WL-TR-91-4061

ULTRAHIGH TEMPERATURE ASSESSMENT STUDY - CERAMIC MATRIX COMPOSITES

E. L. Courtright
Pacific Northwest Laboratory
Richland, Washington 99352

H. C. Graham, A. P. Katz, and R. J. Kerans
Wright Laboratory
Materials Directorate
Metals and Ceramics Division
Wright-Patterson AFB, Ohio 45433

September 1992

Final Report for Period
July 1988 - May 1990

Approved for public release; distribution is unlimited.

MATERIALS DIRECTORATE
WRIGHT LABORATORY
AIR FORCE MATERIEL COMMAND
WRIGHT-PATTERSON AIR FORCE BASE, OHIO 45433-6533

NOTICE

WHEN GOVERNMENT DRAWINGS, SPECIFICATIONS, OR OTHER DATA ARE USED FOR ANY PURPOSE OTHER THAN IN CONNECTION WITH A DEFINITELY GOVERNMENT-RELATED PROCUREMENT, THE UNITED STATES GOVERNMENT INCURS NO RESPONSIBILITY OR ANY OBLIGATION WHATSOEVER. THE FACT THAT THE GOVERNMENT MAY HAVE FORMULATED OR IN ANY WAY SUPPLIED THE SAID DRAWINGS, SPECIFICATIONS, OR OTHER DATA, IS NOT TO BE REGARDED BY IMPLICATION, OR OTHERWISE IN ANY MANNER CONSTRUED, AS LICENSING THE HOLDER, OR ANY OTHER PERSON OR CORPORATION; OR AS CONVEYING ANY RIGHTS OR PERMISSION TO MANUFACTURE, USE, OR SELL ANY PATENTED INVENTION THAT MAY IN ANY WAY BE RELATED THERETO.

THIS REPORT HAS BEEN REVIEWED BY THE OFFICE OF PUBLIC AFFAIRS (ASD/PA) AND IS RELEASABLE TO THE NATIONAL TECHNICAL INFORMATION SERVICE (NTIS). AT NTIS IT WILL BE AVAILABLE TO THE GENERAL PUBLIC INCLUDING FOREIGN NATIONS.

THIS TECHNICAL REPORT HAS BEEN REVIEWED AND IS APPROVED FOR PUBLICATION.

Allan P Katz

ALLAN P. KATZ
Project Engineer

FOR THE COMMANDER

WALTER H. REIMANN, Chief
Materials Development Branch
Metals and Ceramics Division

IF YOUR ADDRESS HAS CHANGED, IF YOU WISH TO BE REMOVED FROM OUR MAILING LIST, OR IF THE ADDRESSEE IS NO LONGER EMPLOYED BY YOUR ORGANIZATION PLEASE NOTIFY WL/MLLM , WRIGHT-PATTERSON AFB, OH 45433-6533 TO HELP MAINTAIN A CURRENT MAILING LIST.

COPIES OF THIS REPORT SHOULD NOT BE RETURNED UNLESS RETURN IS REQUIRED BY SECURITY CONSIDERATIONS, CONTRACTUAL OBLIGATIONS, OR NOTICE ON A SPECIFIC DOCUMENT.

REPORT DOCUMENTATION PAGE

Form Approved
OMB No. 0704-0188

1. AGENCY USE ONLY (Leave blank)	2. REPORT DATE	3. REPORT TYPE AND DATES COVERED
	September 1992	Final Jul 88 - May 90

4. TITLE AND SUBTITLE
Ultrahigh Temperature Assessment Study - Ceramic Matrix Composites

5. FUNDING NUMBERS
MN - FY1457-88-N5052
PE - 62102F
PR - 2420
TA - 01
WU - 01

6. AUTHOR(S)
E. L. Courtright, H. C. Graham, A. P. Katz, R. J. Kerans

7. PERFORMING ORGANIZATION NAME(S) AND ADDRESS(ES)
Pacific Northwest Laboratory
Richland, WA 99352

8. PERFORMING ORGANIZATION REPORT NUMBER

9. SPONSORING/MONITORING AGENCY NAME(S) AND ADDRESS(ES)
Materials Development Branch
Metals and Ceramics Division
Materials Directorate (WL/MLLM)
Wright Laboratory
Wright Patterson Air Force Base OH 45433-6533

10. SPONSORING/MONITORING AGENCY REPORT NUMBER
WL-TR-91-4061

11. SUPPLEMENTARY NOTES

12a. DISTRIBUTION/AVAILABILITY STATEMENT
Approved for public release; distribution is unlimited.

12b. DISTRIBUTION CODE

13. ABSTRACT (Maximum 200 words)

As part of the U.S. Air Force initiative to develop high temperature materials for use in future gas turbine engines, a literature survey coupled with an assessment of recently completed experimental programs sponsored by the Air Force was made to evaluate prospective materials capable of operating at 1650°C or above in oxidizing environments. The assessment reviews fundamental considerations associated with the use of ceramics and ceramic matrix composites in representative environments and includes discussions on potential performance requirements. Key material categories (e.g., borides, carbides, nitrides, silicides, beryllides, and oxides) are evaluated with respect to their strengths and weaknesses. The reinforcements available for high temperature composite applications are reviewed and several prospective composite systems considered. A principal conclusion relative to possible uses for long-term man-rated gas turbine engines is that oxide/oxide composites have the best potential for functional use in oxidizing environments above 1650°C provided adequate single-crystal reinforcement fibers can be developed. Several nonoxide materials and composites were identified for

OVER

14. SUBJECT TERMS	15. NUMBER OF PAGES
Ceramics, composites, ultrahigh temperature, matrix, fiber reinforcement, oxidation, fracture toughness, strength, creep, fatigue	144
	16. PRICE CODE

17. SECURITY CLASSIFICATION OF REPORT	18. SECURITY CLASSIFICATION OF THIS PAGE	19. SECURITY CLASSIFICATION OF ABSTRACT	20. LIMITATION OF ABSTRACT
UNCLASSIFIED	UNCLASSIFIED	UNCLASSIFIED	UNLIMITED

13. ABSTRACT (Continued)

possible uses in short-duty cycle non-man-rated applications. In addition to materials development, there will be critical need for high-temperature test facilities that can be operated in representative oxidizing environments.

ACKNOWLEDGMENTS

The authors wish to acknowledge the technical contributions, guidance, and editorial comments of J. Diefendorf, W. L. Worrell, G. R. St. Pierre, R. A. Rapp, and L. Kaufman, and those who participated in a February 1989 workshop held in Dayton, Ohio. The efforts of Robert Rapp, who carefully reviewed several drafts of this report, are especially appreciated.

The authors would also like to acknowledge J. L. Brimhall, M. D. Merz, and C. H. Henager, Jr., who helped collect literature information on general materials properties, J. L. Biberstine and G. S. Thompson, who helped prepare a workable draft, and W. D. Bennett, who prepared many of the key figures. Editorial assistance was provided by C. A. Anderson and D. K. Hilliard, who helped organize the report and prepare a camera-ready manuscript.

CONTENTS

FIGURES

TABLES

EXECUTIVE SUMMARY

As part of a U.S. Air Force initiative to develop high-temperature materials for use in future gas turbine engines, a literature survey, coupled with an assessment of recently completed experimental programs sponsored by the Air Force, was made to help identify candidate materials capable of operating at 1650°C or above in oxidizing environments. This report focuses primarily on the use of ceramic matrix composites, and a companion report addresses carbon/carbon composites.

The evaluation was done under the assumption that current information is state of the art. The conclusions are therefore subject to change as new data, discoveries, or inventions emerge. This is an important point when drawing conclusions because the entire ultrahigh-temperature area is relatively unexplored and the available data limited. At temperatures of 1650°C or higher, equilibrium is rapidly approached by all systems, thus designers will be unable to use metastable materials--as is presently done in many of today's engineered systems.

The most pertinent conclusions drawn from the assessment are as follows:

1. With the exception of a few materials noted below, most ceramics appear to be marginal for use in jet engines at temperatures above 1650°C, especially for man-rated systems. To achieve satisfactory levels of strength, fracture toughness, and reliability, fiber reinforced composites will be required.

2. Single-crystal oxides are currently the most promising candidates for reinforcements because at 1650°C:

   - all polycrystalline materials creep at rates that are orders of magnitudes too high (desired creep rates: ~10^{-8}/s or less for the matrix and ~10^{-9}/s or less for the fibers)

   - a few single-crystal oxides that include c-axis Al_2O_3 and BeO, and YAG exhibit near satisfactory creep resistance and further improvements appear possible. The creep properties of single-crystal yttrium aluminum garnet (YAG) are particularly encouraging. This compound has cubic crystal structure, which should reduce orientation dependency within the composite and, hence, sensitivity to off-axis loads.

3. Oxides are also the best matrix candidates because:

   - all nonoxide ceramics oxidize faster than allowable (0.1 μm/hr). This is true even if the nonoxide is contained within an oxide matrix.

   - flight-critical components could not oxidize catastrophically and could not depend on protective coatings. This is a necessary requirement for man-rated turbines.

4. In view of (2) and (3) above, an oxide/oxide composite system should be able to meet strength and creep requirements based on single-crystal reinforcements at the lower end of the temperature range of interest (e.g., 1650°C-1700°C).

5. In general, the mechanical properties (e.g., strength, thermal shock resistance, creep, and toughness) of state-of-the-art oxide ceramics are currently marginal for structural applications. Hence, a clear knowledge of the fundamental physical and chemical properties of these materials will be required to optimize properties and achieve acceptable reliability.

6. While nonoxides require protection from oxidation, some limited prospects exist:

   - Silica formers (e.g., SiC, Si_3N_4, $MoSi_2$) are the most promising, but rapidly lose their oxidation protection capabilities with increasing temperature, and will have only marginal usefulness above 1650°C for long-term applications. All other oxides transport oxygen at higher rates than silica and, therefore, cannot be used as coatings to protect nonoxide materials.

   - The strength and short-term oxidation resistance of SiC/HfB_2 or SiC/ZrB_2 composites make them suitable for high-temperature (>1700°C), short-duty cycle (>5 h) applications.

   - The ZrB_2 (pl)/ZrC(Zr) PRC™ platelet reinforced composite produced by Lanxide exhibits excellent strength and toughness and may also be useful in short-duty cycle (non-man rated) applications.

7. In addition to the development of ceramic composite materials, several concurrent technologies must also advance in parallel (these will also be needed for lower temperature composites):

   - processing methodologies

   - oxidation-resistant coatings

- improved polycrystalline fiber and single-crystal fiber manufacturing technologies
- testing/analysis methodology
- high-temperature test facilities that operate in oxidizing environments. (Progress will be slow because the need to test and evaluate in representative oxidizing environments at such high temperatures is a formidable challenge in itself.)

While the assessment that follows reveals a few promising material candidates for use in the ultrahigh-temperature regime above 1650°C, the choices are clearly limited. Further studies, as discussed above, will be needed if these materials are to be transferred from the laboratory into engineering practice.

ULTRAHIGH-TEMPERATURE ASSESSMENT STUDY

INTRODUCTION

U.S. Air Force interest in lightweight structural ceramics began in the 1950s when it became evident that improvements in gas turbine engine performance could be achieved by reducing weight and improving combustion efficiency at higher operating temperatures. Progress toward the development of monolithic structural ceramics has been slow, however, because of low damage tolerance and poor thermal shock resistance. In recent years, research efforts have turned to fiber-reinforced ceramic matrix composites because of evidence that the proper addition of a second phase may prevent catastrophic brittle failure or improve damage tolerance through various energy dissipation processes.[1] For example, studies at the Air Force Materials Directorate, Wright Laboratory, are currently investigating mechanical behavior, failure processes, microstructure/property relationships, the role of fiber/matrix interfaces and environmental stability issues in ceramic composites.[2]

In 1985, an Air Force-sponsored research program on ceramic composites was started to support the Integrated High-Performance Turbine Engine Technology (IHPTET) Initiative by addressing long-term materials technology requirements in the ultrahigh-temperature (UHT) regime (1650°C to 2200°C, 3000°F to 4000°F). As a first step, a workshop was organized to evaluate fundamental considerations regarding temperature and service limitations of known materials.[3] The study topics, which are listed in Table 1, provided the basis needed for identifying R&D projects to examine critical or limiting aspects of high-temperature material behavior. In 1986, twelve research projects were started through a Program Research and Development Announcement (PRDA). Eight of these studies investigated various issues associated with the development of ceramic matrix composites. In 1987, eight new studies were initiated under a PRDA with similar objectives. Project descriptions and key results are listed in Table 2, and Appendices A-E present short summaries of each program. Additional studies, which were directed at improving carbon/carbon oxidation resistance, are discussed in a companion report.

TABLE 1. Agenda for Ultrahigh-Temperature Composite Materials Workshop[3]

Study Topics	Researchers
Materials for High-Temperature Ceramic/Ceramic Composites	T. E. Mitchell, K. M. Vedula, and A. H. Heuer (Case Western Reserve University)
New Options for the Protection of Carbon/Carbon Composites	R. A. Rapp and G. R. St. Pierre (Ohio State University)
Opportunities for the Development of New High-Temperature Materials for Use Under Extreme Conditions	J. L. Margrave (Rice University)
Options for High-Temperature Composites	J. D. Cawley and W. B. Johnson (Ohio State University)
Constituent Materials for 4000°F, Oxidation Resistant Composites	R. Boisvert and J. Diefendorf (Rensselaer Polytechnical Institute)
Deformation Resistance and the Development of High-Temperature Composites	W. S. Williams (Case Western Reserve University)
Potential Materials for Composites and Coatings of Carbon/Carbon Composites at Very High Temperatures	W. L. Worrell (University of Pennsylvania)
Environmental Stability of Materials Having Potential for Ultrahigh-Temperature Use	G. H. Meier and F. S. Pettit (University of Pittsburgh)
The Selection of Materials for Ultrahigh-Temperature Applications	R. R. Mutso and R. W. Guard (University of Texas at El Paso)

Earlier research performed under U.S. Air Force Contract AF33 615-3671 (Research and Development of Refractory Oxidation-Resistant Diborides) and AF33 615-3859 (Stability Characterization of Refractory Materials Under High-Velocity Atmospheric Flight Conditions) are summarized in Appendix F. This work was performed in the 1960s to develop oxidation-resistant refractory metal diborides and to examine the stability characteristics of refractory materials under high-velocity atmospheric flight conditions.

This assessment begins with an examination of the fundamental considerations associated with the use of ceramic matrix composites in gas turbine

TABLE 2. Ultrahigh-Temperature Composite Research Programs

Contractor	Program Description	Key Results
DuPont (Page A.3)	Thermochemical and thermomechanical stability of composite pairs using XRD, TGA, DTA, and microscopy.	• No reaction: C/TiC; HfB_2/TaC; C/TaB_2; HfB_2/TaB_2 to 2200°C. • XRD change, but no TGA/DTA change for: ZrC/TiC; HfN/HfC; TaB_2/ZrC; TaC/TiB_2; TiC/HfB_2; ZrO_2/HfB_2 to 2200°C. • Best CTE match: HfB_2/TaB_2; ZrO_2/HfB_2; TiC/ZrO_2.
Wright State University (Page A.5)	Chemical and oxidative stability of selected material combinations and comparisons with thermodynamic calculations.	• ZrC/ZrO_2; HfC/HfO_2 chemically compatible to 2000°C. • AlN/ZrB_2; AlN/HfB_2 compatible to 1900°C. • $MoSi_2$/ZrB_2; $MoSi_2$/HfB_2 compatible to 1570°C.
Westinghouse R&D (Page A.7)	Diffusion studies of nonoxide/oxide systems (TaC, ZrC, TiB_2, ZrB_2, TaB_2) - ($SrZrO_3$, Y_2O_3).	• Good compatibility between TaC/Y_2O_3; Kr ~8.1 x 10^{-13} cm^2/sec. • Y_2O_3/TaB_2 reaction slight to 1750°C. • $SrZrO_3$ unsuitable due to high vapor pressure.
Ohio State University (Page A.9)	Volatility and microstructural stability of HfO_2, ZrO_2, $CaZrO_3$ and $CaHfO_3$.	• Resistance to mass loss by evaporation HfO_2 > ZrO_2 > $CaHfO_3$ > $CaZrO_3$. • 8 m/o yttria stabilized zirconia can be heated to 1800°C <u>without</u> a disruptive phase transformation.

TABLE 2. (contd)

Contractor	Program Description	Key Results
Ohio State (contd)		• Grain size after 1800°C/μm 72 h: $CaZrO_3$ - 80; $CaHfO_3$ - 33 μm; $HfO_2(Y_2O_3)$ - 20 μm; $HfO_2(Y_2O_3)$ - 14 μm. • Reactivity: $Al_2O_3/CaZrO_3$ - 1700°C $Al_2O_3/CaHfO_3$ - 1800°C.
General Electric R&D (Page A.11)	Thermochemical calculations to identify systems for evaluation of chemical compatibility and microstructural stability.	• Oxides that demonstrate lowest reactivity with carbon: $BeO < Y_2O_3 < Al_2O_3 < Ce_2O_3$. • Oxygen permeation through Al_2O_3 and Y_2O_3 at 1650°C resulted in severe gas evolution at C interface. • Cr and Ir chemically compatible with C in oxidizing environments. • Cr and Ir thermochemically stable with Al_2O_3, Y_2O_3 and $ZrO_2(Y_2O_3)$ to 1650°C in argon.
MSNW (Page A.14)	Acquisition of basic thermodynamic data for selected composite materials.	• Borides and carbides vaporize as the boron and carbon species. • TiB_2/HfC in oxygen reacts at 1027°C. • $SrZrO_3$ and $SrHfO_3$ lose Sr and O_2 between 1527°C-2027°C.

TABLE 2. (contd)

Contractor	Program Description	Key Results
MSNW (contd)		• Yttria-stabilized ZrO_2 and HfO_2 vaporize to Y, YO, ZrO, and HfO at 2227°C. • IrAl preferentially loses Al at 2027°C. Oxygen converts the Al to Al_2O.
Case Western Reserve Univ. (Page A.17)	Compatibility and stability of boride/ oxide systems.	• Neither ZrO_2 or Y_2O_3 prevented oxidation of TiB_2 at 1600°C. • Al_2O_3 did not prevent oxidation of TiB_2. • CaO volatility too high in $CaZrO_3$.
Babcock & Wilcox (Page B.2)	Prospective composite systems evaluated for chemical interaction, oxidation, and creep.	• BN/AlN-SiC stable to 2000°C. Good oxidation resistance to 1600°C. Flexural strength: 192 MPa at 1530°C. • ZrC/ZrB_2-Y_2O_3 exhibits adequate thermal stability - wt gain in 1-2% O_2 at 1650°C ~9.6%.
3M - Ceramic Technology Ctr. (Page B.5)	Chemical and microstructural stability of alkaline-earth zirconates prepared by sol gel.	• Made $MgZrO_3$, $CaZrO_3$, $SrZrO_3$ and $BaZrO_3$ flakes from sol gel derived alkaline zirconates. • Green fibers made from $SrZrO_3$, but rapid grain growth and microstructural instabilities prevent sintering.

TABLE 2. (contd)

Contractor	Program Description	Key Results
UCLA (Page B.7)	Evaluation of $LaCrO_3$ for stability and suitability for fiber making.	• $LaCrO_3$ was made by new solution-based methods. Pre-ceramic precursor fibers were drawn. Attempts to draw continuous filament were not successful. • Young's modulus for KERMAX $LaCrO_3$ measured 97.9 GPa. • Oxidation weight-loss was significantly reduced with Al_2O_3 coating.
UES (Page B.9)	Assessment of morphological and chemical stability of Al_2O_3/mullite.	• Al_2O_3/mullite not a viable composite system due to multiple cracking from large CTE difference.
UES (Page B.9)	Directional solidification of oxide eutectics.	• Six eutectic systems evaluated: $SrO-ZrO_2$; $CaO-ZrO_2$; $La_2O_3-Al_2O_3$; $Y_2O_3-Cr_2O_3$; Al_2O_3-YAG. • Composition and microstructure of alumina - YAG eutectic stable for up to 5 h at 1700°C. • Al_2O_3 - YAG flexural strength ~265 mPa at 1585°C. Fracture toughness ~4 mPa $\sqrt{M}$.
General Electric R&D (Page C.2)	Creep measurements of single crystal oxides.	• Creep in YAG comparable to c-axis sapphire. • In YAG, creep rates for different cubic orientations were similar. • c-axis BeO appears to be very creep resistant in compression.

TABLE 2. (contd)

Contractor	Program Description	Key Results
General Electric R&D (contd)		• Compressive creep data obtained for [100], [110], [111] yttria stabilized zirconia and for [100], [110] thoria. • Stress limits for 2.8 x 10^{-9}/s creep rate at 1650°C: [100] $ZrO_2(Y_2O_3)$ - 14 MPa, [100] ThO_2 - 46 MPa.
University of Texas at El Paso (Page D.2)	Compatibility and Oxidation of HfB_2 - HfO_2 with $HfSiO_4$ interlayers and coatings.	• Hf_2Si forms in reaction between $HfO_2/HfSi_2$ - growth is parabolic.
Refractory Composites (Page D.4)	Oxidation studies of HfB_2-SiC and ZrB_2- SiC.	• Resistance to oxidation for 80% HfB_2 + 20% SiC better than pure HfB_2 at 2000°C.
Pacific Northwest Laboratory and Ohio State University (Page D.6)	Oxidation studies of HfC and HfC with additions of Ta and Pr.	• Provided baseline data on metal-carbide oxidation. • Developed pore diffusion model for low temperature regime where oxide scales are fully dense.
Ohio State University (Page E.2)	Measure vapor pressures, oxygen diffusivities, and gas-solid reaction products for $CaZrO_3$, $BaZrO_3$, $SrZrO_3$, at high temperatures.	• Vaporization of $BaZrO_3$ > $CaZrO_3$ ~1 mg/cm^2/h at 1650°C. • $BaZrO_3$ exhibits lowest diffusion coefficient ~10^9 cm_2/s at 1650°C (extrapolated).

TABLE 2. (contd)

Contractor	Program Description	Key Results
LTV Aerospace (Page E.5)	Oxygen diffusivity measurements in $SrHfO_3$.	• Developed novel method for making tracer diffusivity measurements at temperatures to 2200°C. • Tracer oxygen diffusion coefficients measured for $SrHfO_3$ between 1800°C-2200°C.
Basic Industry Research Laboratories/ Northwestern University (Page E.7)	Oxygen diffusivity measurements for refractory oxides of pyrochlore systems: $Zr_3Y_4O_{12}$, $Zr_3Sc_4O_{12}$, $Zr_3Gd_4O_{12}$, $Zr_3La_4O_{12}$.	• Lowest diffusion coefficients obtained were for Y_2O_3 and $Zr_3Sc_4O_{12}$. At 1200°C both are $\sim 4 \times 10^{-10}$ cm^2/s.
Pacific Northwest Laboratory (Page E.9)	Oxygen permeability measurements for selected oxides from 1200°C-1700°C.	• Oxygen permeability versus temperature curves reported for Y_2O_3, Al_2O_3, BeO, $HfO_2.Y_2O_3$, $ZrO_2.Y_2O_3$, $SrZrO_3$, $HfPr_2O_7$, $HfPr_2O_7$, $CaZrO_3$, and $La_2Hf_2O_7$. • Segregation in oxygen gradient shown to be large for $SrZrO_3$ and very small for $La_2Hf_2O_7$.

engines followed by a short discussion of performance requirements. Key materials categories (e.g., borides, carbides, nitrides, silicides, beryllides, and oxides) are evaluated with respect to their strengths and weaknesses. Reinforcements for composite applications are reviewed and several prospective composite systems are considered. Finally, conclusions relative to possible uses in either limited-life or long-term man-rated gas turbine engines are offered.

The materials for which published data are available were probably not prepared equally with respect to impurity levels, homogeneity, density, or microstructural uniformity. No attempt was made to make judgment decisions

relative to the uncertainty or validity of reported results. If results were clearly questionable or if conclusions were inconsistent and unsupported, the data were not used.

The nomenclature employed throughout this review and assessment to define composite systems is as follows:

• $SiC/MoSi_2$	Reinforcement phase/matrix phase
• SiC p, w, f, pl	Type of reinforcement: particulate (p), whisker (w), fiber (f) platelet (pl)
• ZrC (Zr)	( ) material in parenthesis indicates second phase

FUNDAMENTAL CONSIDERATIONS

A ceramic composite is defined herein as an engineered two-phase material consisting of ceramic fibers, whiskers, platelets, or oriented particulates in a ceramic matrix. The matrix should be thermochemically compatible with the reinforcing phase or its coating and must physically interact in a way that produces synergistic benefits. For example, if the fiber/matrix interface is chemically bonded and very strong, good strength and stiffness may be realized, but the material will probably fracture catastrophically in the same manner as a monolithic ceramic. If the interface is weakly bonded, then cracks do not propagate readily from one phase to the other, enabling the bulk material to resist crack growth and fail in a nontraumatic manner.

The effects of fiber pull-out on the mechanical properties of ceramic matrix composites were reviewed by Thouless and Evans.[4] Toughness is imparted by fibers or whiskers as a result of net traction exerted on the matrix crack by the fibers in the crack wake. Tractions arise from two sources: intact fibers that have been circumvented by the matrix crack and by fibers that fall away from the crack plane. Broken fibers resist crack opening by frictional sliding when the broken ends pull out from the matrix.

In reviewing the need for control of the fiber/matrix interface, Lowden concluded that both qualitative and quantitative analysis of the interfacial shear strength is essential to the development of composites with the necessary combination of strength and toughness.[5] Methods under development to quantify the strength of the interfacial bond generally involve pushing or pulling individual fibers[6] or micro-hardness indentors that apply a force to the end of a fiber embedded in a matrix.[7,8] Kerans et al.[9] reviewed these contemporary experimental techniques with respect to possible mechanistic interpretations and concluded that fiber/matrix characterization can only help establish the best process conditions for optimizing composite properties once the fundamentals of mechanical behavior are better understood.

New design methodologies for ceramic composites emphasize probabilistic life prediction methods,[10,11] whereby analytical or empirical models are used to predict component failures. Traditional criteria involving yield

strength, ductility, toughness, and hardness are giving way to flaw sensitivity, intergranular slow crack growth, and damage tolerance. The mechanical properties of brittle materials are sensitive to the method of specimen preparation, surface condition, environment, and testing approach. Thus, new testing techniques and methodologies must be developed to increase data reliability.

Components exposed to cyclic high-temperature operation, as is the case for many turbine engine components, undergo repetitive straining that induces crack initiation and propagation. In monolithic ceramics, crack propagation is controlled by the distribution of flaws such as pores, surface defects, inclusions, and microstructural features such as large inhomogeneous grains or impurity agglomerates. Time-dependent processes (e.g., slow crack growth) cause fracture to occur at loads significantly below conventional brittle fracture levels, and environmental degradation will likely reduce these levels even further. To account for these complex processes, statistical methods for computing stress deformation and crack propagation are being developed to predict failure probabilities as a function of time. Similar approaches will also be required for the development of ceramic matrix composites in order to achieve reliability.

PERFORMANCE ISSUES AND REQUIREMENTS

Most operational requirements are design specific. From a design perspective, a structural ceramic composite can be directionally reinforced to maximize specific properties such as flexural strength, creep, or toughness. Since ceramics are inherently brittle, a premium is placed on fracture toughness to achieve an acceptable level of reliability. For example, extended life operation may require life-cycle reliability up to 1,000 hours at engine operating temperatures. Another major requirement is thermodynamic stability in oxidizing environments. High temperatures also place emphasis on thermochemical compatibility between components to prevent mechanical degradation.

For propulsion applications, the properties of interest include fracture toughness, oxidation resistance, creep resistance, fatigue resistance, strength, and stiffness.

TOUGHNESS

Before a brittle material can be used in a structural application, tolerance to thermal shock, impact damage, and rapid fracture must be demonstrated. Considerable efforts have been directed toward developing various methods of second phase toughening of ceramic matrices through a variety of energy dissipation processes. As shown in Figure 1, competition between flow and fracture occurs at high temperatures.[12,13] Creep is the dominant deformation process when the flow stress is smaller than the stress needed to induce unstable crack extension.

It is the noncatastrophic decrease in load that gives fiber- and whisker-reinforced ceramics the appearance of being very tough.[14] The general features of load/deflection curves (Figure 2) for flexure and tension tests show an initial elastic region followed by a nonlinear load increase to a maximum, which is then followed by a continuous load decrease. However, comparisons of these load/deflection curves reveal large differences in the regions of nonlinear load increase to the ultimate strength and decreasing load behavior thereafter. Thus, work of fracture does not provide a material

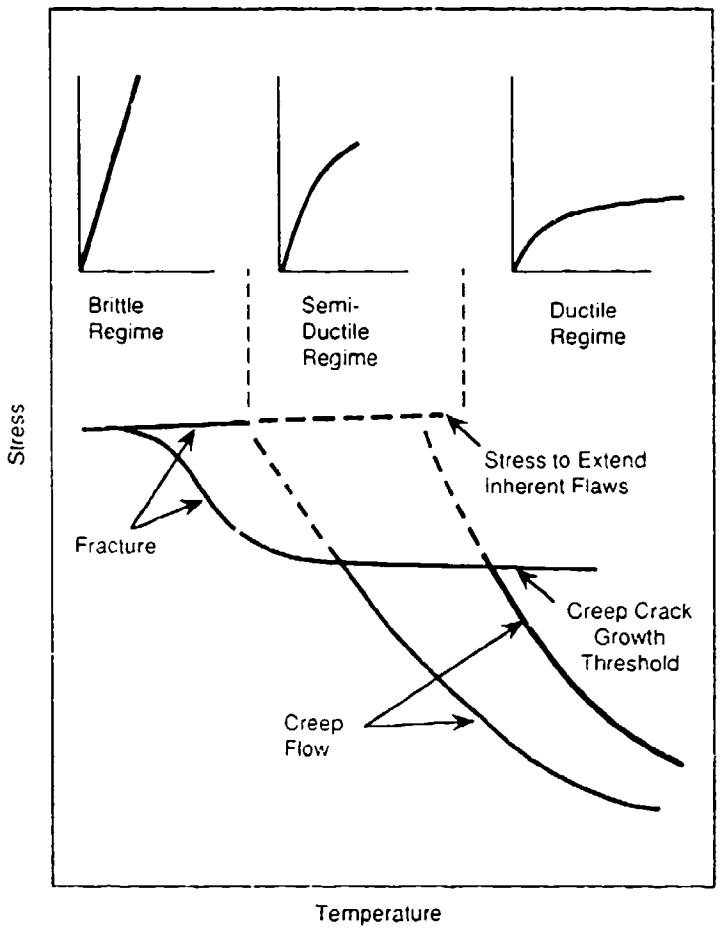

FIGURE 1. Schematic of Fracture and Flow in Ceramics as a Function of Temperature (Ref. 12,13)

property value independent of loading configuration.[15] The consistency between flexure and tension tests is found in the matrix cracking stress, σ_m. This can be written:[14]

$$\sigma_m^c = \frac{2.3\,[K_c^m\,\tau\,E_f V_m^2\,(1 + E_f V_f/E_m V_m)^2]^{1/3}}{E_m R} - \sigma_m^R \qquad (1)$$

where τ is the shear stress of the fiber/matrix interface, K_c^m is the matrix toughness, R the fiber radius and E_f, E_m are the Young's modulus of the fiber

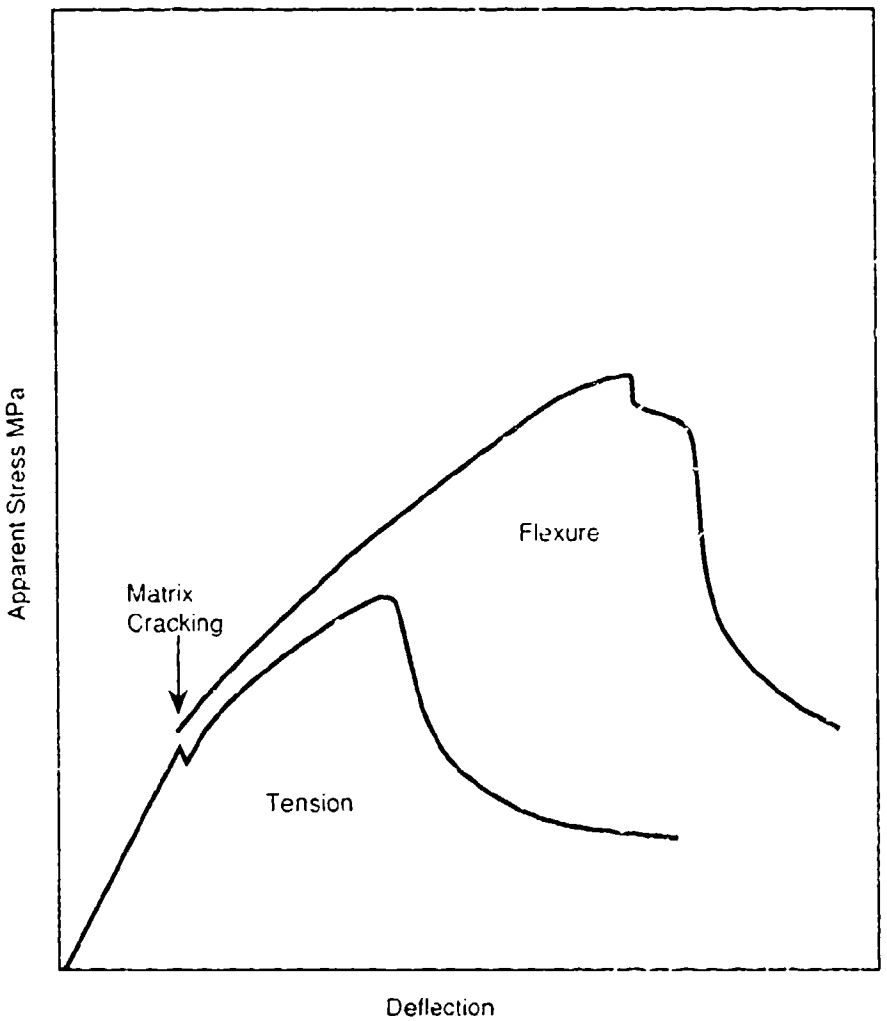

FIGURE 2. Load Deflection Behavior of Fiber-Reinforced Ceramic Matrix Composites (Ref. 15)

and matrix, respectively. The residual stress term σ_m^R is important if large differences in thermal coefficient between fiber and matrix exist. The shear strength of a fiber reinforced composite is generally less than the tensile strength and can be described by an equation of the type:[14]

$$\tau \alpha \frac{V_f^{1/4} V_m K_c^m}{(1+V_f) \sqrt{R}} \qquad (2)$$

An important term common to both equations (1) and (2) is the dependence on K_c^m, which is the toughness of the unreinforced matrix.

In both fiber and whisker reinforced composites, the matrix cracking strength σ_{mc} and the ultimate tensile strength, σ_{uc}, at fiber bundle failure are useful design properties analogous to the yield strength and ultimate tensile strength for structural alloys.[14] An additional consideration at elevated temperatures is potential exposure of the fibers to the environment once matrix cracking has occurred. Environmental degradation of the fibers or the fiber/matrix interface could significantly alter the toughness of the material.

The concept of fracture resistance in a qualitative sense or some measure of toughness in a quantitative sense is very important to the functional design of structural ceramics, particularly for engine applications. Reliability will have to be ensured at some acceptable level of damage tolerance that can be accurately measured on a representative sample of material. The interpretation of fracture toughness measured from notched-beam tests is somewhat subjective due to relative degrees of matrix cracking, fiber pullout, and various crack deflection processes. Thus, quantitative use of fracture toughness numbers obtained from ceramic materials must be applied with caution. However, measurements of this type are qualitatively useful for comparing relative resistance to brittle failure, and a fracture toughness of 10 MPa$\sqrt{m}$ probably represents a functional minimum.

Unfortunately, only a few ceramic composites concurrently meet or exceed this value. Fracture toughnesses approaching 10 MPa $\sqrt{m}$ have been reported for TiB$_2$ particulate reinforced SiC[18] and 8 MPa $\sqrt{m}$ for SiC whisker strengthened MoSi$_2$.[19] Values as high as 20 MPa $\sqrt{m}$ have been reported for phase-toughened zirconia.[18] Fiber toughened composites exhibit better fracture toughness than whisker reinforced materials, emphasizing the importance of fiber length/fiber diameter aspect ratio, L/d, in "pull out" toughening.[20] In SiC fiber-toughened Si$_3$N$_4$, fracture toughness values as high as 13 MPa $\sqrt{m}$ have been reported,[20] and values in excess of 10 MPa $\sqrt{m}$ have been achieved with long whiskers (L/d ~40) compared with 6 to 8 MPa $\sqrt{m}$ for particles and smaller aspect ratio whiskers.[21]

The use of Linear Elastic Fracture Mechanics has not proved effective in predicting failure in monolithic ceramics, and observations of noncoplanar failure indicate that fracture is not uniformly controlled by K_{IC}.[11] As previously discussed, work of fracture does not give a quantity that is independent of the loading configuration.[15] Despite these problems, the concept of toughness, even if in a qualitative sense, is very important to the proper design and utilization of structural ceramics. Two practical performance concerns are resistance to thermal shock and to foreign object impact damage. These real operational concerns must be satisfied at an acceptable level of reliability that can be accurately measured and interpreted by some toughness related value.

CREEP

As shown in Figure 1, creep is a dominant flow process at high temperatures, and steady-state creep will likely be an important design criterion in any high-temperature structural application. Composite creep rates will have to be on the order of 10^{-8}/s or lower for extended service applications. To achieve these levels, a very creep-resistant fiber will be needed to reinforce less creep-resistant matrices.

The creep behavior of a reinforced ceramic composite is not easy to predict. In modeling short-fiber (whisker) reinforced materials, the fiber volume fraction and fiber aspect ratio are predicted to have a dominant effect on creep behavior; however, low values of fiber/matrix bonding will increase the creep rate only by a factor of two or so.[22] The latter prediction is important because easy interface sliding is desirable for toughness.

The stress dependencies of steady-state creep in ceramics are similar to those in metallic systems. Cannon[23,24] reports that the stress exponent (n) typically varies from three to five in the dislocation climb regime and is in the range of one to two when diffusional mechanisms are operable. If we assume that high-temperature tensile creep of ceramic fiber and matrix materials can be described by a common power law expression,[25] and the

strain rate, $\dot{\epsilon}_c$, in the composite at a stress, σ_c, is weighed according to the volume fraction of the two phases present,[26] then the composite stress can be related to the composite creep rate by:

$$\sigma_c = \frac{\sigma_{fo} V_f \dot{\epsilon}_c^{1/n}}{\dot{\epsilon}_{fo}^{1/n}} + \frac{\sigma_{mo} V_m \dot{\epsilon}_c^{1/m}}{\dot{\epsilon}_{mo}^{1/m}} \qquad (3)$$

where σ_{fo}, $\dot{\epsilon}_{fo}$, σ_{mo}, $\dot{\epsilon}_{mo}$ are constants obtained from empirical stress/strain rate relationships, and m and n are the stress components for the matrix and fiber, respectively.

This equation allows us to calculate the stress required to sustain a steady-state creep rate (e.g., 10^{-8}/s) in a continuous fiber-reinforced composite assuming that both fiber and matrix are creeping at the same rate and there is no interfacial slippage. Two hypothetical examples are shown in Table 3.

For case I, a polycrystalline alumina matrix is reinforced by 20 v/o YAG single crystals. The composite is predicted to creep at 10^{-8}/s (Temp=1500°C) when the composite stress reaches 50 MPa. In case II, single-crystal sapphire is reinforced with 30 v/o single-crystal YAG. For this situation, a creep rate of 10^{-8}/s occurs when a stress of 100 MPa is reached at 1700°C. In the first case, the creep rate of the matrix was very high (~3 x 10^{-5}/s) and the fiber had to carry almost the entire load. In the second case, the matrix creep rate (~3 x 10^{-8}/s) was only slightly lower than that for the fiber (3 x 10^{-9}/s), and the two phases shared the load about equally. These two examples demonstrate the need for a very creep-resistant fiber (~10^{-9}/s or better) to achieve the necessary degree of creep resistance in a composite.

In a whisker-reinforced system, some incremental increase in creep resistance is expected because the matrix can creep unrestrained at the end of the whiskers. It has been shown that the shear stress profile along the fiber will be uniformly distributed if the stress exponent (m) in the matrix is greater than four and the aspect ratio (L/d) is greater than two.[29] In addition, the load transfer from matrix to fiber becomes fairly constant at

TABLE 3. Examples of Creep in Prospective Oxide/Oxide Composites*

Case I:	Fiber	YAG	Single crystal	n=6 [110] (Re: 27)
	Matrix	Al_2O_3	Polycrystalline	m=1.6 (Re: 28)
	Temp	1500°C		
	Vol fraction fiber:	20%		
	Creep rate:	10^{-8}/s		
	σ_c =	50 MPa		
Case II:	Fiber	YAG	Single crystal	n=2.7 [100] (Re: 27)
	Matrix	Al_2O_3	Single crystal	m=4.5 [c-axis] (Re: 27)
	Temp	1700°C		
	Vol fraction fiber:	30%		
	Creep rate:	10^{-8}/s		
	σ_c =	100 MPa		

*Assume creeping fibers - fully bonded interface

m>4 and for fiber volume fractions of 30% or greater. Bullock, McLean, and Miles[26] also show that for V_f constant, the minimum creep rate in the composite can be reduced by two orders of magnitude if the fiber radius is reduced from 4 to 0.4 μm. These considerations suggest that useful whisker-reinforced composites can be engineered given proper choice of stress exponents, fiber radius, and aspect ratio.

FATIGUE

In metals and metal alloys, fatigue cracks initiate and propagate in regions of high strain concentrations, which are usually associated with flaws or defects. Under cyclic loading, a plastic zone develops at or near the defect. This zone is an initiation site for cracks, which can propagate

through the material when driven by the applied stress. The concept of crack tip plasticity may be achieved in brittle materials only at very high temperatures.

Although time-dependent failure or loss of strength is known to occur in ceramics, it is normally attributed to microstructural changes and material quality factors. For example, strength retention in monolithic Si_3N_4 and SiC exposed to long-term cyclic conditions in a combustion environment becomes better as the material density increases.[19] Dauskardt and Ritchie[30] studied fatigue crack propagation in alumina (Al_2O_3), partially stabilized zirconia (PSZ), zircona-toughened alumina (ZTA), and silicon nitride (Si_3N_4). Cyclic crack growth in the range of 10^{-6} to 10^{-10} m/cycle was power law dependent. In their studies, the ceramics exhibited mean-stress, crack closure, and environmental effects that were analogous to metals.

Ewart and Suresh[31] studied crack propagation in ceramics under cyclic compression. These authors found that a zone of residual tensile stress was created at the notch tip if the deformation within the notch tip process zone leaves permanent strains upon unloading from the maximum nominal compressive stress. This mechanism is thought to be the principal driving force for mode I crack growth in ceramics stressed in cyclic compression. While early compression cycles may cause appreciable damage in the form of microcracking at the root of the notch, coalescence of microcracks to form microscopic fatigue flaws can only be achieved over tens-of-thousands of subsequent cycles. Intergranular fracture promotes the accumulation of debris within the cracks, resulting in the progressive development of closure in the wake of the crack tip leading to crack arrest. In SiC whisker-reinforced Si_3N_4, crack growth continued at a monotonically diminishing rate following the early compression cycles, but the whiskers generally lowered the fatigue resistance compared with the unreinforced matrix.[32]

Relative slippage between fiber and matrix above σ_m^c, Equation (1), will most likely enhance fatigue damage in addition to promoting environmental susceptibility. Thus, it may be necessary for the design stress to be below the matrix cracking stress. This value has not been rigorously established

for a wide variety of ceramic composites, but is expected to be about 2/3 of the ultimate strength. For example, Nikkila and Mantyla [33] reported that the fatigue limit for Si_3N_4 was on the order of 2/3 of the flexural strength.

Current design strategies for structural ceramics are based primarily on strength and toughness measurements. Cyclic fatigue behavior must also be included as an essential element in any comprehensive design analysis. Suresh, Han, and Petrovic [32] suggest that fatigue crack growth measurements can be obtained under farfield cyclic compression tests during the process of precracking notch specimens for fracture toughness measurements. Such an approach, if rigorously adopted, would greatly add to the mechanical property data base needed to evaluate and properly design composite systems for structural applications.

OXIDATION

Many of the composite systems involve one or more phases that are sensitive to either oxidation or other forms of environmental degradation. A linear recession value of <0.1 μm/h is a reasonable goal. This implies a total recession of ~100 μm (4 mil) in 1000 hours, which would amount to a significant fraction of a turbine foil cross-section that might be acceptable for a larger and thicker structure. If a protective coating is applied, it must have sufficiently low permeability to oxygen and other corrosive species to prevent an equivalent amount of attack to the underlying substrate. A simple one-dimensional diffusion argument leads to a permeability limit of 10^{-12} g O_2/cm•s if the coating thickness is 1 μm, or 10^{-10} g O_2/cm•s if the thickness is 100 μm.[34] Currently, pure SiO_2 is the only oxide capable of meeting these criteria above 1650°C (see Figure 3 for comparison with other refractory oxides and noble metals). A range of values for silica was obtained by converting oxidation and diffusivity data to obtain the permeability constant as a function of temperature.

Because of the importance of oxidation protection for nonoxide ceramics and carbon/carbon composites, three Air Force UHT programs (Appendix E) measured the tracer diffusivity of oxygen in several compound oxides thought

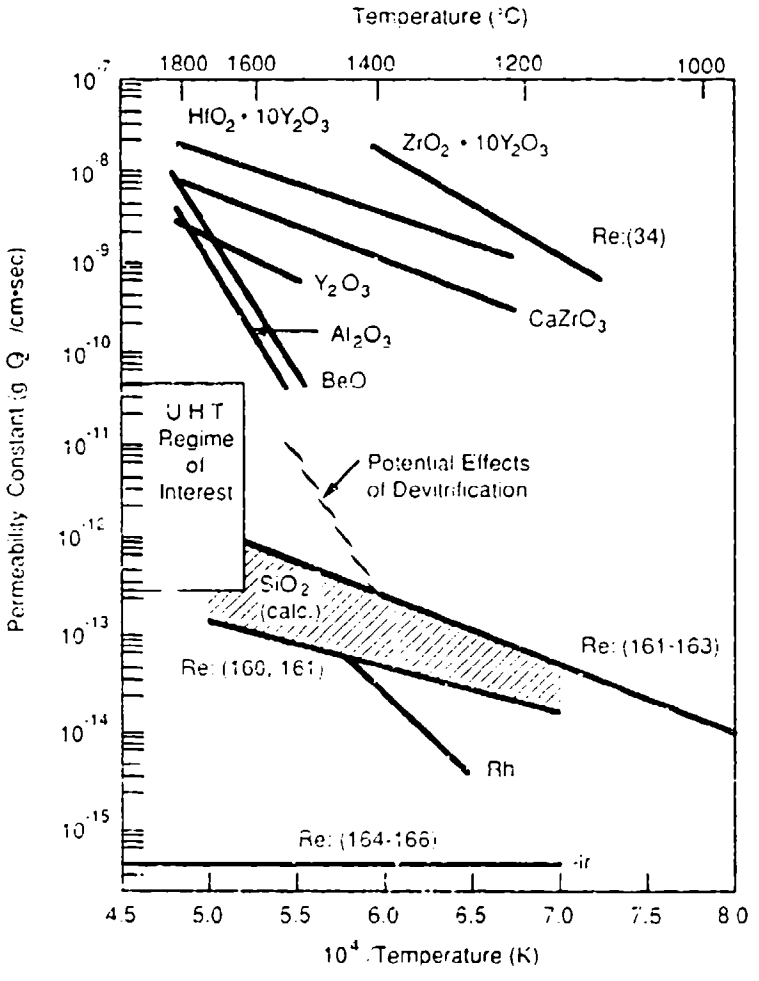

FIGURE 3. Range of Oxygen Permeability Through Several Oxides and Noble Metals

to have potentially better resistance to the diffusion of oxygen than the refractory fluorites (e.g., ZrO_2 and HfO_2). Barium zirconate was reported to have the lowest diffusion coefficient for several zirconates and hafnates including $SrHfO_3$.[35,36] Compound oxides containing strontium exhibited unfavorably high vapor pressures.[36] The oxygen diffusivity through several pyrochlore compounds has also been measured.[37] The compound $Zr_3Sc_4O_{12}$ was found to have a similar oxygen diffusion coefficient ~4 x 10^{-10} cm^2/s to Y_2O_3 at 1200°C.

A comparison of parabolic oxidation rates for several nonoxide ceramics is made in Figure 4. The regime of interest for UHT applications is in the lower left-hand corner of the figure. An acceptable rate constant is about 10 $\mu m^2/h$ or lower. The data were taken from a variety of sources,[38-46] and were typically obtained from experiments that measured thickness increase by metallography or weight-gain from gravimetric measurements. Where possible, parabolic rates were taken from a plot of thickness (μm) versus the square-root of time ($\sqrt{h}$) according to the recommendation of Pieraggi,[47] since this method properly delineates the transient oxidation period.

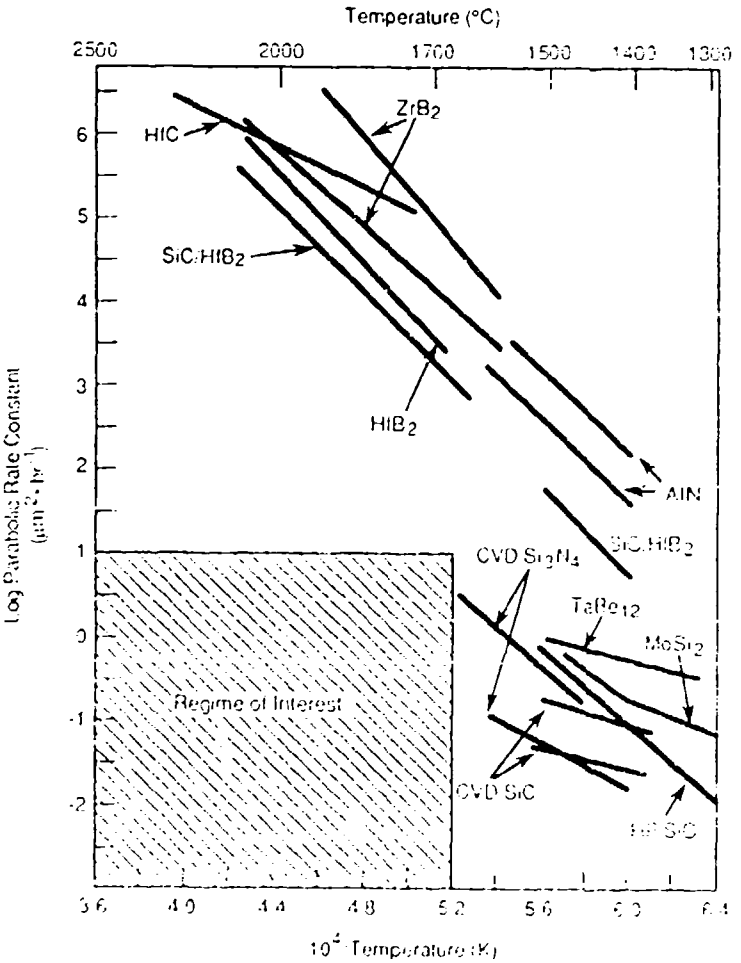

FIGURE 4. Oxidation of High-Temperature Ceramics (Refs. 38-46)

The conversion of weight-gain data to recession rates assumes that one knows the proper oxidation reactions and the density of the oxide scale (theoretical density is usually chosen). For example, consider the reaction:

$$2\ AlN + 3/2\ O_2 \rightarrow Al_2O_3 + N_2 \qquad (4)$$

For every two moles of AlN converted, one mole of Al_2O_3 is formed. Therefore, 48 g mol of O_2 are consumed and 28 g mol of N_2 are lost, providing a net increase of 20 g. While this approach is not precise, it does provide a method for making useful comparisons between data derived by different experimental methods, and easily distinguishes the materials which exhibit the better oxidation resistance when the parabolic rate constants differ by an order of magnitude or more.

Only the silica-formers Si_3N_4 and SiC are able to meet the desired requirement of 10 $\mu m^2/h$ or less above 1650°C. Other carbides, borides, and even the nitrides oxidize at rates that are several orders of magnitude too high. One of the Air Force sponsored UHT programs (Appendix D.6) provided data on the oxidation kinetics of hafnium carbide.[45] Praseodymium and tantalum were included with the idea of increasing scale resistance to oxygen permeation, but these additions actually increased the oxidation kinetics. While the oxidation rate for HfC was found to be parabolic owing to the formation of HfO_2, the kinetics are several orders of magnitude higher than the regime of interest and are not particularly favorable with respect to other nonoxide ceramics.

ELASTIC MODULUS

By the reasoning of Hillig,[48] ceramics should exhibit comparable stiffness on an equal weight basis to superalloys. For a typical nickel-base superalloy, the modulus to density ratio E/ρ is approximately 1.7×10^6 m at 1000°C, where E is about 140 GPa and ρ is in g/cc. The calculated temperatures (T_{max}) for which this specific E/ρ value is reached are shown for several monolithic ceramics in Table 4. Alumina and beryllia would appear to

TABLE 4. Calculated Maximum-Use-Temperature Based on Stiffness[48]

Material	ρ (g/cc)	E_o[a] (GPa)	T_{melt} (°C)	T_{max}[b] (°C)
ThO_2	10.0	180	3220	1117
Al_2O_3	4.0	490	2054	1937
MgO	3.6	350	2825	2637
BeO	3.0	380	2570	2437
AlN	3.3	270	2760[c]	2537[c]
HfC	12.7	410	3827	2927

(a) E_o=Modulus at room temperature, 1GPa = 10^8 kg/m^2
(b) T_{max}=Temperature at which the modulus to density ratio drops to 1.7×10^6 m
(c) AlN decomposes congruently at 2300K

satisfy this criterion up to temperatures approaching their respective melting points, while the more dense and more refractory materials are lower.

STRENGTH

With the exception of carbon and graphite, most polycrystalline ceramics rapidly lose strength at high temperatures (Figure 5). Hillig[48] suggests that the strength in brittle materials should decrease proportionally to the 3/2 power of T/T_{melt} and will be approximately half the room temperature value at 0.5 T_{melt}, where T_{melt} is the melting temperature. Diffusion-controlled processes dominate at high temperatures and grain boundaries play a major role in the deformation process. Thus, impurities or sintering additives can reduce strength or cause the formation of glassy grain boundary phases that lead to a precipitous loss in strength.

While loading conditions will be design specific, a minimum strength requirement of about 150 to 200 MPa will be needed for extended life operation; and higher values (>200 MPa) required for short-duty cycles (5 h/50 cycles).[49] The duty cycle is application and component dependent. In general, engine materials have to withstand the stresses induced by thermal gradients during lift-off, shut-down, and general cyclic use, in addition to

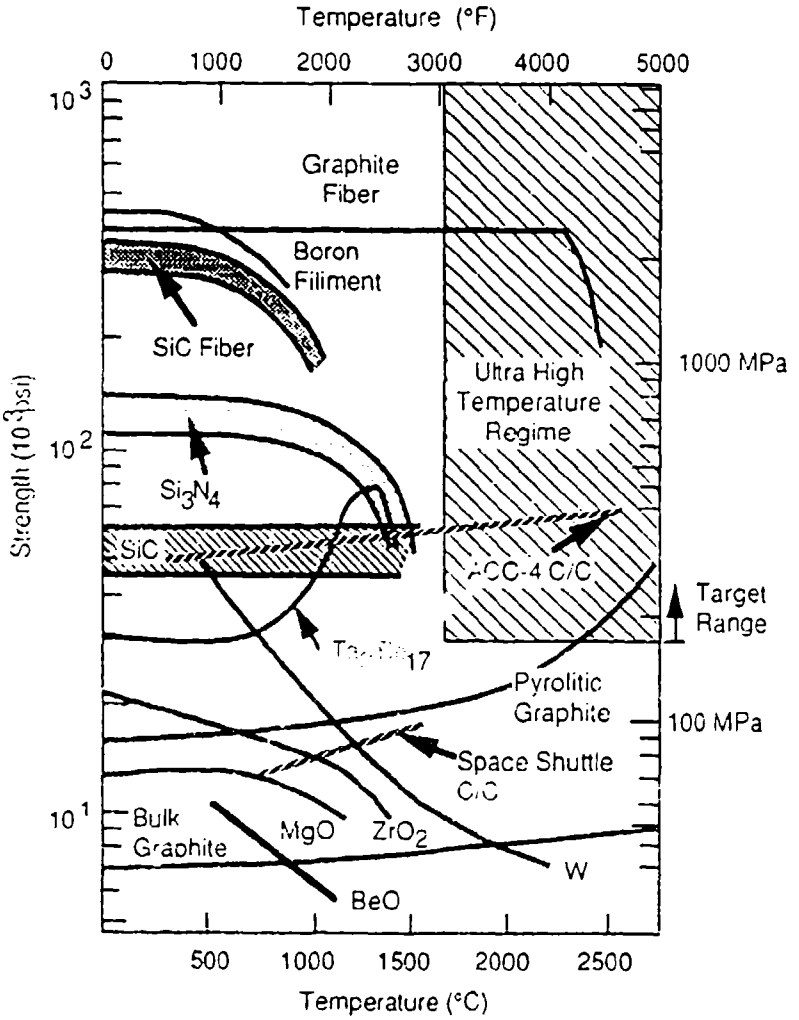

FIGURE 5. Tensile and Flexural Strengths of High-Temperature Materials[19,50,82,167] (Flexure: Si_3N_4, SiC, and Ta_2Be_{17})

the stresses and temperatures of maximum power engine operation.[19] Thermal transients will probably dictate peak stresses in ceramic components. Above 1650°C, a few borides and carbides [e.g., TaC and TiB_2 (Figure 6)] may be capable of meeting these postulated strength requirements in the UHT regime. Solid solution[51] and precipitation[52] hardened zirconia have been shown to exceed 100 MPa at 1400°C in air, but a considerable loss in strength is expected by 1650°C.

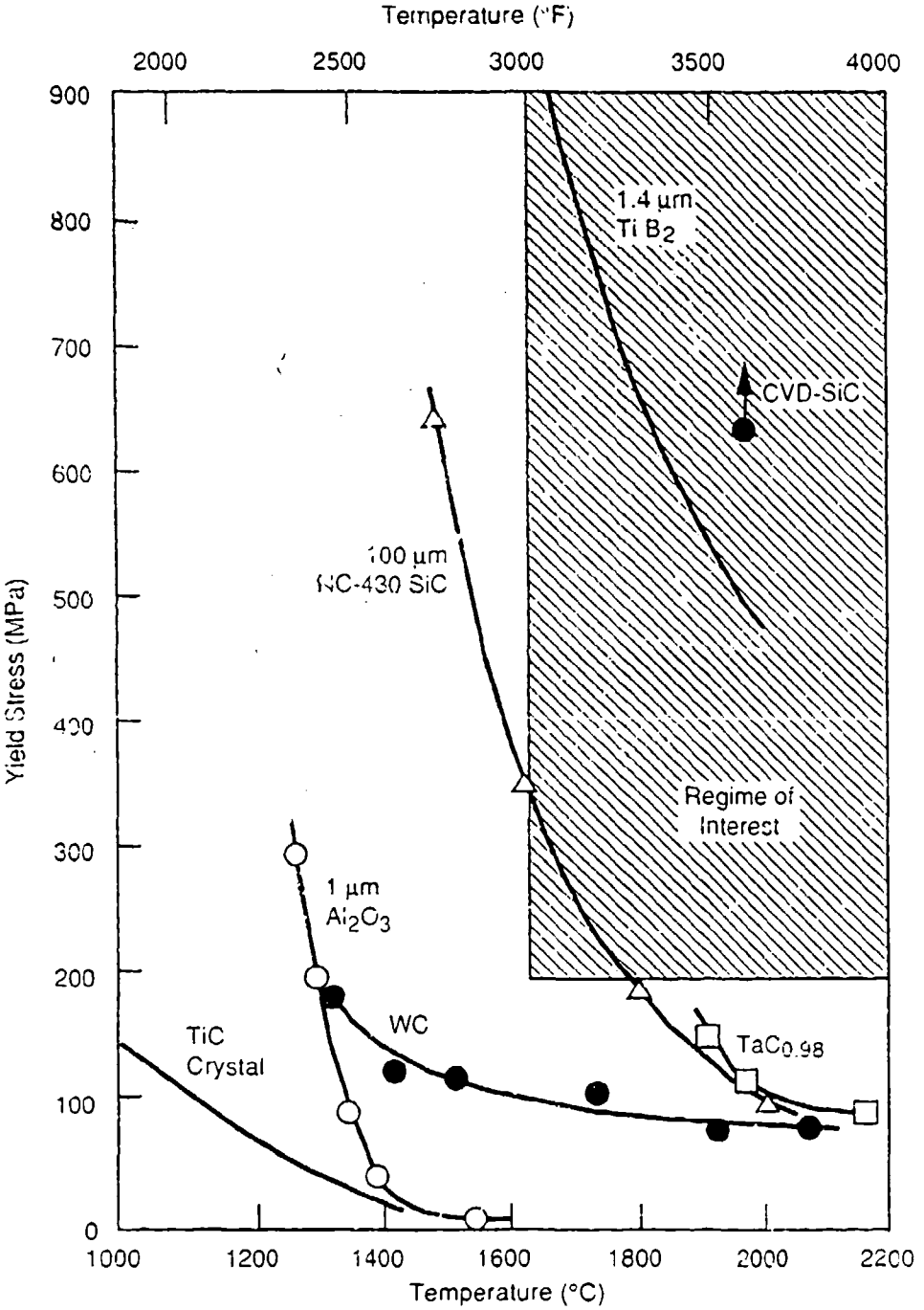

FIGURE 6. Yield Strength Data for Selected Structural Ceramics (Ref. 50)

MATERIALS

In this section, the properties of several classes of ceramic compounds are reviewed relative to performance needs.

BORIDES

Refractory metal diborides have high melting points and high strength retention as a result of strong covalent bonding characteristics. Romberg, Wolfe, and Williams[54] report that the lower bound for plastic yielding in fine grained TiB_2 is on the order of 500 MPa at 1900°C (Figure 6). Such a high strength at this temperature suggests that TiB_2 is a prime candidate for a reinforcement fiber. The physical properties of HfB_2, TiB_2, and ZrB_2 are listed in Table 5. Thermal expansion coefficients vary systematically with melting temperature and size of the transition metal atom.[55]

Oxidation resistance of some borides is surprisingly good despite the formation of a fluid B_2O_3 protective layer. Tripp and Graham[38] performed careful studies on the oxidation behavior of zirconium diboride (ZrB_2), and showed that liquid B_2O_3 glass forms below 1100°C where the oxidation kinetics are parabolic. Above 1000°C, B_2O_3 vaporizes rapidly, thus reducing its effectiveness as a diffusion barrier; and above 1400°C, the rate of vaporization is comparable to the rate of formation. When 20 v/o SiC is added, appreciably more SiO_2 glass is formed in the temperature range between 1100°C and 1300°C.[56] The formation of this glass continues to provide oxidation resistance at higher temperatures due to good wetability and surface coverage.

The Air Force supported extensive studies in the mid-1960s to develop oxidation-resistant refractory metal diborides. The results of this work are summarized in Appendix F. Short-term recession rates on the order of 12 μm/h were reported for HfB_2-20% SiC at 2000°C.[42,57] This may be acceptable for short-duty cycle engines, but is significantly greater than the 0.1 μm/h needed for long-life applications. Simpson and Paquette[58] recently corroborated the oxidation behavior of diborides at high temperatures up to 2000°C and the benefits of SiC additions (Appendix page D.4).

TABLE 5. Physical Property Data for Selected Nonoxides (Ref. 59-62,168)

Material	Temperature, T_m (°C)	Material Density, ρ (g/cm^3)	(E) Young's Modulus (GPa)	Thermal Expansion Coefficient (in/in·°C x 10^6) 20°C	Thermal Expansion Coefficient (in/in·°C x 10^6) 1000°C	Thermal Conductivity (W/cm·°C)	Crystal Structure	Comments: Advantage	Comments: Disadvantage
HfC	3890	12.67	324	4.9	7.2	0.22	FCC	High M.P	Rapid oxidation
SiC	2827	3.21	414	3.3	5.8	0.40	Polytypes	High temp. strength/ Beta-Cubic	Sensitive to impurities SiO_2 former
TaC	3880	14.50	510	5.6	7.3	0.11	Cubic	Good carbon barrier	Rapid oxidation
TiC	3140	4.92	448	6.4	8.9	0.50	FCC	---	---
ZrC	3420	6.56	386	4.0	8.3	0.40	FCC	High M.P.	Rapid oxidation and high creep rate
AlN	2300d[a]	3.26	345	2.6	6.4	0.33	Hexagonal	H.T. strength and	Rapid oxidation and high retentionvapor pressure
BN	2500d[a]	2.28	69	1.8	7.1	0.17	Hexagonal	High temp.	Rapid oxidation strength/toughness
Si_3N_4	1870	3.18	296	0.8	3.7	0.45	Hexagonal	Low CTE,	High vapor pressure SiO_2 former
TiN	2950	5.44	600	5.3	10.4	0.33	Cubic	---	Creep > 1400°C
HfB_2	3250	11.20	---	5.8	7.9	---	Hexagonal	High strength	Rapid oxidation Compatible with SiC
TaB_2	3100	12.60	248	6.5	7.4	0.11	Hexagonal	---	---
TiB_2	2980	4.52	496	7.2	9.2	0.60	Hexagonal	High strength	Rapid oxidation
ZrB_2	3050	6.09	496	5.2	8.2	0.42	Hexagonal	High strength/	Rapid oxidation Compatible with SiC
$MoSi_2$	2030	6.26	379	6.8	9.6	0.49	Tetragonal	SiO_2 former -	Low high temp strength good oxidation
WSi_2	2165	9.87	448	7.2	9.7	0.48	Tetragonal	Good oxidation	--- resistance

(a) decomposes

CARBIDES

Metal carbides are known to have high strength[50] at high temperatures as indicated in Figures 6 and 7. For example, the yield strength for both TaC and pure SiC is approximately 100 MPa at 2000°C. However, the creep resistance for zirconium carbide (ZrC) has been reported to be as low as 10^{-4}/s at 1400°C under a load of 100 MPa.[63] Metal carbides also exhibit brittle to ductile transitions in the range from 1725°C to 1980°C depending on stoichiometry. Additions of boron carbide (B_4C) have been shown to significantly degrade SiC oxidation, and (B_4C) is also incompatible with ZrC,

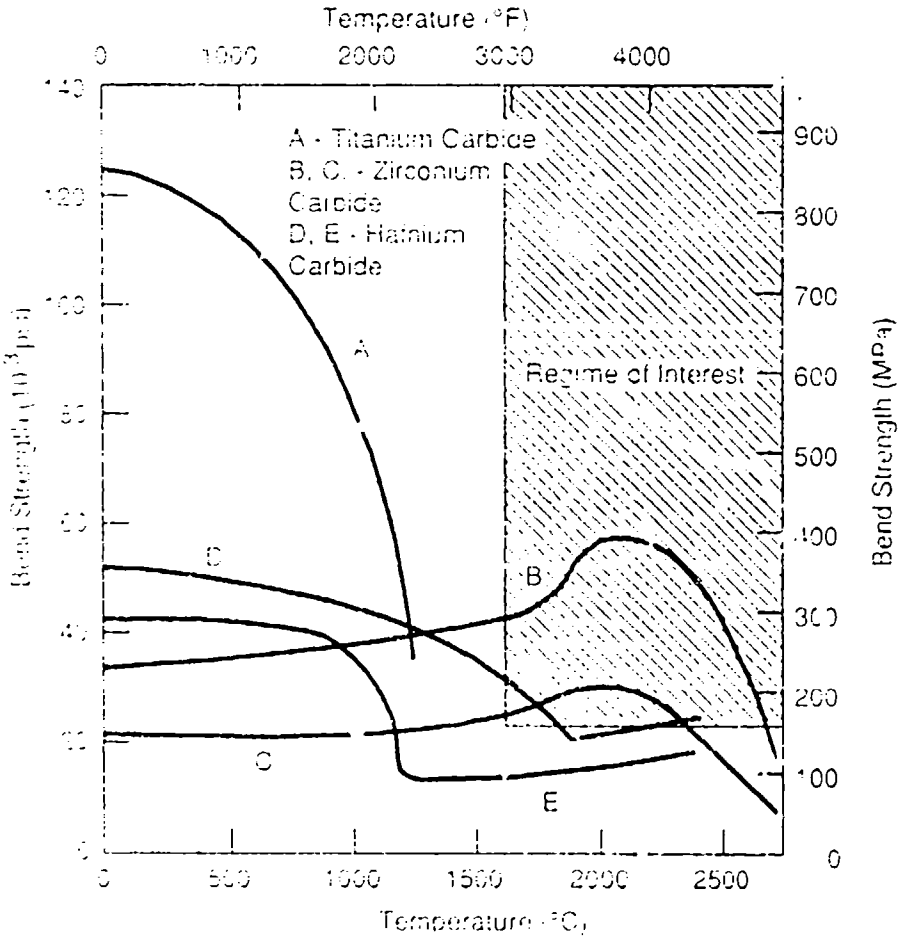

FIGURE 7. Bend Strengths of Titanium, Zirconium, and Hafnium Carbides (Ref. 59)

HfC, and TaC.[64-67] The oxidation of HfC is parabolic and very rapid above 1600°C.[45] At lower temperatures, the scale is not compact, and the kinetics are controlled by gaseous diffusion through the porous scale. Physical properties for HfC, SiC, TaC, TiC, ZrC are listed in Table 5.[59-62]

NITRIDES

Mazdiyasni[68] and DeWith[69] report good room temperature flexure strength for aluminum nitride (AlN) (>300 MPa). Aluminum nitride also shows good strength retention to about 1200°C. The elastic modulus is high (~320 to 340 GPa at room temperature), but fracture toughness is relatively poor, about 2.7 Mpa $\sqrt{m}$. Flexural strengths for hot-pressed BN/AlN composites are almost a factor of two below that for unreinforced AlN at room temperature, but strengths are maintained to 1500°C with little or no decrease.[68] The oxidation resistance of AlN is equivalent to borides and carbides (see Figure 3), but is not as good as Si_3N_4 or SiC.[39] At temperatures above 1500°C, the protective Al_2O_3 scale shows a tendency to crack due to the evolution of nitrogen which causes rapid degradation.

Silicon nitride has been extensively studied for advanced automotive gas turbine engine applications.[70] Hot-pressed silicon nitride (HPSN) exhibits excellent strength at room temperature, but loses strength rapidly above 1000°C. Reaction-sintered silicon nitride (RSSN) has been improved over the years by controlling the processing methods and currently has better strength retention with increasing temperature than HPSN due to its higher purity. The creep rate of RSSN is on the order of 10^{-8}/s at applied stresses up to 300 MPa and temperatures of 1500°C, which is also superior to HPSN. The oxidation resistance of Si_3N_4 is limited to temperatures below the point (1730°C) where the nitrogen partial pressure exceeds 1 atm[40] and disrupts the protective SiO_2 scale. Several authors[39-41] have reported that the oxidation resistance of SiC is slightly better than that of Si_3N_4 except at low temperatures (Figure 5). Both hot-pressed and reaction-sintered silicon nitride are heavily doped with other cations to improve fabricability, and these additions can diffuse rapidly in the bulk to decrease the protective properties of the SiO_2 scale.

Luthra[71] has suggested, on the basis of thermodynamic arguments, that the oxidation kinetics of Si_3N_4 are controlled by a combination of oxygen diffusion through the SiO_2 scale and an interface reaction that forms silicon oxynitride. Du, Tressler, Spear, and Pontano[72] performed careful experiments that confirm the formation of a duplex scale on Si_3N_4 consisting of SiO_2 and an inner layer of Si_2N_2O.

For SiC_2-forming systems, conditions could exist under which a protective SiO_2 layer does not form. This occurs when a low flux of oxygen resulting from exposure to a reduced total pressure or a dilute oxygen concentration (low partial pressure) in an inert carrier gas is insufficient to support the formation of a protective oxide. This active (versus passive) oxidation behavior was first reported by Wagner,[73] who observed that a clean silicon surface would rapidly react with a low oxygen flux to form SiO molecules instead of a protective SiO_2 film. The regime of active oxidation for SiC and Si_3N_4 was studied by Hinze, Tripp, and Graham.[74,75]

SILICIDES

While several refractory silicides have melting points as high as 2500°C, molydisilicide ($MoSi_2$) and titanium silicide (Ti_5Si_3) appear to be the best choice for structural applications in the 1000°C to 1600°C range.[76] Possible reinforcements include titanium diboride (TiB_2), zirconium diboride (ZrB_2), silicon carbide (SiC), and aluminum oxide (Al_2O_3). There is a pronounced exchange reaction of Ti_5Si_3 with ZrB_2, but not with TiB_2. Titanium silicide (Ti_5Si_3) exhibits a tensile strength of 350 MPa at 1200°C with strains to failure on the order of 7%, which is unusually high ductility for a ceramic. Molybdenum disilicide grows a self-healing scale that is protective for up to 3000 hours at 1700°C.[77] Early work with $MoSi_2$[78] reported accelerated low-temperature oxidation due to a phenomenon called "pest oxidation." This term is used to describe a process whereby rapid oxidation, sometimes localized at grain boundaries, occurs at a low temperature even though the same material may exhibit excellent oxidation resistance at higher temperatures. The phenomenon occurs in many compounds and intermetallics, and is not well understood.[79] Recent work suggests that pest oxidation does not occur in $MoSi_2$ of high density and purity.[80]

BERYLLIDES

The most refractory beryllides are lightweight intermetallic compounds with large beryllium contents (e.g., $Be_{12}M$ and $Be_{17}M_2$) where M can be Zr, Nb, Ta, or Y. These intermetallics are characterized by high hardness and modulus, but modest melting points in the range of 1800°C to 2000°C.[81] They exhibit good strength retention to high temperatures (e.g., 178 MPa at 1500°C) and display the unusual behavior of increasing strength with increased temperature (Figure 5).[82] It is not clear whether this unusual strength versus temperature behavior is an inherent property or a manifestation of porosity in the test specimens, which sinter to higher densities during the testing process.

The beryllides have low specific gravity due to their very high beryllium content, but the thermal expansion coefficient is very high and thermal shock resistance may be questionable. Beryllides reportedly have good oxidation resistance to at least 1500°C (Figure 4) as a result of a compact BeO film formation,[83,84] although there is some concern that degradation occurs in the presence of moisture. The beryllium intermetallics would appear to have a potential use-range between 1400°C and 1600°C if strength and oxidation behavior can be confirmed and if creep resistance, for which there are few data, is acceptable.

OXIDES

Several refractory oxides with high-temperature melting points (e.g., MgO, CaO, and Cr_2O_3) exhibit high evaporation rates or produce high vapor pressures when reacting with oxygen, and are therefore unsuitable for structural applications. A few refractory compound oxides (e.g., zirconates and hafnates) also suffer high volatility loss[36,85,86] and exhibit excessive grain growth,[36,85] thereby eliminating these compounds from consideration. La_2O_3, MgO, and CaO, are also hygroscopic and are subject to structural degradation if exposed to atmospheric moisture[85,87] (Appendix pages A.9, B.9).

Most polycrystalline oxides exhibit relatively low strength and creep resistance at high temperatures.[88] Despite these shortcomings, oxides remain the preferred choice for high temperature composite systems because of

intrinsic environmental stability in oxidizing atmospheres. The physical properties of several refractory oxides that have potential applications in UHT composite systems are presented in Table 6. These data, together with those in Table 4, were collected from a variety of sources and reviews.[60-62,89] The single-crystal oxides with the best high-temperature strengths are shown in Figure 8,[90] but new work that is currently being performed on yttrium aluminum garnet and oxide eutectics suggests that these materials may have potential for even better strength retention at high temperatures.

TABLE 6. Physical Property Data for Selected Oxides (Ref. 60,61,89,168)

Material	Temperature, T_m (°C)	Material Density, ρ (g/cm^3)	(E) Young's Modulus (GPa)	Thermal Expansion Coefficient (in./in. °C x 10^6) 25°C	1000°C	Thermal-Conductivity (W/cm °C)	Crystal Structure	Comments: Advantage	Comments: Disadvantage
Al_2O_3	2040	3.98	443	5.4	9.9	0.38	Hexagonal	Low O_2 perm.	Low M.H.T.
BeO	2570	3.01	400	6.3	11.6	2.20	Hexagonal Low O_2 Perm.	Low density too toxic	Moisture susceptible
CaO	2610	3.32	---	11.2	11.2	0.29	Cubic (Rock Salt)	---	High vapor pressure Moisture sensitivity
CeO_2	2615	7.28	169	9.5	14.1	0.12	Cubic	---	---
Cr_2O_3	2270	5.21	---	8.8	7.6	---	Hexagonal	---	High vapor pressure
HfO_2	2845	9.68	---	3.8	9.7	0.17	Cubic (Flourite)	Low vap. pres./ H.T. phase trans.	Low O_2 permeability
La_2O_3	2540	6.57	---	10.8	---	---	Hexagonal	---	Moisture sensitivity
MgO	2800	3.58	387	10.2	15.7	0.63	Cubic (Rock Salt)	---	Moisture sensitivity High vapor pressure
Pr_2O_3	2485	6.32	---	7.8	9.2	---	Cubic	---	High vapor pressure
Sc_2O_3	2480	3.84	225	6.6	11.3	0.08	C-Type R_2O_3	High strength?/ creep?	---
SiO_2	---	2.32	74	0.5	---	0.01	Fused	Low O_2 perm./ Low CTE	Low viscosity at H.T.
SrO	2455	4.70	---	1.14	1.14	---	Cubic (Rock Salt)	---	High vapor pressure
Ta_2O_5	2155	8.02	---	---	6.6	---	Orthorhombic	Glassy	---
ThO_2	3220	9.86	253	7.7	10.6	0.14	Cubic (Fluorite)	Very high M.P./ Low vap. pres.	Radioactive
TiO_2	1850	4.25	288	7.5	10.5	0.11	Tetragonal	---	Poor oxidation Low temperature
UO_2	2840	10.96	204	9.4	12.0	0.13	Cubic	---	Density/Radioactive

TABLE 6. (contd)

Material	Temperature, T_m (°C)	Material Density, ρ (g/cm^3)	(E) Young's Modulus (GPa)	Thermal Expansion Coefficient (in./in. °C x 10^6) 25°C	1000°C	Thermal-Conductivity (W/cm °C)	Crystal Structure	Comments: Advantage	Comments: Disadvantage
Y_2O_3	2420	5.03	169	7.3	9.2	0.17	C-Type R_2O_3	Low O_2 Perm./ No Phase Trans.	H.T. Creep
ZrO_2	2765	5.83	253	8.8	10.5	0.17	Cubic (Flourite)	Env. Stable/ Low Vap. Pres.	L.T. Phase Trans./ High Oxygen Perm./ Thermal Shock
$CaHfO_3$	2470	6.05	---	---	---	0.096	Tetragonal	---	High Vap. Pres./ Grain Growth
$CaZrO_3$	2325	4.76	---	7.9	13.9	0.035	Monoclinic	---	High Vap. Pres./ Not Stable/ Grain Growth
HfO_2 (Y_2O_3)	2400	9.70	---	---	---	---	Cubic	No Phase Trans./ Env. Stab.	Very High O_2 Perm./ Thermal Shock
$LaCrO_3$	2510	---	---	---	8.5	---	Cubic	---	---
$MgO{\cdot}Al_2O_3$	1995	3.59	239	7.0	10.6	0.12	Hexagonal	Light Wt./ High Flow Stress	H.T. Strength/Low O_2 Perm/Ductive Brittle Trans.
$3Al_2O_3$ $2SiO_2$	1850	3.20	148	---	5.0	0.06	Cubic	Good Strength/ Toughness/Thermal Shock	Not Compatible with Al_2O_3
$SrZrO_3$	2650	5.48	84	0.75	1.21	0.027	Orthohombic	---	High Vap. Pres./ Segregates in O_2 grad.
ZrO_2	2800 (Y_2O_3)	5.6-6.1	294	---	10-13	---	Cubic	---	---
$La_2Hf_2O_7$	2285	8.02	---	---	~8	0.19	---	No Phase Trans. Low Vap. Pres.	Moisture Sensitive?
$Y_3Al_5O_{12}$	1995	4.55	----	---	---	---	---	---	---

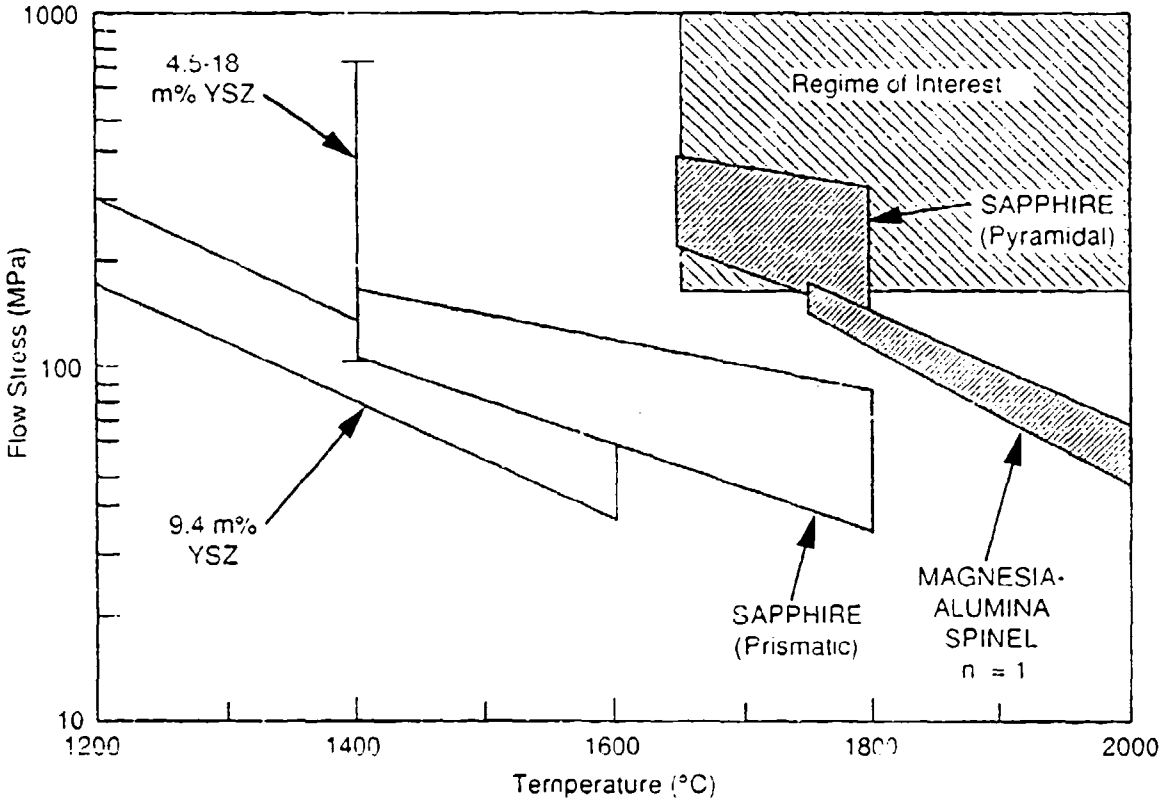

FIGURE 8. Flow Stress vs. Temperature for Single-Crystal Sapphire, Magnesia-Alumina Spinel, and Zirconia (Ref. 90)

REINFORCEMENTS

Properties of several ceramic fibers, some of which are under development as commercial reinforcement materials for composite applications, are listed in Table 7. Tensile strengths and elastic moduli at room temperature are typically very high and in the desirable range for a reinforcing medium. Pysher and Tressler [91,92] report that fiber tensile strength and modulus decrease significantly above 1000°C as shown in Figures 9 and 10. With the exception of carbon, and perhaps CVD silicon carbide, the creep rates for commercially available fibers are also too high (Figure 11).

Although creep in polycrystalline oxide fibers is significantly higher than the 10^{-8}/s rate needed for long-life structural applications, single-crystal oxides are more promising (Figure 12). For example, c-axis sapphire exhibits a creep rate of about 10^{-7}/s at 1750°C and 100 MPa. Recent results from one of the Air Force sponsored UHT programs[25] indicates that the creep rate of $Y_3Al_5O_{12}$ (YAG) is almost an order of magnitude lower (see Appendix page C.2). Yttrium aluminum garnet is cubic, and the absence of a crystallographic orientation dependence is a significant advantage for off-axis loading conditions.

Chrysoberyl ($BeO \cdot Al_2O_3$) also exhibits excellent compressive creep resistance, $<7 \times 10^{-9}$/s at 1820°C and 280 MPa.[93] Limited compressive creep testing performed on c-axis BeO indicated that the creep strength in the c-axis orientation is very high (too high to measure), but specimens tested along the [1011] axis crept severely (Appendix C.1, page C-3). Anisotropic behavior of creep and other mechanical properties could pose problems in the design and engineering of practical composite systems.

Many proposed fibers and reinforcements are also not thermochemically compatible with the host matrices. Weak interfacial bond strength is desirable if toughness is the major consideration. Interface reactivity is generally not desirable. To optimize composite properties, considerable attention is directed at either modifying or coating fiber surfaces. For example, the SCS-6 fiber developed by Textron has a 3 μm outer SiC layer which

TABLE 7. Room Temperature Properties for Ceramic Fibers of Potential Use in Advanced Composites (Ref. Mfg. Data Sheets)

Manufacturer	Fiber Designation	Composition (wt%)	Tensile Strength (GPa)	Modulus (GPa)	Density (g/cc)	Nominal Diameter (μm)
Several	High Modulus	C	2.0-2.5	300-500	1.7-1.8	6-10
Several	High Strength	C	2.5-4.0	200-300	1.8-1.9	6-10
Nippon Carbon	Nicalon					
	HVR	59 Si, 31 C, 10 O	2.5-3.3	180-193	2.35	13-16
	Ceramic Grade	59 Si, 31 C, 10 O	2.5-3.3	193-207	2.55	13-16
	Low Oxygen	63.5 Si, 36 C, 0.5 O	2.75	262	2.75	13-16
Ube	Tyranno	Si, Ti, C, O	3.0	220	2.3-2.5	8-10
Dow Corning	HPZ	59 Si, 10 C, 28 N, 3 O	2.4-3.1	186	2.41	10-12
Dow Corning	SiC	>99 SiC, Beta Trace Alpha	2.3 max	414	3.1	8-12
Textron	SCS-6	CVD SiC on carbon	3.9	406	3.0	143
3M	Nextel 312	62 Al_2O_3 24 SiO_2 14 B_2O_3	1.725	138	2.7	10-12
3M	Nextel 440	70 Al_2O_3 28 SiO_2 2 B_2O_3	2.07	186	3.05	10-12
3M	Nextel 480	70 Al_2O_3 28 SiO_2 2 B_2O_3	2.24	221	3.05	10-12
3M	Nextel 550	73 Al_2O_3 27 SiO_2	2.0	193	3.03	10-12
Sumitomo	Altex	85 Al_2O_3 15 SiO_2	1.8-2.6	210-250	3.2	9-17
Dupont	FP*	>99 αAl_2O_3	1.4	385	3.9	20
Dupont	PRD-166*	Al_2O_3 15-25 ZrO_2	2.1-2.4	385	4.2	20
Mitsui Mining	Almax	99.5% Al_2O_3 Polycrystalline	1.77	323	4.0	10
3M	Nextel 610	>99% Al_2O_3	1.90	373	3.75	10-12
Saphikon	Sapphire	Al_2O_3 single crystal	2.8-3.4	435	3.9	25

*Not currently in Production

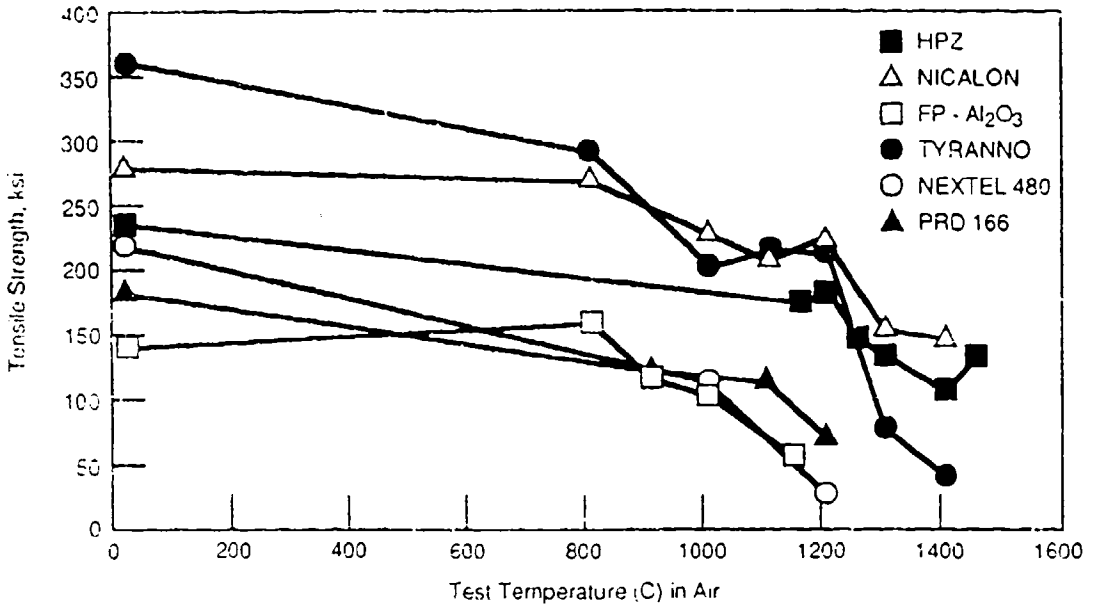

FIGURE 9. Short-Term Strength of Some Ceramic Fibers (Refs. 91,92)

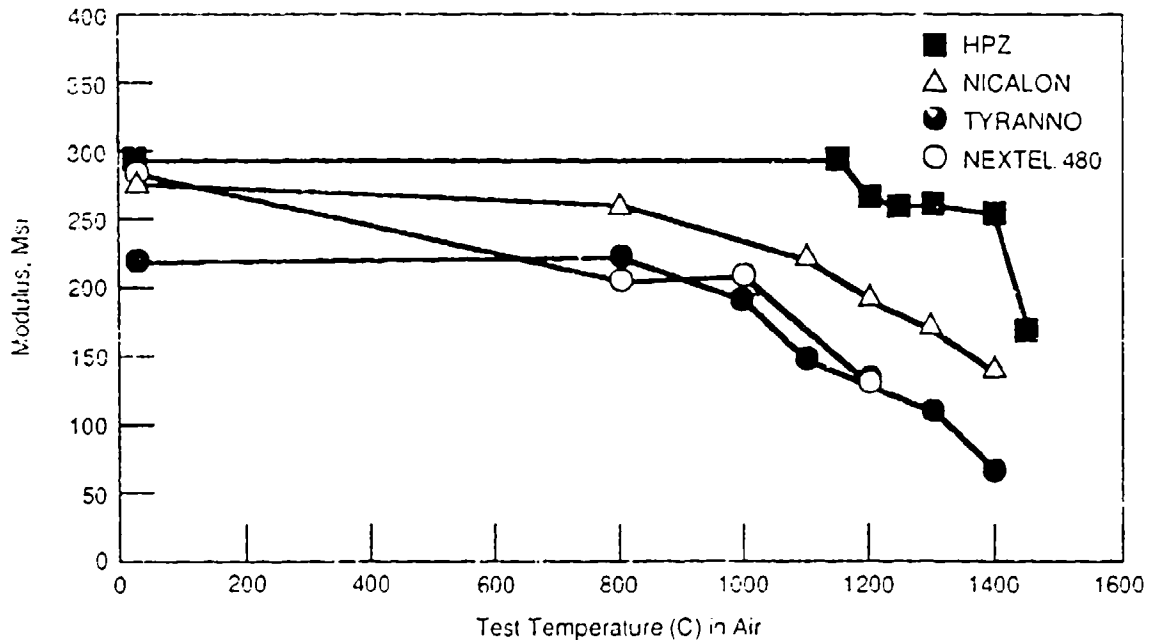

FIGURE 10. Fiber Tensile Modulus Tested at Temperature in Air (Refs. 91,92)

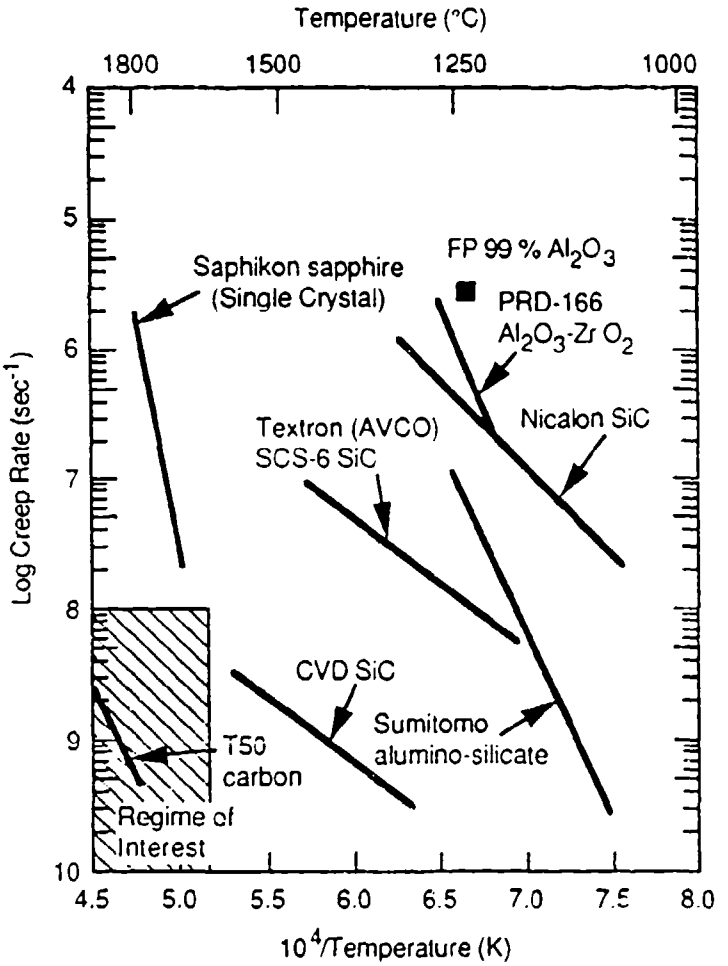

FIGURE 11. Creep Behavior of Several Commercial Fibers at an Applied Stress of 100 MPa (Refs. 96-101)

is carbon-rich relative to the underlying SiC.[94] This carbon-rich layer is designed to protect the fiber from strength degradation and to enhance thermo-chemical compatibility with matrices that might otherwise strongly react with SiC. Coatings on small diameter fibers are very difficult to apply in a consistent manner. A protective coating must be of high quality and very thin, approximately 1 μm. If the fiber is oxygen sensitive, the coating must also serve as an oxygen barrier. Since very little reaction by the underlying fiber is acceptable, oxygen permeability through a coating needs to be

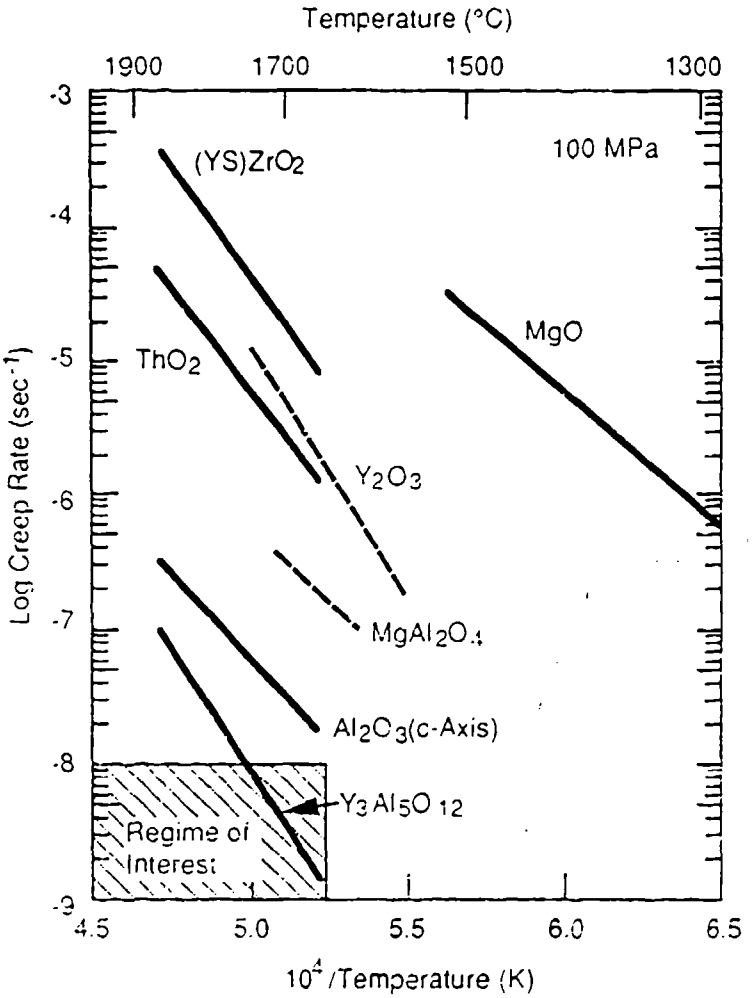

FIGURE 12. Creep Behavior of Several Single-Crystal Oxides (Ref. 102-106)

10^{-12} g O_2/cm•s or lower.[34] Luthra and Park[95] (Appendix page A.11) experimentally demonstrated the importance of oxygen diffusion in compatibility experiments between C/Al_2O_3 and C/Y_2O_3. Both oxides are chemically compatible with carbon in an inert atmosphere. However, when these materials are exposed to an oxygen environment at 1650°C, very high gas pressures develop at the carbon/oxide interface as a result of rapid oxygen permeation through the oxide phase.

PROSPECTIVE COMPOSITES

This section evaluates a few selected composites divided into three reinforcement/matrix categories: nonoxide/nonoxide, oxide/oxide, and nonoxide/oxide.

NONOXIDE/NONOXIDE COMPOSITES

Refractory metal diborides alloyed with 20 v/o SiC particulates[57] show good mechanical properties and some short-term oxidation resistance at high temperatures even in flowing gas environments (see Appendices D and F for discussion). If carbon is added, fracture toughness and thermal shock resistance are improved. These systems develop protective boria-silica or silicate glass scales that are effective in preventing catastrophic or runaway oxidation at very high temperatures (up to 2000°C) for short periods of time (less than 1 hour).

Richerson, Stuffle, and Griffen[107] have attempted to reinforce SiC (Ti, Hf, Zr)B_2 with SiC and carbon fibers. The best compatibility was achieved with AVCO SCS-6 SiC which exhibited little reaction with the diborides up to the 2000°C hot pressing temperature. A composite system composed of ~30 v/o (SCS-6) in a SiCp/HfB_2 matrix was reported to exhibit flexure strengths as high as 1000 MPa at room temperature. Oxidation resistance at 1600°C in static air showed weight-gains on the order of 0.6% to 5.0% (no rates were given). Although high-temperature mechanical properties have not yet been measured, this composite displays potential for very good high-temperature strength and possibly creep resistance. However, long-term oxidation resistance would have to be improved by the application of a suitable protective coating.

Composites made of SiC/SiC have received a great deal of attention for applications in gas turbines and heat exchangers. As shown in Table 7, commercially available silicon carbide fibers are impure and are either amorphous or two phase. It is also difficult to achieve full densification with a SiC matrix, and most composites exhibit some open porosity with total porosities ranging from 15% to 25%. Considerable effort is being directed towards chemical vapor infiltration (CVI) under controlled temperature

gradients to enhance densification and to minimize the need for repeated, time consuming infiltrations.[109] Other techniques include forced flow and pulse methods where the reactants are cyclically forced into the preform by pressurization.[110]

Room temperature bend strengths close to 350 MPa for two-dimensional SiC_f/SiC laminates and 700 MPa for one-dimensional (uniaxial) reinforcement have been reported for as-fabricated material.[108] Incompletely dense composites exhibit bend strengths on the order of 100 MPa up to 1500°C.[108] Room temperature fracture toughness is also good with values ranging between 12 and 18 MPa $\sqrt{m}$, although the low density may in part be responsible for the good toughness. Rapid loss of composite strength occurs around 1100°C, which is characteristic of state of the art SiC fibers (see Figure 9). This is not a fundamental limit as pure SiC has the potential for very high intrinsic strength (Figure 6).

Oxidation behavior will depend on the thermochemistry. As silicon is depleted to form a protective SiO_2, carbon may be precipitated in the matrix, thereby increasing the carbon activity. This would lower the temperature at which disruptive gas bubbles form to about 1585°C.[110] In addition, mass loss by evaporation could exceed 0.1 $\mu m/h$ above 1600°C, but parabolic oxidation rates do not exceed 10 $\mu m^2/h$ below 1730°C. While it is doubtful that SiC composites could be used in extended life applications in oxidizing atmospheres at temperatures much higher than 1600°C, SiC/SiC may have utility in short term exposures at temperatures up to 1750°C. Chemical vapor infiltrated carbon/SiC is being developed commercially because high-temperature strength is more promising than for Nicalon/SiC. The addition of SiC as the matrix phase or as a co-woven fiber helps to obtain a better CTE match and also provides improved compatibility with oxidation resistant coatings.[111] Carbon/SiC composites have successfully survived for short periods (20 to 40 s) in arc plasma tests to 2360°C.[112]

Silicon carbide reinforced Si_3N_4 is of interest in automotive turbines for improved high-temperature strength and toughness. Although the high-temperature properties of monolithic Si_3N_4 have improved dramatically since 1976,[113] and sinterable, net-shaped components with good high temperature

strength retention (~500 mPa at 1400°C) can now be produced, the high-temperature strength of Si_3N_4 drops below for SiC above 1400°C. Silicon nitride reinforced with 30 v/o SCS-6 exhibits linear elastic strength properties comparable to monolithic material, but with continued load support after matrix cracking, and flexural strength at 1370°C is 365 MPa, which is on the order of 60% of the strength of the same material at room temperature.[113] The oxidation behavior of Si_3N_4 is comparable to SiC (see Figure 3); however, dissolution of densification aids can significantly increase oxygen permeability in the SiO_2 scale.

A new commercially available platelet-reinforced ceramic, Lanxide PRC™,[114,115] consists of a refractory zirconium carbide (ZrC) matrix reinforced with zirconium diboride platelets and can contain up to 30 v/o zirconium metal continuously dispersed as a grain boundary phase [ZrB_2pl/ZrC(Zr)]. The metal phase imparts good thermal shock resistance, and room-temperature fracture toughness values as high as 16 to 18 MPa $\sqrt{m}$ have been reported.[114] Flexural strengths at room temperature are in the range of 1800 to 1900 MPa. Creep resistance may be poor due to the metal (Zr) phase in the grain boundaries. The high-temperature oxidation resistance of this material is unknown, but could be enhanced by a siliconized coating.

A SiC/$MoSi_2$ composite would be expected to have good high-temperature oxidation resistance. If the interface sequence $SiO_2/MoSi_2/Mo_5Si_3/SiC$ forms, the silicon activity in the $MoSi_2$ is reduced to a low value corresponding to equilibrium coexistence of the two moly-silicides. This should effectively lower the interfacial SiO(v) pressure. The intermediate Mo_5Si_3 would provide a barrier to carbon transport, thus reducing the carbon activity (and CO pressure) at the $SiO_2/MoSi_2$ interface. Additions of 20% SiC whiskers have been shown to impart toughness (~8 MPa $\sqrt{m}$) to the molybdenum disilicide at room temperature where $MoSi_2$ is brittle, and to provide increased strength at elevated temperatures.[17] Both pure $MoSi_2$ and the 20 vol% SiC whisker-$MoSi_2$ matrix composites exhibited significant plastic deformation in bending, with the pure $MoSi_2$ generally showing more ductility than the composite.[116] The composite yield strength at 1400°C is about 20 MPa, which is nearly four times that of pure $MoSi_2$.

OXIDE/OXIDE COMPOSITES

An oxide fiber-reinforced refractory oxide matrix is the most attractive composite system from the standpoint of high-temperature resistance to oxidation. The two oxides chosen must be chemically compatible and have adequate thermal stability. To achieve the desired strengthening effect, the fiber or whisker phase should have a higher elastic modulus and better creep resistance than the matrix. To achieve toughness, which may be the more important criterion, a weak interface between the phases is required so that cracks do not easily propagate from the matrix into the fiber.

Although most oxide systems are expected to be stable in an oxygen environment, compound oxides that are used as one phase of a two-component composite system, or that form at an interface, can demix in the presence of an oxygen gradient. Schmalzried and Laqua[117] defined the conditions that lead to demixing of homogeneous solutions or compound oxides in an oxygen potential gradient. If a stable ternary oxide, ABO_x, is subjected to an oxygen gradient, and if the diffusion coefficient D_A is $> D_B >> D_O$, the crystal enriches in AO at the side of the higher oxygen potential. Demixing can also occur in a nonoxide/oxide composite as the nonoxide reinforcement serves as an internal oxygen sink.

Studies of alumina-YAG[118] (Appendix B) funded by the Air Force UHT program suggest that this oxide composite can be produced by eutectic solidification, and may have structural promise if the lamellar Al_2O_3 structure can be controlled to impart adequate toughness. The eutectic composition appears to be stable to at least 1650°C. Li and Bradt[119] developed methods for calculating micromechanical stresses in composites and were able to determine the residual stress for two orientations of anisotropic sapphire whiskers and for isotropic alumina fibers in a YAG matrix as a function of L/d shown in Figure 13. The stresses in polycrystalline alumina fibers in a YAG matrix are on the order of -250 MPa (compressive) in the axial direction. This value is intermediate to the strengths in the < 1210 > and < 0001 > sapphire single-crystal orientations. Similar stress calculations for alumina single-crystal whiskers in a mullite matrix show much higher stress levels in tension

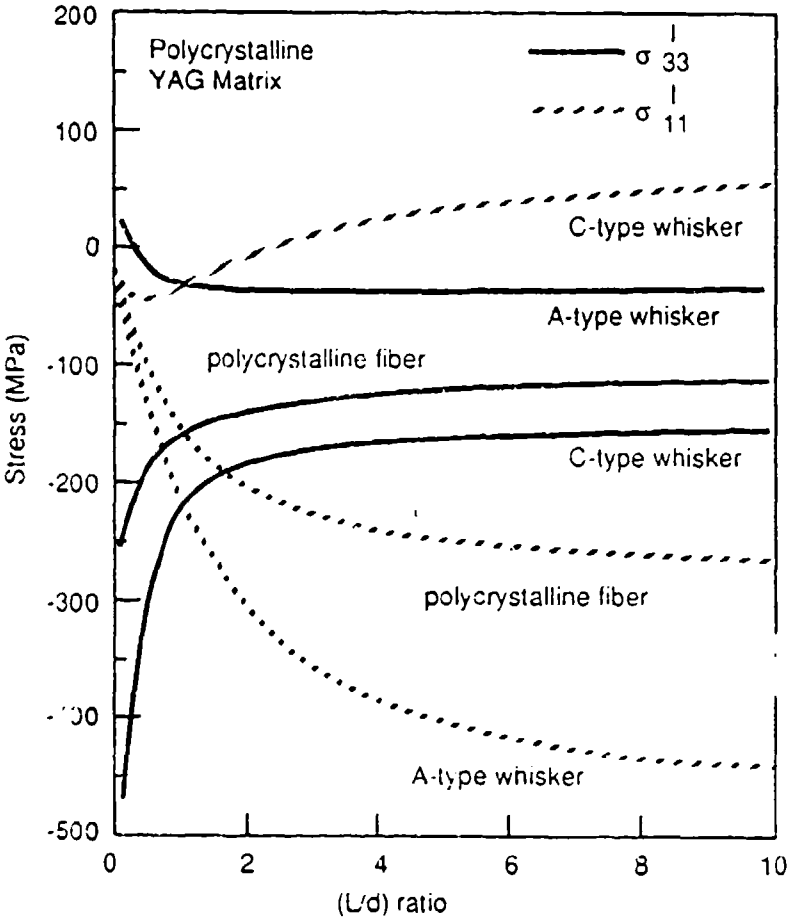

FIGURE 13. Residual Stress of Anisotropic Sapphire Whiskers and Isotropic Alumina Fibers in a YAG Matrix (Work of Li and Bradt, Ref. 119)

(~500 MPa), which are consistent with observed fiber microcracking. These calculated results corroborate the experimental findings of Mah[87] and confirm that $Al_2O_{3(w)}$/mullite is not a viable composite system.

Another oxide matrix candidate for an Al_2O_3-reinforced composite is lanthanum chromite ($LaCrO_3$) (see Appendix B for discussion). Mackenzie and Ono[120] reported some diffusional interaction between the $LaCrO_3$ and Al_2O_3 after 72 hours in air at 1600°C. It was not clear whether the extent of this reaction is sufficient to cause interfacial degradation. Lanthanum chromite exhibits appreciable CrO_3 vapor pressure above 1400°C,[121] thus a coating would be required to minimize weight-loss. MacKenzie and Ono[120] demonstrated

that an alumina coating reduces $LaCrO_3$ weight-loss by a factor of six. Thermal expansion compatibility between $LaCrO_3$ and Al_2O_3 is not currently known.

Lanthanum hafnate ($La_2Hf_2O_7$) is another oxide compound of interest. It has a pyrochlore (distorted fluorite) structure and exhibits several very attractive properties (e.g., the compound congruently melts at approximately 2300°C with low mass evaporation loss even after 8 hours at 1925°C).[122] Lanthanum hafnate also has one of the lower oxygen permeability constants reported for mixed oxides, and does not segregate in an oxygen gradient at high temperatures.[34] The chemical and thermal expansion compatibility between Al_2O_3 and $La_2Hf_2O_7$ is not currently known.

Composite systems consisting of Al_2O_3 reinforcement in matrices of alumina, hafnium, zirconia or yttrium aluminum garnet are of potential interest. However, the Al_2O_3/ZrO_2 transformation-toughened (partially stabilized zirconia PSZ) materials have generally been studied at temperatures lower than the UHT regime.[18] Weddell[123] reports that Al_2O_3 forms a liquid phase with both zirconia and hafnia at approximately 1865°C (see Appendix A). Composites of Al_2O_3/ZrO_2 or Al_2O_3/HfO_2 would probably be limited to applications at operating temperatures around 1400°C due to both strength and creep considerations.

Selected composite systems in which the reinforcement phase and the matrix are composed of the same material (e.g., Al_2O_3/Al_2O_3 or YAG/YAG) may prove useful. The interface between phases will be formed from low angle grain boundaries as opposed to the interphase boundaries predominantly found in most composite systems.[9] While it is usually beneficial for the reinforcement phase to exhibit higher stiffness $Ef/Em > 2$ to enhance load transfer, similar benefits may be imparted through single crystals that exhibit highly directional properties.

Solute additions may also be useful if controlled segregation to the reinforcement/matrix interface can be used to increase interface energy and, hence, preferentially reduce rupture strength.[9] It may be possible, in this way, to engineer the interface between phases and thereby achieve enhanced toughening. The achievement of high density and good interface contact during fabrication could present problems, although the directed metal oxidation

process, Dimox™, developed by Lanxide Corp., offers a particularly attractive approach to producing dense Al_2O_3/Al_2O_3 with low-angle grain boundary interfaces.

A major concern associated with the use of oxide/oxide composites is their poor thermal shock resistance. Thermal shock failures have been observed at heat flux levels as low as 136 Btu/ft^2•s for yttria-stabilized zirconia compared to heat flux thresholds on the order of 250 and 750 Btu/ft^2•s for refractory diboride and hypereutectic carbides, respectively.[124] The material properties that generally determine thermal shock resistance in ceramics are tensile strength, modulus of elasticity, Poisson ratio, coefficient of thermal expansion, thermal conductivity, and thermal emissivity. For a composite system, the volume fraction of fibers or whiskers that constitutes the reinforcing phase, the material properties of the reinforcement, and the matrix porosity will also be factors. A two-phase composite, in which one phase has a higher Young's modulus than the other, may be more resistant to thermal shock damage. This is due to a potential decrease in the elastic energy stored at fracture coupled with potential increases in the effective surface energy required for crack propagation.[125]

NONOXIDE/OXIDE COMPOSITES

The thermochemical stability of refractory diboride reinforcements in an oxide matrix is of concern where the composite is exposed to an oxygen atmosphere. For example, Vedula[126] (Appendix page A.17) shows that zirconia and yttria matrices do not prevent the oxidation of imbedded diboride particles above 1650°C. Thermodynamically compatible systems such as HfB_2/ZrO_2 [this pair also exhibits a complementary CTE match[123]], or TiB_2, HfB_2, and ZrB_2 with ThO_2[127] will degrade due to high oxygen permeability in the matrix. Oxidation of SiC/ZrB_2-(Y_2O_3) produced a very frothy and nonprotective YBO_3 reaction product,[128] (Appendix page B.2).

Even stable refractory oxides with very low negative Gibbs free energy of formation are not always stable in the presence of a nonoxide at high temperatures. For example, when a $HfO_2/HfSi_2/HfB_2/HfO_2$ composite was reacted at 1800°C, a product layer formed at the oxide silicide interface and its

growth was parabolic with time (see Figure D.1). The composite system TiB_2/Al_2O_3 showed significant reactivity at temperatures below 1650°C.

Clearly, refractory diboride-reinforced oxide matrix composites have little potential as structural materials in oxidizing environments. Oxygen permeability through the oxide matrix results in diboride oxidation, and the oxidation products react with the matrix to produce further degradation.

Composites made with SiC whiskers or particles in Al_2O_3, mullite, and magnesia aluminate have received considerable attention, and $SiC_{(p,w)}/Al_2O_3$ composites are produced in commercial quantities. However, the permeation of oxygen through even dense Al_2O_3 is sufficient to cause interface reactions between the matrix and fiber. Large weight-gains are observed when SiC/Al_2O_3 is subjected to oxidation at temperatures greater than 1200°C.[129] During oxidation, the SiC first oxidizes partially to form an SiO_2 layer, which then reacts with the Al_2O_3 matrix to form mullite. The formation of mullite disrupts the protective nature of the SiO_2 layer, which causes further oxidation of the SiC. The oxidation rates of SiC in an oxide matrix (SiC/Al_2O_3 and SiC/mullite) is a factor of three higher than for monolithic SiC.[130,131] This result is a consequence of the large oxygen potential gradient and the segregation that occurs as the more rapidly diffusing cations preferentially diffuse towards the highest oxygen activity.

Dramatic evidence of cation demixing has also been shown for the $SiC/MgAl_2O_4$ system in an oxidizing atmosphere.[132] At 1250°C, magnesium atoms leave the low PO_2 interface reaction product and rapidly migrate to the high oxygen activity. The result is an outer scale of essentially pure MgO, an intermediate layer of $MgAl_2O_4$, and a porous nonprotective inner layer composed of $MgO + Al_2O_3 + SiO_2$. These results are particularly significant in view of the fact that the $SiC/MgAl_2O_4$ is thermodynamically stable in a nonoxidizing environment and underscores the importance of evaluating prospective systems in a representative oxidizing environment.

The TaC/Y_2O_3 composite is stable in argon to 1750°C,[133] and other carbide/oxide pairs, such as ZrC/ZrO_2 and TiC/ZrO_2, which are also stable in nonoxidizing environments to 1650°C (Appendix page A.7). However, chemical compatibility in oxidizing environments is also expected to degenerate rapidly

in all these systems as oxygen diffuses through the oxide matrix to the carbide/oxide interface, where disruptive CO gas will be evolved, Appendix page A.5.[95,110]

SUMMARY

MATERIALS

An approach commonly employed in choosing high temperature ceramic composites is to use some fraction of the melting point (T_{melt}) as a guideline. For example, Fleischer[134] suggests that a practical operating limit for creep should lie between 0.5 and 0.66 T_{melt}. This would imply that materials with melting points between 2500°C and 3300°C would be required for 1650°C operation. There are over 130 known refractory ceramics that fit this melting point range. Other important factors, such as chemical compatibility and oxidation resistance, must also be considered.

In general, many borides and carbides have the requisite high-melting points and also exhibit good high-temperature strength.[43,57,59] Titanium diboride (TiB_2) and SiC are both expected to exhibit adequate high-temperature strength and possibly creep resistance if impurity levels can be minimized.[53] Other carbides, for example ZrC, exhibit reasonably good high-temperature strength but poor creep behavior.[63,64]

A major disadvantage of most, if not all, carbides and diborides is their very poor oxidation resistance. The addition of 20% to 30% SiC to HfB_2 does improve short-term oxidation resistance at temperatures as high as 2000°C, where the material recession rate is approximately 12 μm/h,[43] but this is almost two orders of magnitude greater than needed for extended applications. Long-term operation at temperatures much above 1000°C may not be feasible since volatilization of B_2O_3 becomes appreciable at this temperature.[55]

Both aluminum nitride (AlN) and boron nitride (BN) exhibit high thermal conductivity. This property greatly enhances thermal shock resistance. Unfortunately, nitrides do not have good high-temperature oxidation resistance (Figure 3). Silicon nitride (Si_3N_4) is the exception owing to the formation of a protective SiO_2 scale. Silicon nitride also exhibits good creep resistance to 1500°C. However, the properties of Si_3N_4 (e.g., oxidation, creep, strength) generally deteriorate rapidly above 1500°C, partly because impurities are added to obtain high density during fabrication.[70]

Less is known about the properties of beryllides and silicides. Beryllide intermetallics are lightweight, brittle, and appear to have good strength at high temperatures[81,82] although the data are limited and confirmation is needed. Oxidation resistance appears to be good (see Figure 3), even under cyclic conditions.[84] Silicides should have the best oxidation resistance of all the nonoxide ceramics. Molybdenum disilicide is known to have good oxidation resistance to 1700°C.[80] Germanium addition increases the coefficient of thermal expansion of the SiO_2 scale, and good cyclic oxidation resistance has been reported.[135,136] Silicides appear to lose strength rapidly above 1000°C and, for that reason, are not candidates for reinforcements. If compatible reinforcements can be developed, good oxidation resistance and toughness make $MoSi_2$, Ti_5Si_3, and perhaps the silicides of zirconium and hafnium, attractive matrix candidates.

Oxide compounds are favored in situations where oxidizing environments are encountered. Unfortunately, volatility is too high for CaO, SrO, MgO, and for many of the hafnate and zirconate compounds.[36,85,86] High-temperature creep and tensile strength are also generally very poor for polycrystalline ceramic oxides. Single crystals exhibit much better creep behavior (Figure 11) than polycrystalline fibers.

Solid solution or precipitation hardening may further increase strength in some single-crystal oxides. Increasing the Y_2O_3 content to 18 m/o in ZrO_2 promotes solution hardening, and the engineering stress is about 275 MPa compared with 160 MPa for 9.4 m/o when tested at 1400°C in air.[51] By appropriate aging, Heuer, Lanteri, and Dominguez-Rodriguez[52] also increased the yield strength in two-phase 4.5 m/o Y_2O_3 partially-stabilized ZrO_2 to 550 MPa. These results were also obtained at 1400°C in air.

Thermodynamic stability in oxidizing environments is good for most single oxides that have acceptably low vapor pressures, but some compound oxides exhibit segregation (demixing) in an oxygen gradient.[137] While many oxides and oxide compounds do not have good thermal shock resistance or fracture toughness, it may be possible to engineer these properties into an oxide matrix composite.

REINFORCEMENTS

A variety of carbon fibers that meet the requisite high-temperature mechanical property requirements are available, but are extremely sensitive to oxidizing environments and cannot be used uncoated. Luthra[95] demonstrated that both Y_2O_3 and Al_2O_3 are stable in contact with carbon at high temperatures in inert atmospheres. However, when oxygen is present, the permeability of oxygen through the protective oxide layer causes rapid degradation at the interface due to the release of CO gas at pressures exceeding 1 atm (see Appendix page A.11). There are no other known coating materials, oxide or nonoxide, that will protect carbon fibers and allow them to be used in ceramic composite systems above 1650°C in oxidizing environments.

Fibers made from polymer precursors yield a less-than-pure silicon carbide (e.g., Si-C-O or Si-C-N-O) and exhibit good mechanical strength below 1100°C. However, non-stoichiometry causes strength to decrease rapidly when temperatures exceed 1200°C[96] (see Figure 9). Chemical vapor deposited SiC is generally of higher purity and typically has very good high-temperature strength[53] and creep,[138,139] but fully stoichiometric CVD fibers have not yet been produced on a commercial scale. Recent progress reported by Lipowitz, Rabe, and Zonk[140] indicates that strengths as high as 1725 MPa at 1400°C have been reached on limited quantities of SiC from new polymer precursors.

Silicon carbide has an advantage over other nonoxide ceramics in that it exhibits good high-temperature-oxidation resistance. One limit is the evolution of CO gas at the SiO_2/SiC interface.[110] Expected short-term operating temperatures are on the order of 1750°C, although 1650°C may be a more practical upper limit; and for long-term use, the limit could be lower. Active oxidation, mass loss by evaporation, and decreasing SiO_2 viscosity are areas of concern at temperatures above 1650°C.

Titanium diboride is of interest as a reinforcing medium for ceramic composites because of its potential high-temperature mechanical properties. Efforts are under way to develop TiB_2 fibers for use in intermetallic composites, but the intended applications are below the UHT composite temperature

range of interest, and little is currently known about the high-temperature creep properties of TiB_2. Oxidative stability does not appear to be good.[126]

Although polycrystalline oxide fibers have not exhibited sufficient high-temperature strengths or creep resistance to be considered for use at 1650°C or higher,[88] studies on single-crystal oxides performed under the UHT Composite Program show that c-axis Al_2O_3, BeO, Al_2O_3•BeO, and yttrium aluminum garnet (YAG) approach the desired 10^{-8}/s needed for a creep-resistant material.[27] The YAG results are particularly encouraging because the material is cubic and the creep rates do not show a strong orientation dependency. This feature is of particular importance to both design and fabrication of composite systems since off-axis loads and complex stresses can be accommodated. Questions of commercial availability and problems associated with fabricability into engineered composites need to be addressed, however.

NONOXIDE/NONOXIDE COMPOSITES

Prior work under the Man Labs programs (see Appendix F) selected SiCp/HfB_2(C) as the best candidate for high velocity, oxidative environment applications from a number of nonoxide composite systems. High-temperature strength and thermal shock resistance are good, but little has been reported concerning fracture toughness or creep (although the materials were apparently machinable, especially with added carbon). Mechanical properties might be improved by adding SiC fibers, whiskers, or platelets to the SiC/HfB_2 matrix. The strength and short-term oxidation resistance of SiC/HfB_2 or SiC/ZrB_2 composites make them suitable for high-temperature (>1700°C) short-duty-cycle (<5 h) applications. However, long-term service applications would probably be limited to 1000°C due to B_2O_3 volatilization. Studies to determine the potential enhancement of strength and creep through selective reinforcement, and to evaluate long-term cyclic oxidation behavior are needed to establish the full potential of this composite system.

Composites of SiC/SiC made by CVI and SiC/Si_3N_4 by reactive sintering are being developed. Densities of these composites are gradually increasing as a result of process improvements and progress in controlling the kinetics of high-temperature gas-phase reactions. Composite strength and fracture toughness values are attractive.[20,21,108,109] Improved SiC fibers that do not

lose strength at temperatures above 1200°C will significantly improve these composites. Oxidation in both systems will eventually be limited by the carbon activity and purity levels. Measurements of the high-temperature creep and fatigue properties are needed.

A platelet-reinforced (PRC)™ ZrB_2(pl)/ZrC(Zr) composite exhibits excellent strength and toughness.[114,115] High-temperature creep data are not currently available, and the presence of even a small fraction of a zirconium metal phase will probably exacerbate creep at high temperatures. The reaction synthesis process can be controlled to reduce the volume fraction of zirconium metal, but at the expense of toughness. High-temperature oxidation rates are not expected to be significantly different from those of other boride or carbide compounds.

Composites of SiC/$MoSi_2$ exhibit good toughness and oxidation resistance, but poor strength and creep behavior[17] at temperatures of interest to UHT applications. This system will be a more viable candidate as SiC reinforcements with better high-temperature strength retention become available. Similarly, SiC/TiB_2 is not a good UHT candidate because its oxidation resistance is very poor, although toughness and strength are promising.[16]

OXIDE/OXIDE COMPOSITES

Most oxide/oxide composites are expected to be stable in oxidizing environments, which eliminates the need for external oxidation protection coatings. Two inherent weaknesses in oxide/oxide systems are low strengths and high creep rates at temperatures of interest. Recent studies suggest that a few single-crystal oxides may meet the proposed 10^{-8}/s creep rate.[27] Alumina and beryllia (BeO) show promising creep resistance in the c-axis orientation only. Single-crystal fibers with proper alignment must be produced and directionally incorporated into a ceramic matrix to take full advantage of their preferred mechanical properties. This is not an easy task from the standpoint of fabricating engineered composite systems.

Yttrium aluminum garnet (YAG) single crystals have also exhibited creep rates in the range of interest.[27] This compound oxide is cubic and the creep rates are similar in all directions, which implies that there is not one preferred slip plane for which the critical resolved shear stress can activate off-axis slip. This is a significant advantage in structural applications. YAG/Al_2O_3 composites have been made by directional solidification,[118] but optimum control of phase morphology must still be developed. Fracture toughness values for the directionally solidified eutectic composition are modest (~4 MPa $\sqrt{m}$), thus further work is needed to optimize microstructure and property relationships.

If we make the assumption that the matrix phase bears no load and provides no creep resistance, the fibers in a composite with 20% reinforcement would need creep rates of almost 10^{-10}/s to compensate for the stress dependency. This translates to a maximum operating temperature of 1350°C for c-axis Al_2O_3 and 1530°C for YAG if the stress exponent (n) is 3.0, which is close to a value of 2.7 reported by Corman[27] for the [100] orientation. More exploratory research is needed to identify single-crystal compounds with creep rates that are 10^{-9}/s or lower above 1650°C, and a better understanding of fiber/matrix interactions will also be needed. Experimental composites must be prepared with carefully oriented fibers to measure and establish the upper limits for strength at a given temperature.

Not all compound oxides are thermodynamically stable in oxidizing environments if there is a significant oxygen pressure gradient. When the diffusion rate of one cation is significantly higher than the second cation in a compound oxide lattice, significant demixing can occur; the faster diffusing species preferentially move to the side with the highest oxygen activity.[34,117,132,137]

A few oxide/oxide composite systems can be postulated that would meet strength and creep requirements based on single-crystal reinforcements. Thus, it seems plausible that the UHT goals are achievable, particularly at the lower end of the temperature range of interest (i.e., 1650°C to 1700°C).

NONOXIDE/OXIDE COMPOSITES

Currently, the only commercially available ceramic fibers that exhibit potentially good high-temperature creep strength are nonoxides (e.g., C, SiC). Titanium diboride (TiB_2) fibers are not yet commercially available, but this compound has been shown to have good high-temperature strength (Figure 6). It would be desirable to find thermochemically compatible oxidation-resistant coatings for these materials so that they could be incorporated into oxide matrices. Attempts to coat carbon with yttria or alumina resulted in significant degradation of the carbon fiber despite the fact that the components are thermochemically stable.[35] This is because of rapid permeation of oxygen through the oxide to the carbon interface where the reaction product results in the disruptive evolution of CO gas.

Boride/oxide composites exhibit unacceptable degradation at high temperatures as a result of oxygen permeation in the oxide lattice and formation of reaction products at the fiber/matrix interface. Composites of SiC/Al_2O_3[133] and $SiC/MgAl_2O_4$[132] also degrade in oxidizing environments around 1200°C. There currently appears to be no nonoxide/oxide composite system that warrants further investigation in the UHT regime of interest because of potential interface degradation and the lack of suitable coating materials.

COMPARISON OF SYSTEMS

In Table 8, properties for selected ceramic reinforcements and composite systems are presented for purposes of comparison. Striking features of this table are the lack of fatigue data and the limited amount of fracture toughness and creep data available. Virtually all available fracture toughness information has been taken at room temperature. It would be desirable to have values for higher temperatures and an indication of the temperature dependence of the various mechanical properties including any environmental effects. Room temperature fracture toughness values are probably a reasonable indication of thermal shock resistance and the ability to withstand thermal transients.

TABLE 8. Comparison of Selected Ceramic Reinforcements and Composites

Materials	Flexure or Bend Strength (MPa) Room Temp	Flexure or Bend Strength (MPa) Elevated Temp	Creep @ 100 MPa (Sec^{-1})/Temp	Room Temp Fracture Toughness (MPa $\sqrt{\mu m}$)	Fatigue	Oxidation Resistance
Reinforcements						
Carbon	2000-4000	~2560 @ 2300°C	$1X10^{-11}$ @ 1600°C	U	U	Catastrophic
TiB_2/TiB(C)	370-1560	900 @ 1000°C	U	U	U	Poor
SiC (CVD)	-	1725 @ 1400°C	$3X10^{-9}$ @ 1600°C	U	U	Good
C-axis Al_2O_3	1400-3300	-	$1X10^{-8}$ @ 1600°C	U	U	Not Affected
C-axis BeO	-	~40 @ 1000°C	$1X10^{-9}$ @ 1750°C	U	U	Not Affected
YAG	U		$5X10^{-10}$ @ 1600°C	U	U	Not Affected
Nonoxide/Nonoxide						
BNp/AlN-SiC	-	28 @ 1530°C	U	U	U	Fair to 1600°C
SiC/SiC	350-750	-	U	18	U	$<10\mu m^2$/hr @ 1600°C
SiCp/HfB_2	380	28 @ 1600°C	$\sim 10^{-5}$ @ 1600°C	U (Good Thermal Shock)	U	12μm @ 2000°C
SiC_f/HfB_2-SiC	1000					5% wt gain @ 1600°C
SiC/$MoSi_2$	310	20 @ 1400°C	U	~8	U	$<10\mu m^2$/hr @ 1600°C
ZrB_{2pl}/ZrC(Zr)	1800-1900	U	U	18	U	Not known
20 v/o SiC_w/Si_3N_4	620	365 @ 1370°C	U	13	*	Good
Oxide/Oxide						
Al_2O_{3w}/Mullite	~180	-	U	U	U	Dissolution Reaction
Al_2O_3/ZrO_2	500-900	-	U	U	U	Not Affected
YAG/Al_2O_3	373	198 @ 1650°C	U	4	U	Not Affected
Nonoxide/Oxide						
SiC/ZrB_2-Y_2O_3	-	16 @ 1530°C	U	U	U	Poor
TiB_2/ZrO_2	U	U	U	U	U	Poor
SiC/Al_2O_3	600-800	U	10^{-5} @ 1525°C	5-9	U	Poor > 1200°C
30 v/oSiC/ZrO_2	600	400 @ 1000°C	U	12	U	Degrades > 1000°C

U = Unknown

* = 0.2 μm crack growth after 500,000 cycles in compression @ 42 MPa

CONCLUSIONS

Of the reinforcements, carbon is clearly in a class by itself from the standpoint of elevated temperature strength and creep resistance. However, the oxidation resistance of carbon is unacceptable, and no satisfactory coating or oxidation protection method has yet been developed. Of the nonoxide ceramics, silicon carbide is a promising reinforcement and will become more prominent when high-temperature strength properties are improved and approach theoretical values. More data are needed to assess the potential of TiB_2. Single-crystal oxide fibers appear to have great promise, and may reach the desired 10^{-9}/ creep rates; however, their utility in actual composite systems must yet be demonstrated.

For engines with lifetime requirements shorter than 5 hours, two nonoxide/nonoxide composites with potential are SiCp/HfB_2 and ZrB_2pl/ZrC(Zr). Both of these systems have good room-temperature strength and thermal-shock resistance, but lack long-term high-temperature oxidation resistance. However, they both should be able to withstand a limited life cycle without debilitating oxidation loss. The SiC_p/HfB_2 system can withstand temperatures in excess of 2000°C for short periods, but the platelet-reinforced composite will be limited to the melting point of the free zirconium (~1850°C). While both composites have modest high-temperature strength and creep resistance, these properties are not so critical for a short duty cycle where good thermal shock resistance is probably more important.

For long-term applications, only oxide/oxide composites will be able to survive in oxidizing environments. Several single-crystal oxide fibers (e.g., BeO, c-axis Al_2O_3, and YAG) appear capable of achieving creep rates on the order of the $^{-}10^{-9}$/s needed to adequately reinforce less creep-resistant oxide matrices. Fabrication into composite structures without some reduction in single-crystal properties has not been demonstrated and may be difficult. Single-crystal YAG fibers are particularly attractive because of their cubic symmetry. Isotropic property behavior will result in less loss of strength or creep resistance when subjected to off-axis loading conditions. The Al_2O_3/YAG

eutectic (see Appendix B.9) is also a promising composite; however, fracture toughness levels on the order of ~4 MPa $\sqrt{m}$ will have to be improved.

There are two nonoxide composite systems that also show some long-range promise. These are the silicon-base composites: SiC/SiC and SiC/$MoSi_2$. Both systems appear to be limited by high-temperature strength and creep resistance. Better high-temperature SiC fiber properties are expected as fabrication technologies, control of stoichiometry, and purity levels are improved, and better quality fibers should directly lead to improvements in high-temperature strength and creep resistance in these systems. Both composites form adherent protective SiO_2 scales with low permeability to oxygen at the lower temperature range of interest for UHT composite applications (e.g., 1650°C). Thus, the concurrent development of improved SiC reinforcements, together with improvements in methods for producing high-density composites from these two systems, warrant further investigation.

Nonoxide reinforced oxide matrix composites do not appear to offer as much promise as the other composite systems. The main reason is rapid oxygen permeation through the matrix leading to the formation of undesirable reaction products at the fiber/matrix interface. All nonoxide ceramics, with the exception of SiC, Si_3N_4, and $MoSi_2$, oxidize at rates that exceed 10 $\mu m^2/h$. In some cases, these rates even increase within an oxide matrix. Flight critical components cannot suffer catastrophic oxidation or debilitating reductions in mechanical properties; hence, it is questionable that nonoxide composites warrant further study for UHT application.

REFERENCES

1. T. M. Mah, M. G. Mendiratta, A. P. Katz, and K. S. Mazdiyasni. "Recent Developments in Fiber-Reinforced High-Temperature Ceramic Composites." Ceramic Bulletin 66(2):304-307. (1987)

2. A. P. Katz and R. J. Kerans. "Structural Ceramics Program at AFWAL Materials Lab." Ceramic Bulletin 67(8):1360-1366. (1988)

3. R. J. Kerans and L. S. Theibert. "Proceedings of the Ultrahigh-Temperature Composite Materials Workshop." AFWAL-TR-87-4142, Wright-Patterson Air Force Base, Ohio. (1987)

4. M. D. Thouless and A. D. Evans. "Effects of Pull-out on the Mechanical Properties of Ceramic-Matrix Composites." Acta Metall. 36(3):517-522. (1988)

5. R. A. Lowden. "Characterization and Control of the Fiber-Matrix Interface in Ceramic Matrix Composites." ORNL/TM-11039. Oak Ridge National Laboratory, Oak Ridge, Tennessee. (1989)

6. J. F. Mandell, K. C. Hong, and D. H. Grande. "Interfacial Shear Strength and Sliding Resistance in Metal and Glass-Ceramic Matrix Composites." Ceram. Eng. Sci. Proc. 8(7-8):937-940. (1987)

7. R. W. Goettler and K. T. Faber. "Interfacial Shear Stresses in SiC and Alumina Fiber-Reinforced Glasses." Ceram. Eng. Sci. Proc. 9(7-8):861-72. (1988)

8. D. B. Marshall. "An Indentation Method for Measuring Matrix-Fiber Frictional Stresses in Ceramic Components." J. Am. Cer. Soc. 67(12):C259-260. (1984)

9. R. J. Kerans, R. S. Hay, N. J. Pagano, and T. A. Parthasarathy. "The Role of the Fiber-Matrix Interface in Ceramic Composites." Ceramic Bulletin 68(2):429-442. (1989)

10. D. E. Sokolowski, ed. "Toward Improved Durability in Advanced Aircraft Engine Hot Sections." NASA Technical Memorandum 4087, Lewis Research Center, Cleveland, Ohio. (1989)

11. J. S. Cuccio, J. H. Adams, and H. L. Kington. "Probabilistic Design Technology For Ceramic Components." 3rd International Symposium on Ceramic Materials and Components For Engines, ed. V. J. Tennery, pp. 1273-1288. (1988)

12. A. G. Evans and B. J. Dalgleish. "Some Aspects of the High-Temperature Performance of Ceramics and Ceramic Composites." Ceram. Eng. Sci. Proc. 7(9-10):1073-1094. (1986)

13. G. R. Terwilliger and K. C. Radford. "High-Temperature Deformation of Ceramics: I, Background." Ceramic Bulletin 53(2):172-180. (1974)

14. A. G. Evans. "Engineering Property Requirements for High Performance Ceramics." Mater. Sci. Eng. 71:3-21. (1535)

15. D. B. Marshall and A. G. Evans. "Failure Mechanisms in Ceramic-Fiber/Ceramic-Matrix Composites." J. Amer. Cer. Soc. 68(5):225-31. (1985)

16. C. H. McMurtry, W.O.G. Boecker, S. G. Seshadri, J. S. Zanghi, and J. E. Garnier. "Microstructure and Materials Properties of SiC-TiB_2 Particulate Composites." Am. Ceram. Soc. Bull. 66(2):325-329. (1987)

17. D. H. Carter, J. J. Pertrovic, R. E. Honnell, and W. S. Gibbs. "SiC-$MoSi_2$ Composites." Ceram. Eng. Sci. Proc. 10(9-10):1121-1129. (1989)

18. A. H. Heuer. "Transformation Toughening in ZrO_2 - Containing Ceramics." J. of Amer. Cer. Soc. 70(10):689-698. (1987)

19. D. Carruthers and L. Lundberg. "Critical Issues For Ceramics For Gas Turbines." 3rd International Symposium on Ceramic Materials and Components For Engines, ed. V. J. Tennery, pp. 1258-1272. (1988)

20. H. Kodoma and T. Miyoshi. "Fabrication and Properties of Si_3N_4 Composites Reinforced by SiC Whiskers and Particles." Ceram. Eng. Sci. Proc. 10(9-10):1072-1082. (1989)

21. P. D. Shalek, J. J. Petrovic, G. F. Hurley, and F. D. Gac. "Hot-Pressed SiC Whiskers/Si_3N_4 Matrix Composites." Am. Ceram. Soc. Bull. 65(2):351-56. (1986)

22. Y. R. Wang, D. S. Liu, P. P. Majidi, and T. W. Chow. "Creep Characterization of Short Fiber-Reinforced Ceramic Composites." Ceram. Eng. Sci. Proc. 10(9-10):1154-1163. (1989)

23. W. R. Cannon. "Creep of Ceramics - Part I Mechanical Characteristics." J. of Material Sci. 18:1-50. (1983)

24. W. R. Cannon. "Creep of Ceramics - Part II An Examination of Flow Mechanisms." J. of Material Sci. 23:1-20. (1988)

25. J. D. Luban and R. P. Felgar. "Plasticity and Creep of Metals." New York: J. Wiley & Sons, p. 175. (1961)

26. E. Bullock, N. M. Mclean, and D. E. Miles. "Creep Behavior of a Ni-Ni_3Al-Cr_3C_2 Eutectic Composite." Acta Metall. 25:333-344. (1977)

27. G. S. Corman. "Creep of Oxide Single Crystals." WRDC-TR-90-4059, Wright-Patterson Air Force Base, Ohio. (1990)

28. A. H. Choksi and J. R. Porter. "Creep Deformation of an Alumina Matrix Composite Reinforced With Silicon Carbide Whiskers." J. Am. Ceram. Soc. 68(6):C144-C145. (1985)

29. A. Kelby and K. N. Street. "Creep of Discontinuous Fiber Composites II Theory for the Steady State." Proceedings Royal Society London A. 328, pp. 283-293. (1972)

30. R. H. Dauskardt and R. O. Ritchie. "Cyclic Fatigue-Crack Propagation Behavior in Advanced Ceramics." Ceram. Eng. Sci. Proc. 10(9-10):1146. (1989)

31. L. Ewart and S. Suresh. "Crack Propagation in Ceramics Under Cyclic Load." J. Mater. Sci. 22:1173-1192. (1987)

32. S. Suresh, L. X. Han, and J. J. Petrovic. "Fracture of Si_3N_4-SiC Whisker Composites Under Cyclic Loads." J. Amer. Cer. Soc. 71(3):6158-6151. (1988)

33. A. P. Nikkila and T. A. Mantyla. "Cyclic Fatigue of Silicon Nitrides." Ceram. Eng. Sci. Proc. 10(7-8):646-656. (1989)

34. E. L. Courtright, J. T. Prater, E. H. Greenwell, and C. H. Henegar, Jr. "Oxygen Permeability in Refractory Oxides in the Range 1200°C-1700°C." WL-TR-91-4006, Wright-Patterson Air Force Base, Ohio. (1991)

35. J. D. Cawley, G. R. St. Pierre, J. D. Kalen, J. C. Amante, K. Gourishonkar, and K. S. Goto. Thermodynamic and Diffusivity Measurements in Potential Ultrahigh-Temperature Composite Materials. WRDC-TR-90-4058, Wright-Patterson Air Force Base, Ohio. (1990)

36. D. Freitag. "Oxygen Diffusion in $SrHfO_3$ For Use In Ceramic Matrix Composites at Ultrahigh Temperatures." WRDC-TR-89-4029, Wright-Patterson Air Force Base, Ohio. (1989)

37. R. P. Turcotte. "Oxygen Diffusivity Measurements in Pyrochlore Compounds." WL-TR-91-4059 to be issued.

38. W. C. Tripp and H. C. Graham. "Thermogravmetric Study of the Oxidation of ZrB_2 in the Temperature Range of 800°C to 1500°C." J. Electro Chem. Soc. 118(7):1195-99. (1971)

39. J. R. Strife and J. E. Sheehan. "Ceramic Coatings for Carbon-Carbon Composites." Ceramic Bulletin 67(2):369-374. (1988)

40. G. H. Schiroky, R. J. Price, and J. E. Sheehan. "Oxidation Characteristics of CVD Silicon Carbide and Silicon Nitride." GA-AI8696, General Atomics, La Jolla, California. (1986)

41. J. Schlichting. "Oxygen Transport Through Silica Surface Layers on Silicon-Containing Ceramic Materials." High Temperatures-High Pressures 14:717-724. (1982)

42. Kaufman, E. V. Clougherty, and J. B. Berkowitz-Mattuck. "Oxidation Characteristics of Hafnium and Zirconium Diboride." Trans. Metal. Soc. AIME 239:458. (1967)

43. E. V. Clougherty, R. L. Pober, and L. Kaufman. "Synthesis of Oxidation-Resistant Metal Diboride Composites." Trans. Metal. Soc. AIME 242:1077. (1968)

44. V. A. Laurenko and A. F. Alexeev. "Oxidation of Sintered Aluminum Nitride." Ceramic International 9:80. (1983)

45. J. T. Prater. "Modification of Hafnium Carbide for Enhanced Oxidation Resistance Through Additions of Tantalum and Praseodymium." AFWAL-TR-88-4141, Wright-Patterson Air Force Base, Ohio. (1988)

46. J. Doychak, J. L. Smialek, and C. A. Barrett. "The Oxidation of Ni-Rich Ni-Al Intermetallics." In Oxidation of High-Temperature Intermetallics, eds. T. Grobstein and J. Doychak, TMS, Warrendale, Pennsylvania, pp.41-55. (1989)

47. B. Pieraggi. "Calculations of Parabolic Rate Constants." Oxidation of Metals 27(3,4):177-185. (1987)

48. W. B. Hillig. "Prospects for Ultrahigh-Temperature Ceramic Composites." Tailoring Multiphase and Composite Ceramics, eds. R. E. Tressler, et al., pp. 697-712. Plenum Press. (1986)

49. D. Carruthers. Private Communications Courtesy of Garrett Auxiliary Power Division, Allied-Signal Aerospace Company. (1990)

50. J. W. Warren. "Ceramic Matrix Composites for High Performance Structural Applications." TMS/AIME Publication Advanced Fibers and Composites for Elevated Temperatures, eds. J. Ahmad and B. R. Noton. (1980)

51. A. Dominguez-Rodriguez, K.P.D. Lagerlof, and A. H. Heuer. "Plastic-Deformation and Solid Solution Hardening of Y_2O_3-Stabilized ZrO_2." J. Amer. Cer. Soc. 69(3):281-283. (1986)

52. A. H. Heuer, V. Lanteri, and A. Dominguez-Rodriguez. "High-Temperature Precipitation Hardening of Y_2O_3 Partially-Stabilized ZrO_2 (Y-PSZ) Single Crystal." Acta Metall. 37(2):559-567. (1989)

53. W. S. Williams. "Deformation Resistance and the Development of High-Temperature Composites." AFWAL-TR-87-4142, pp. 169-185. (1987)

54. J. R. Romberg, C. F. Wolfe, and W. S. Williams. "Resistance of Titanium Diboride to High-Temperature Plastic Yielding." J. Amer. Ceram. Soc. 68(3):C78-C79. (1985)

55. B. Lonnberg. "Thermal Expansion Studies on the Group IV-VII Transition Metal Diborides." J. Less Common Metals 141:145-156. (1988)

56. W. C. Tripp, H. H. Davis, and H. C. Graham. "Effect of an SiC Addition on the Oxidation of ZrB_2." Ceramic Bulletin 52(8):612-616. (1973)

57. J. R. Fenter. "Refractory Diborides as Engineering Materials." SAMPE 2,1(3):1-15. (1971)

58. M. Simpson and E. Paquette. "Diboride/Carbide Ceramics for Elevated Temperature Oxidation Resistance." WRDC-TR-90-4077, Wright-Patterson Air Force Base, Ohio. (1990)

59. Battelle Columbus Laboratories. Engineering Property Data on Selected Ceramics, Vol 2: Carbides. Metals and Ceramics Information Center, Battelle Columbus Laboratories, Report MCIC-HB-07-Vol 2, Aug. 1979. (Avail. NTIS, AD-A087519.) (1979)

60. N. J. Shaw, J. A. Dicarlo, N. S. Jacobson, S. R. Levine, J. A. Nesbitt, H. B. Probst, W. A. Sanders, and C. A. Stearns. "Materials for Engine Applications Above 3000°F - an Overview." NASA Technical Memorandum 100169, Lewis Research Center, Cleveland, Ohio. (1987)

61. J. F. Lynch, C. G. Rederer, and W. H. Duckworth. "Engineering Properties of Selected Ceramic Materials." J. Amer Ceram Soc. (1966)

62. Battelle Columbus Laboratories. Engineering Property Data on Selected Ceramics, Vol. 1: Nitrides. Metals and Ceramics Information Center, Battelle Columbus Laboratories, Report MCIC-HB-07-Vol. I, Mar. 1976 (Avail. NTIS, AD-A023773.) (1976)

63. H. J. Frost and M. F. Ashby. "Deformation-Mechanism Maps - The Plasticity and Creep of Metals and Ceramics." Pergamon Press. (1982)

64. E. Rudy, S. Windisch, and Y. A. Chang. Ternary Phase Equilibria in Transition Metal-Boron-Carbon-Silicon Systems, Part I. Related Binary Systems, Vol. I. Mo-C System. Prepared under Contract No. AF33(615)-1249, Aerojet-General Corporation, Materials Research Laboratory, Sacramento, California, AFML-TR-65-2, Part I, Vol. I. (1965)

65. E. Rudy. Ternary Phase Equilibria in Transition Metal-Boron-Carbon-Silicon Systems, Part II. Ternary Systems, Volume I. Ta-Hf-C System. Prepared under Contract No. AF33(615)-1249, Materials Research Laboratory of Aerojet-General Corporation, Sacramento, California, AFML-TR-65-2, Part II, Vol. I. (1965)

66. E. Rudy. Ternary Phase Equilibria in Transition Metal-Boron-Carbon-Silicon Systems, Part I. Related Binary Systems, Volume IV. Hf-C Systems. Prepared under Contract No. AF33(615)-1249, Materials Research Laboratory of Aerojet-General Corporation, Sacramento, California, AFML-YR-65-2, Part I, Vol. IV. (1965)

67. E. Rudy and D. P. Harmon. Ternary Phase Equilibria in Transition Metal-Boron-Carbon-Silicon Systems, Part I. Related Binary System, Volume V. Ta-C System. Partial Investigation in the Systems Nb-C and V-C. Prepared under Contract AF33(615)-1249, Materials Research Laboratory of Aerojet-General Corporation, Sacramento, California, AFML-TR-65-2, Part I, Vol. V. (1966)

68. K. S. Mazdiyasni, R. Ruh, and E. Hermes. "Phase Characterization and Properties of AlN-BN Composites." Am. Ceram. Soc. Bull. 64(8):1149-54. (1985)

69. G. DeWith and N. Hattu. "High-Temperature Fracture of Hot-Pressed AlN Ceramics." Material Science 18:503-507. (1983)

70. D. C. Larsen, et al. "Ceramic Materials for Advanced Heat Engines." Hoyes Publications, Park Ridge, New Jersey. (1985)

71. K. L. Luthra. "Oxidation of Silica-Forming Materials." General Electric Report, 89CRU088. (1989)

72. H. Du, R. E. Tressler, K. E. Spear, and C. G. Pontano. "Oxidation Study of Crystalline CVD Silicon Nitride." J. Electrochem. Soc. 136:1527-36. (1989)

73. C. Wagner. "Passivity During the Oxidation of Silicon at Elevated Temperatures." J. Appl. Phys. 29(9):1295-1297. (1958)

74. J. W. Hinze, W. C. Tripp, and H. C. Graham. "Active Oxidation in Silicon and Silicon Base Materials." In Metal-Slag-Gas Reactions and Processes, eds. W. W. Smelter and Z. A. Forovus. The Electrochemical Society. (1975)

75. J. W. Hinze and H. C. Graham. "The Active Oxidation of Si and SiC in the Viscous Gas-flow Region." J. Electrochem. Soc. 123(7). (1976)

76. P. J. Meschter and D. S. Schwartz. "Silicide-Matrix Materials for High-Temperature Applications." The Journal of Minerals, Metals, and Materials Society 41(11):52-55. (1989)

77. E. Fitzer and J. Schwab. J. Metall. 9:1062. (1955)

78. J. B. Berkowitz-Mattuck, M. Rossetti, and D. W. Lee. "Enhanced Oxidation of Molybdenum Disilicide Under Tensile Stress: Relation to Pest Mechanisms." Metall. Trans. I:479-483. (1970)

79. G. H. Meier. "Fundamental of the Oxidation of High-Temperature Intermetallics in Oxidation of High-Temperature Metals," eds. T. Grobstein and J. Doychak, The Minerals, Metals, and Materials Society, Warrendale, Pennsylvania, pp. 1-16. (1988)

80. J. Schlichting. "Molybdenum Dislilicide as a Component of Modern High-Temperature Composites," High Temp-High Pressures. 10(3):241-269. (1978)

81. J. M. Marder and A. J. Stonehouse. "A Review of Beryllides For Very High-Temperature Service." 2nd International SAMPE Metals and Metals Processing Conference 2:357-367. (1988)

82. A. J. Stonehouse, R. M. Paine, and W. W. Beaver. "Mechanical Properties of Intermetallic Compounds." ed., J. H. Westbrook, Wiley Publ., New York. (1960)

83. F. Grensing. "Oxidation Behavior of Beryllide Intermetallic Compounds." In Oxidation of High-Temperature Metals, eds T. Grobstein and J. Doychak, The Minerals, Metals, and Materials Society, Warrendale, Pennsylvania, pp. 279-293. (1988)

84. E. L. Courtright. "The Oxidation of $TaBe_{12}$ and $NbBe_{12}$ Coatings on Niobium." To be published in Proceedings of the 14th Annual Conference on Composites, Materials, and Structures. (1990)

85. J. D. Cawley. "High-Temperature Screening Experiments on HfO_2, ZrO_2, $CaZrO_3$, and $CaHfO_3$." AFWAL-TR-88-4008, Wright-Patterson Air Force Base, Ohio. (1987)

86. J. Porter and G. Reynolds. "Determination of Fundamental Thermodynamic Properties of Constituent Materials and Performance Screening of Candidate Systems." WRDC-89-4035, Wright-Patterson Air Force Base, Ohio. (1989)

87. T. Mah, M. G. Mendiratta, and L. A. Boothe. "High-Temperature Stability of Refractory Oxide-Oxide Composites." AFWAL-TR-88-4015, Wright-Patterson Air Force Base, Ohio. (1988)

88. R. E. Tressler, L. E. Jones, and S. Sabol. "Creep of Ceramic Fibers." NASA HiTemp Review 1989. NASA Conference Publication 10039. (1989).

89. Battelle Columbus Laboratories. "Engineering Property Data on Selected Ceramics, Vol. 3: Single Oxides." Metals and Ceramics Information Center, Battelle Columbus Laboratories, Report MCIC-HB-07-Vol. III, July 1981. (Avail. NTIS, AD-A104538.) (1981)

90. A. H. Heuer. "Precipitates, Dislocations, and Phase Transformations in Y_2O_3 Partially-Stabilized ZrO_2 Single Crystals." Presented at the 15th Annual Conference on Composites and Advanced Ceramics, January 13-16, 1991, Cocoa Beach, Florida. (1991)

91. D. J. Pysher and R. E. Tressler. "Strength of Ceramic Fibers at Elevated Temperatures." J. Amer. Ceram. Soc. 72:284-288. (1989)

92. R. E. Tressler. "Mechanical Behavior of Fibers." 3rd Annual Report, Center for Advanced Materials, Penn State University, University Park, Pennsylvania. (1989-1990)

93. P. J. Whalen, D. Narasimhan, C. J. Gasdaska, E. W. O'Dell and R. C. Morris. "New High-Temperature Oxide Composite Reinforcement Material: Chrysoberyl." Presented at the 15th Annual Conference on Composites and Advanced Ceramics, Jan. 13-16, 1991, Cocoa Beach, Florida. (1991)

94. J. DiCarlo. "Thermal Stability of SCS-6 SiC Fibers." Proceedings of 2nd Annual HiTemp Review. NASA Conference Publication 10039, 69(1-11). (1989)

95. K. L. Luthra and H. D. Park. "Chemical Compatibility in Ceramic Composites." AFWAL-TR-89-4009, Wright-Patterson Air Force Base, Ohio. (1989)

96. G. Simon and A. R. Bunsel. "Creep Behavior and Structural Characterization at High Temperatures of Nicalon SiC Fibers." J. Mater. Sci. 19:3658-3670. (1984)

97. C. D. Pears. "A Technical Note on Yarn Properties That Relate to Processing." Special Edition Carbon-Carbon Materials, Current Awareness Bulletin, Issue No. 7, Metals and Ceramics Information Center, Battelle Columbus Laboratories. (1980)

98. D. J. Pysher and R. E. Tressler. "Creep Rupture Studies of Two Alumina-based Ceramic Fibers." Submitted to J. Mater. Sci.

99. K. Jukus and V. Tulluri. "Mechanical Behavior of a Sumitomo Alumina Fiber at Room and High-Temperature." Submitted to J. Amer. Ceram. Soc.

100. J. A. DiCarlo. "Creep of Chemically Vapor Deposited SiC Fibers." NASA Tech Memo. 86897, prepared for 8th Annual Conference on Composites and Advanced Ceramic Materials, J. Amer. Ceram. Soc. (Jan. 15-18, 1984), Cocoa Beach, Florida. (1984)

101. R. F. Firestone and A. H. Heuer. "Creep Deformation of 0° Sapphire." J. Amer. Ceram. Soc. 59(1-2):24-29. (1976)

102. H. A. Clauer and B. A. Wilcox. "High-Temperature Tensile Creep of Magnesium Oxide Single Crystals." J. Amer. Ceram. Soc. 59(3-4):89-96. (1976)

103. R. J. Garboriande. "Fluage Haute Temperature du Sesquioxyde d'Yttrium: Y_2O_3." Phil. Mag. 44A:(3):561-587. (1981)

104. R. Duclos, N. Doukhan, and B. Escaig. "High-Temperature Creep Behavior of Nearly Stoichiometric Alumina Spinel." J. Mat. Sci. 13:1740. (1978)

105. W. J. Minford. "Microstructure, Crystallography, and Creep of Directionally Solidified Oxide Eutectics." Ph.D. Thesis, The Pennsylvania State University. (1977)

106. D. M. Kotchick and R. E. Tressler. "Deformation Dynamics of Doped and Undoped a-Axis and c-Axis Sapphire." Ph.D. Thesis in Ceramic Science, The Pennsylvania State University. (1978)

107. D. W. Richerson, K. L. Stuffle, and C W. Griffen. "Development of Continuous Fiber-Reinforced Group IVB Diboride Composites." 13th Conference on Metal Matrix, Carbon, and Ceramic Matrix Composites. NASA Publication 3054, Part 1, pp. 119. (1989)

108. A. J. Caputo, R. A. Lowden, and H. H. Moeller. "Fiber Reinforced Ceramic Tubular Components." ORNL/TM 10466, Oak Ridge National Laboratory, Oak Ridge, Tennessee. (1988)

109. W. J. Lackey. "Review, Status, and Future of the Chemical Vapor Infiltration Process for Fabrication of Fiber Reinforced Ceramic Composites." Ceram. Eng. Sci. Proc. 10(7-8):577-584. (1989)

110. R. A. Rapp and G. R. St. Pierre. "New Options For The Protection of Carbon/Carbon Composites." Proceedings of the Ultrahigh-Temperature Composite Workshop. AFWAL-TR-87-4142, pp. 27-62. (1987)

111. M. Keller. "Hybrid Fiber Carbon-Carbon Composites for Improved Compatibility with Oxidation Resistant Coatings." AFWAL-TR-88-4107, Wright-Patterson Air Force Base, Ohio. (1988)

112. R. A. Williamson and M. P. Kandell. "Arc Heater Screening of Oxidation Resistant Carbon-Carbon Materials." NSWL-TR-85-268. (1985)

113. W. Foulds, J. F. LeCostaquec, C. Londry, S. D. Pietro, and T. Vasilos. "Tough Silicon Nitride Matrix Composites Using Textron Silicon Carbide Monofilaments." Ceram. Eng. Sci. Proc. 10(9-10):1083-1099. (1989)

114. W. B. Johnson, T. D. Claar, and G. H. Schiroky. "Preparation and Processing of Platlet Reinforced Composites (PRC™) by the Lanxide™ Process." Ceram. Eng. Sci. Proc. 10(7-8):588-598. (1939)

115. T. D. Claar, W. B. Johnson, C. A. Anderson, and G. H. Schiroky. "Microstructure and Properties of Platelet-Reinforced Composites (PRC™) by the Lanxide™ Process." Ceram. Eng. Sci. Proc. 10(7-8):599-609. (1989)

116. W. S. Gibbs, J. J. Petrovic, and R. E. Honnell. "SiC Whisker-$MoSi_2$ Matrix Composites." Ceram. Eng. Sci. Proc. 8(7-8):645-648. (1987)

117. H. Schmalzried and W. Laqua. "Multi-Component Oxides in Oxygen, Potential Gradients." High-Temperature Corrosion, NACE-6, ed, R. A. Rapp, pp. 115-120. (1983)

118. T. Mah, T. A. Parthasarthy, L. A. Boothe, M. D. Petry, and L. E. Matson. "Directional Solidification of Refractory Oxide Ceramic Eutectic Composites." WRDC-TR-90-4081, Wright-Patterson Air Force Base, Ohio. (1990)

119. Z. Li and R. C. Bradt. "Micromechanical Stresses in SiC-Reinforced Whiskers Al_2O_3 Composites," Jour. Amer. Ceram. Soc., Vol. 72, No. 1, pp. 70-77. (1989)

120. J. D. Mackenzie and K. Ono. "Oxide Ceramic Fibers by the Sol-gel Method." AFWAL-TR-88-44199, Wright-Patterson Air Force Base, Ohio. (1989)

121. D. B. Meadowcraft and J. B. Wimmer. "Oxidation and Vaporization Processes in $LaCrO_3$." Bull. Amer. Ceram. Soc. 58(6):610. (1979)

122. J. P. Pemsler. Private communication.

123. J. K. Weddell. "Screening Investigation of Materials For Ultrahigh-Temperature Ceramics." AFWAL-TR-88-4048, Wright-Patterson Air Force Base, Ohio. (1989)

124. L. Kaufman and H. Nesor. "Additional Studies." Part V in Stability Characterization of Refractory Materials Under High Velocity Atmospheric Flight Conditions. AFML-TR-69-84. (1970)

125. D.P.H. Hasselman and P.T.B. Shaffer. "Factors Affecting Thermal Shock Resistance of Polyphase Ceramic Bodies." WADD-TR-60-749, Part II, Wright-Patterson Air Force Base, Ohio. (1962)

126. K. Vedula. "Ultrahigh-Temperature Ceramic-Ceramic Composites." WRDC-TR-89-4089, Wright-Patterson Air Force Base, Ohio. (1989)

127. H. S. Edward, A. F. Rosenburg, and J. T. Bittel. "Thorium Oxide Diffusion of Oxygen, Compatibility with Borides, and Feasibility of Coating Borides by Pyrohydrolysis of Metal Halides." ASD-TR-63-635. (1963)

128. J. D. Lee. "Ultrahigh Temperature Composites Concepts Evaluation." AFWAL-TR-88-4114, Wright-Patterson Air Force Base, Ohio. (1988)

129. R. A. Marra and D. J. Bray. "Thermochemical Characterization of SiC Whiskers in Al_2O_3 Matrices." Proceedings of the 10th Annual Conference on Composites and Advanced Ceramic Materials, Jan. 19-24, 1986, Cocoa Beach, Florida, pp. 945-946. (1986)

130. W. P. Borom, M. K. Brun, and L. E. Szala. "Kinetics of Oxidation of Carbide and Silicide Dispersed Phases in Oxide Matrixes." Proceedings of the 11th Annual Conference on Composites and Advanced Ceramic Materials. Ceram. Eng. Sci. Proc. 8(7-8):654-670. (1987)

131. K. L. Luthra. "Oxidation of SiC - Containing Compounds." Proceedings of the 11th Annual Conference on Composites and Advanced Ceramic Materials Ceram. Eng. Sci. Proc. 8(7-8):649-653. (1987)

132. E. E. Hermes and R. J. Kerans. "Degradation of NonOxide Reinforcement and Oxide Matrix Composites." Mat. Res. Soc. Symposium Proc. (125):93-94. (1988)

133. J. C. Bowker. "Oxide Matrix Composite Systems." WRDC-TR-89-4017. (1989)

134. R. L. Fleischer. "High-Temperature, High-Strength Materials - An Overview." J. Met 37(12):16-20. (1985)

135. J. Schlichting and S. Neuman. "GeO_2/SiO_2 Glasses from Gels to Increase the Oxidation Resistance of Porous Silicon-Containing Ceramics." J. of Non-Crystalline Solids 49:185-194. (1982)

136. J. Schlichting. Report No BMVG-FBWT-79-32. (1979)

137. H. Schmalzried and W. Laqua. "Multicomponent Oxides in Oxyyen Potential Gradients." Oxid. of Metals 15(3/4):339-353. (1981)

138. J. A. DiCarlo. "Creep of Chemically Vapor Deposited SiC Fibers." J. Mater. Sci. 21:217-224. (1986)

139. C. H. Carter, R. F. Davis, and J. Bentley. "Kinetics of High-Temperature Creep in Silicon Carbide: II, Chemically Vapor Deposited." J. Am. Ceram. Soc. 67(11):732-740. (1984)

140. J. Lipowitz, J. A. Rabe, and G. A. Zonk. "Crystalline Silicon Fibers Derived from Organosilicon Polymers." Proceedings of 2nd Annual HiTemp Review, NASA Conference Publication 10039, pp. 71(1-6). (1989)

141. L. Kaufman and E. V. Clougherty. "Investigation of Boride Compounds for Very High-Temperature Applications." RTD-TDR-63-4096, Part I. (1963)

142. L. Kaufman and E. V. Clougherty. "Investigation of Boride Compounds for Very High-Temperature Applications." RTD-TDR-63-4096, Part II. (1965)

143. L. Kaufman and E. V. Clougherty. "Investigation of Boride Compounds for Very High-Temperature Applications." RTD-TDR-63-4096, Part III. (1966)

144. E. V. Clougherty, D. Kalish, and E. T. Peters. "Research and Development of Refractory Oxidation Resistant Diborides." AFML-TR-68-190, Wright-Patterson Air Force Base, Ohio. (1968)

145. E. V. Clougherty. "Research and Development of Refractory Oxidation Resistant Diborides, Part II, Volume I: Summary." AFML-TR-68-190, Wright-Patterson Air Force Base, Ohio. (1970)

146. E. V. Clougherty, R. H. Hill, W. H. Rhodes, and E. T. Peters. "Research and Development of Refractory Oxidation Resistant Diborides, Part II, Volume II: Processing and Characterization." AFML-TR-68-190, Part II, Volume II, Wright-Patterson Air Force Base, Ohio. (1969)

147. E. V. Clougherty and E. T. Peters. "Research and Development of Refractory Oxidation Resistant Diborides, Part II, Volume III: Thermochemical Stability Characteristics," AFML-TR-68-190, Wright-Patterson Air Force Base, Ohio. (1969)

148. W. H. Rhodes, E. V. Clougherty, and D. Kalish. "Research and Development of Refractory Oxidation Resistant Diborides, Part II, Volume IV: Mechanical Properties." AFML-TR-68-190, Part II, Volume IV, Wright-Patterson Air Force Base, Ohio. (1969)

149. E. V. Clougherty, K. E. Wilkes, and R. P. Tye. "Research and Development of Refractory Oxidation Resistant Diborides, Part II, Volume V: Physical, Thermal, Electrical and Optical Properties." AFML-TR-68-190, Wright-Patterson Air Force Base, Ohio. (1969)

150. E. V. Clougherty, D. E. Niesz, and A. L. Mistretta. "Research and Development of Refractory Oxidation Resistant Diborides, Part II, Volume VI; Thermal Stress Resistance." AFML-TR-68-190, Part II, Volume VI, Wright-Patterson Air Force Base, Ohio. (1969)

151. E. V. Clougherty and F. M. Anthony. "Research and Development of Refractory Oxidation Resistant Diborides, Part II, Volume VII; Application Evaluations and Design Considerations." AFML-TR-68-190, Part II, Volume VII, Wright-Patterson Air Force Base, Ohio. (1969)

152. L. Kaufman and H. Nesor. "Summary of Results." Part I-I in Stability Characterization of Refractory Materials Under High Velocity Atmospheric Flight Conditions, AFML-TR-69-84, Wright-Patterson Air Force Base, Ohio. (1970)

153. L. Kaufman and H. Nesor. "Facilities and Techniques Employed For Characterization of Candidate Materials." Part II-I in Stability Characterization of Refractory Materials Under High Velocity Atmospheric Flight Conditions, AFML-TR-69-84, Wright-Patterson Air Force Base, Ohio. (1970)

154. L. Kaufman and H. Nesor. "Facilities and Techniques Employed For Cold Gas/Hot Wall Tests." Part II-II, in Stability Characterization of Refractory Materials Under High Velocity Atmospheric Flight Conditions, AFML-TR-69-84, Wright-Patterson Air Force Base, Ohio. (1970)

155. L. Kaufman and H. Nesor. "Facilities and Techniques Employed For Hot Gas/Cold Wall Tests." Part II-III in Stability Characterization of Refractory Materials Under High Velocity Atmospheric Flight Conditions, AFML-TR-69-84, Wright-Patterson Air Force Base, Ohio. (1970)

156. L. Kaufman and H. Nesor. "Experimental Results of Low Velocity Cold Gas/Hot Wall Tests." Part II-I in Stability Characterization of Refractory Materials Under High Velocity Atmospheric Flight Conditions, AFML-TR-69-84, Wright-Patterson Air Force Base, Ohio. (1970)

157. L. Kaufman and H. Nesor. "Experimental Results of High Velocity Cold Gas/Hot Wall Tests." Part III-II in Stability Characterization of Refractory Materials Under High Velocity Atmospheric Flight Conditions, AFML-TR-69-84, Wright-Patterson Air Force Base, Ohio. (1970)

158. L. Kaufman and H. Nesor. "Experimental Results of High Velocity Hot Gas/Cold Wall Tests." Part III-III in Stability Characterization of Refractory Materials Under High Velocity Atmospheric Flight Conditions, AFML-TR-69-84, Wright-Patterson Air Force Base, Ohio. (1970)

159. L. Kaufman and H. Nesor. "Theoretical Correlation of Material Performance with Stream Conditions." Part IV-I in Stability Characterization of Refractory Materials Under High Velocity Atmospheric Flight Conditions, AFML-TR-69-84, Wright-Patterson Air Force Base, Ohio. (1970)

160. L. Kaufman and H. Nesor. "Calculation of the General Surface Reaction Problem." Part IV-II in Stability Characterization of Refractory Materials Under High Velocity Atmospheric Flight Conditions, AFML-TR-69-84, Wright-Patterson Air Force Base, Ohio. (1970)

161. K. Motzfeldt. "On the Rates of Oxidation of Silicon and of Silicon Carbide in Oxygen, and Correlation With Permeability of Silica Glass." Acta Chemica Scandinavica 18:1596-1606. (1964)

162. K. Muehlenbachs and H. A. Schaeffer. "Oxygen Diffusion in Vitreous Silica-Utilization of Natural Isotopic Abundances." Canadian Mineralogist 15:179-184. (1977)

163. E. L. Williams. "Diffusion of Oxygen in Fused Silica." J. Amer. Cer. Soc. 48:190-194. (1965)

164. J. M. Criscione, H. F. Volk, J. W. Nuss, B. A. Mercuri, S. Sarian, and F. W. Mezaros. "High-Temperature Protective Coatings For Graphite." ML-TDR-64-173, Part II. (1964)

165. J. M. Criscione, et al. "High-Temperature Protective Coatings For Graphite." ML-TDR-64-173, Part III. (1965)

166. J. M. Criscione, et al. "High-Temperature Protective Coatings For Graphite." ML-TDR-64-173, Part IV. (1966)

167. R. E. Yeager. Courtesy of LTV Aerospace Corporation.

168. D. T. Vier. "Thermal and Other Properties of Refractories." LA-5937-MS, Los Alamos Scientific Laboratory, Los Alamos, New Mexico. (1975).

APPENDICES

Summaries of twenty UHT programs funded by the Air Force in support of the Integrated High-Performance Turbine Engine Technology Initiative are included in the Appendices A through D. These studies, initiated in 1986 and 1987, were small (~$100 k/yr) one- and two-year efforts intended to assess the potential of a broad range of candidate constituents and composite systems to operate above 1650°C. The objective of each study was to address some fundamental or performance limiting issue. Prior Air Force studies are covered in Appendix F. A cross reference of topical categories by page numbers is shown below:

MATERIAL	RESEARCH TOPIC				
	THERMO-DYNAMICS	COMPATIBILITY	MECHANICAL PROPERTIES	OXIDATION AND OXYGEN DIFFUSION	THERMAL-STABILITY
Borides	A3,A5,A14	A3,A5,A7,A17 B15	B2,F2	A5,A17,B 5 D2,D4,F2	A7,A14,B2 F2
Carbides	A3,A5,A14	A3,A5,A7	F2	A5,B17,D4 D6	A7,A14
Nitrides	A3,A5	A3,A5	B2	A5	B2
Oxides	A3,A5,A9 A11,A14 B13	A3,A5,A7,A9, A11,A17,B8,B15	B8,B10,C2	A5,A11,B13 B15,E2,E5, E7,E9	A7,A9.A14 B2,B6,B8 E2,E5
Reinforce-ments		B6,B8	C2		B6,B13
Composites		B2,B15	B2,B10,F2	B2,B17,F2	B2,B10 B15

APPENDIX A

COMPATIBILITY STUDIES

Ceramic composites are typically composed of two or more materials with different properties. Most composites are designed so that the reinforcement, in combination with the matrix, enhances the structural performance and reliability of the material.

Compatibility issues determine which systems are feasible. For example, the fiber/matrix interface must exhibit thermochemical stability to prevent undesirable reactions and by-products that could influence mechanical behavior considerations. Many of the prospective fiber reinforcement materials (e.g., SiC, TiB_2, carbon, etc.) are susceptible to oxidation. Fiber properties can deteriorate even while embedded in an oxidation-resistant matrix if oxygen permeates or forms undesirable reaction products.

Differential thermal expansion between the fiber and matrix is a major factor in mechanical performance. Induced stresses depend upon the degree of bonding between the two phases and the processing temperatures employed. These can either enhance or detract from structural stability at operating temperatures. The initial criterion for materials selection in UHT composite studies is often melting point. Strength and modulus rapidly decrease with increasing T/T_{melt} and chemical reactivity increases. Chemical compatibility is a major selection criterion in all UHT considerations.

The objective of the programs summarized in Appendix A was to identify material systems that are thermodynamically compatible at ultrahigh temperatures and suggest possible ceramic composite systems for future development. In many cases, powdered mixtures were heated to high temperatures in inert environments and their reactivity was studied by conventional analytical techniques (e.g., XRD, SEM, TGA, DTA, etc.). These results often revealed only the most incompatible combinations. Environmental considerations, not the least of which is oxidation, can destroy otherwise stable interfaces. This situation is demonstrated for C/Al_2O_3, C/Y_2O_3, TiB_2/ZrO_2 and other combinations. In a structural composite, where the fiber/matrix interface controls

many of the properties, even limited interface diffusion can significantly alter properties. These important, but subtle, effects are generally not revealed in these basic compatibility studies which, for the most part, attempted to identify major instabilities.

CHEMICAL COMPATIBILITY OF MATERIAL COMBINATIONS

DuPont
Wilmington, Delaware
Principal Investigator: J. K. Weddell
Report: AFWAL-TR-88-4048

The thermochemical and thermomechanical stability for more than 170 pairs of materials were initially considered. Selections for further evaluation were based on the ability to withstand high temperatures, coefficient of thermal expansion match, and chemical compatibility. The list was narrowed to 35 pairs, based on the initial thermodynamic calculations.

Starting materials for the constituents in each of the 35 pairs were characterized by OES, XRF, XRD, SEM/EDX. These analytical techniques were also employed to evaluate changes after heating intimately mixed compounds through various stages to 2200°C. The results rank potential high-temperature materials pairs, as shown in Figure A.1.

Four potential composite systems that undergo no significant change to 2200°C were identified. Six other systems showed some reaction by X-ray diffraction, but no TGA/DTA degradation, and twelve systems exhibited some degree of change between 1650°C and 2200°C, but the reactions may not be severe enough to affect performance significantly. Three pairs seem particularly noteworthy because they also exhibit a very good CTE match: HfB_2/TaB_2, ZrO_2/HfB_2, and TiC/ZrO_2. Two of these are of particular interest because they involve a nonoxide reinforced/oxide matrix system.

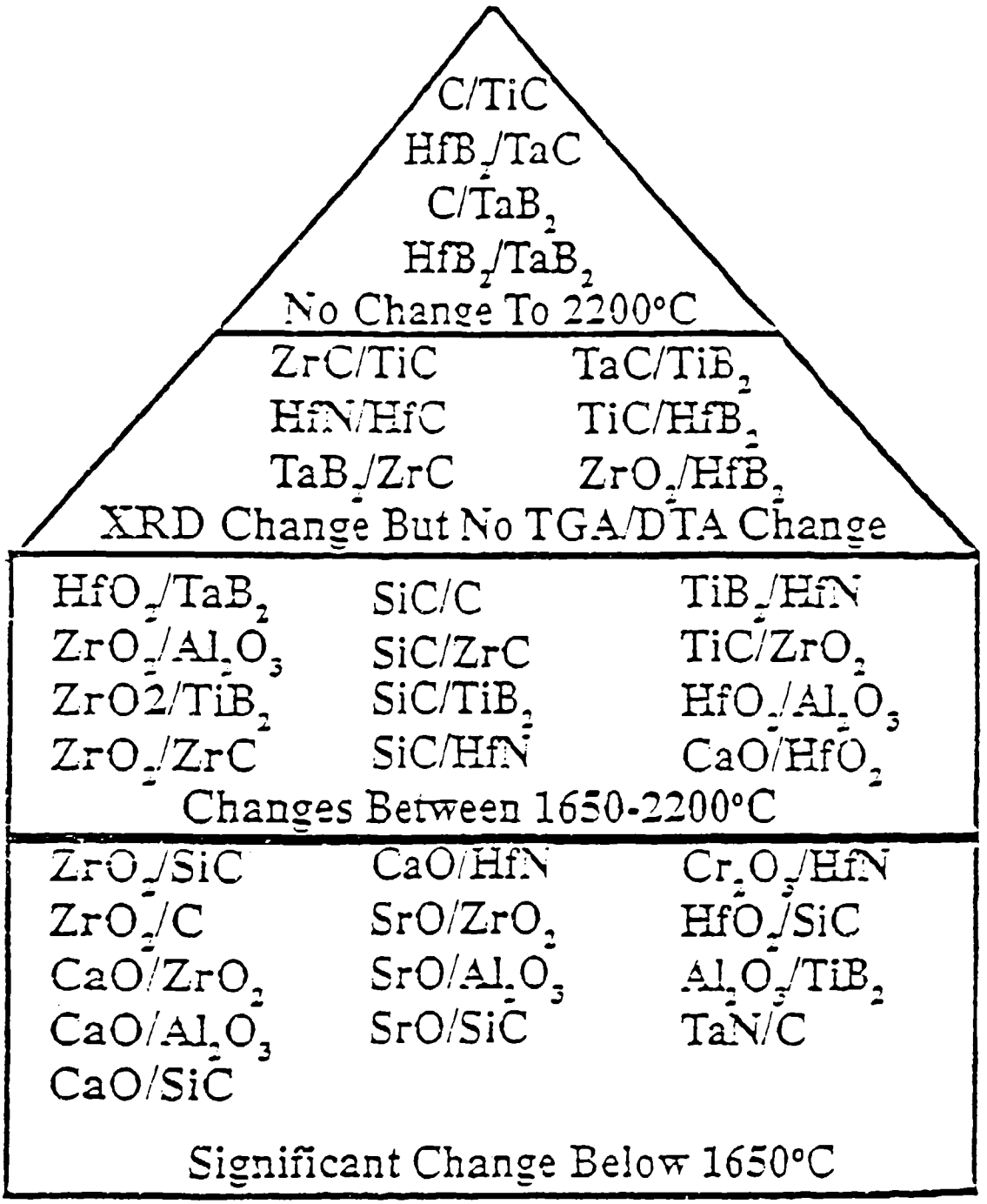

FIGURE A.1. Ranking of High-Temperature Material Pairs (Ref. 123)

CHEMICAL AND OXIDATIVE STABILITY OF SELECTED MATERIALS

Wright State University
Dayton, Ohio
Principal Investigator: G. M. Mehrota
Report: WRDC-TR-90-4127

In this work, the oxidation and chemical compatibilities (in vacuum) of several prospective composite systems were investigated. Titanium carbide (TiC) was not compatible with zirconium diboride (ZrB_2) above 1535°C or with hafnium diboride (HfB_2) at or above 1900°C. Aluminum nitride (AlN) appeared to be compatible with zirconium diboride (ZrB_2) and hafnium diboride (HfB_2) to 1900°C, but $MoSi_2$ was only compatible with the same diborides to 1570°C. The carbide-oxide pairs ZrC-ZrO_2 and HfC-HfO_2 both appeared to be chemically compatible up to 2000°C.

Compacts prepared by hot-pressing 50 vol% of each phase were not fully dense. Characterization was performed by X-ray diffraction and microscopic examination (optical SEM, EDX). Diffusion couples of TiC and ZrB_2 (or HfB_2) were prepared by embedding a TiC compact in ZrB_2 (or HfB_2) powder, followed by hot-pressing. Some low-temperature (1000°C) oxidation tests were performed. While this temperature is below the range of principal interest, the results provided some indication of oxidative stability. Hot-pressed specimens of ZrB_2, HfB_2, SiB_6, 50% AlN - 50% ZrB_2, 50% $MoSi_2$ - 50% ZrB_2, 50% AlN - 50% HfB_2, 50% $MoSi_2$ - 50% HfB_2, 50% ZrC - 50% ZrO_2, and 50% HfC - 50% HfO_2 all oxidized significantly at 1000°C in air. Weight gains per unit area were the least for composites containing $MoSi_2$ and maximum for the specimens of 50% ZrC - 50% ZrO_2 and 50% HfC - 50% HfO_2. The rate of oxidation for TiN dispersed in a matrix of ZrO_2 was found to be greater than for pure TiN alone.

X-ray diffraction results for hot-pressed and oxidized specimens are presented in Table A.1.

TABLE A.1. X-Ray Diffraction Results for Hot-Pressed and Oxidized Specimens

Composition	Phases Identified	
	Unoxidized	Oxidized (1000°C)
100 TiC	TiC	
100 ZrB_2	ZrB_2	ZrO_2 (monoclinic), ZrB_2, B_2O_3 ? (one broad peak)
100 HfB_2	HfB_2	HfO_2 (monoclinic), HfB_2 (only one peak)
100 TiB_2	TiB_2	TiO_2 (rutile), Ti_4O_7, TiB_2 (low intensity)
100 SiB_6	SiB_6	
100 ZrC	ZrC	
100 TiN	TiN	TiO_2 (rutile)
100 $MoSi_2$	$MoSi_2$	$MoSi_2$, SiO_2 (one peak only)
100 AlN	AlN	
100 ZrO_2	ZrO_2	
50 TiC-ZrB_2	ZrC, TiB_2, TiC	
50 TiC-HfB_2	HfC, TiB_2	
50 ZrC-TiB_2	ZrC, TiB_2	
50 HfC-TiB_2	HfC, TiB_2	
50 AlN-ZrB_2	AlN, ZrB_2	ZrO_2 (monoclinic), AlN, ZrB_2
50 AlN-HfB_2	AlN, HfB_2	
50 $MoSi_2$-ZrB_2	$MoSi_2$, ZrB_2	ZrO_2 (monoclinic), B_2O_3, SiO_2, (low intensity peaks), ZrB_2 (broad peaks), $MoSi_2$
50 $MoSi_2$-HfB_2	$MoSi_2$, HfB_2	
50 ZrC-ZrO_2	ZrC, ZrO_2	
50 HfC-HfO_2	HfC, HfO_2	
50 TiN-ZrO_2	TiN, ZrO_2	TiO_2 (rutile), ZrO_2 (mono.)
50 SiB_6-ZrB_2	ZrB_2, only one peak of SiB_6	
50 SiB_6-HfB_2	HfB_2, SiB_6 (only one peak)	
50 TiC-AlN	TiC, AlN	
50 SiB_6-TiC	TiC, TiB_2, SiB_6 (only one peak)	TiO_2

DIFFUSION STUDIES OF NONOXIDE/OXIDE SYSTEMS

Westinghouse R&D
Pittsburgh, Pennsylvania
Principal Investigator: J. C. Bowker
Report: WRDC-TR-89-4017

This program determined the compatibility in argon of several borides and carbides with $SrZrO_3$ and Y_2O_3. The objective was to identify reactions between potential oxide matrices and nonoxide reinforcement candidates using diffusion couples. Argon purity was reportedly very good because of the gettering action of the host molybdenum containment tube.

High-density materials were prepared by (a) direct carbonization of metal to form carbides, (b) hot-pressing and HIPing diboride powders, and (c) sintering in air to make oxide samples. Sample couples were reacted for 64 and 171 hours at 1750°C in argon. Results for the 64 hour samples are presented in Table A.2. The best compatibility was shown between TaC and Y_2O_3, for which a reaction rate constant of $8.1 \times 10^{-13} cm^2/s$ was deduced. Reaction between Y_2O_3 and TaB_2 appears to have been slight, but limitations of post-exposure sample preparation make this result ambiguous.

All other pairs showed moderate or severe reaction. $SrZrO_3$ is unsuitable because of its high vapor pressure. Titanium diboride formed a liquid phase in contact with Y_2O_3. Yttria reacted strongly with materials containing zirconium. Zirconium diboride was less reactive than ZrC. Diffusion coefficients as a function of composition in the Y_2O_3/ZrO_2 system could be determined from the severely reacted 171 hour Y_2O_3/ZrC couple.

TABLE A.2. Relative Reaction After 64 h/1750°C in Argon

Relative Reactivity		
Slight	Moderate	Severe
$SrZrO_3/TiB_2$	$SrZrO_3/ZrC$	$SrZrO_3/TaC$
Y_2O_3/TaC	$SrZrO_3/TaB_2$	Y_2O_3/TiB_2
Y_2O_3/ZrB_2	$SrZrO_3/ZrB_2$	
	Y_2O_3/ZrC	
	Y_2O_3/TaB_2	

VOLATILITY AND MICROSTRUCTURAL STABILITY OF HfO_2, ZrO_2, $CaZrO_3$, and $CaHfO_3$

Ohio State University
Columbus, Ohio
Principal Investigator: J. D. Cawley
Report: AFWAL-TR-88-4008

The stabilities of calcium zirconate ($CaZrO_3$) and calcium hafnate ($CaHfO_3$) were compared with yttria-stabilized hafnia and zirconia. Mass loss by evaporation in air in order of increasing severity was $HfO_2 < ZrO_2 < CaHfO_3 < CaZrO_3$. The high mass losses for both calcium zirconate and calcium hafnate were due to calcium evaporation which, in turn, caused significant deviations from stoichiometry.

Stability studies indicated that the $CaZrO_3$ and 4 m/o yttria-stabilized zirconia undergo disruptive phase changes. However, 8 m/o yttria-stabilized zirconia and yttria-stabilized hafnia could both be heated to 1800°C without evidence of a disruptive transformation.

Grain growth was by far the most extensive in the $CaZrO_3$ samples. This material had the largest grain size under all annealing conditions. A sample of $CaZrO_3$ annealed at 1800°C for 72 hours had an average grain size in excess of 80 μm. Calcium hafnate exhibited grain sizes on the order of 33 μm when fired under similar conditions compared to an average grain size of about 20 μm for yttria-stabilized zirconia and 14 μm for yttria-stabilized hafnia. The average grain size for the hafnia systems as a function of annealing history is shown in Table A.3.

Chemical reactivity with alumina was also measured for $CaZrO_3$ and $CaHfO_3$. The zirconate reacted at 1700°C, whereas there was no reaction between $CaHfO_3$ and Al_2O_3. The reactivity limit for the hafnate was not established due to inconclusive results, but it was suggested to be 1800°C or less.

TABLE A.3. Average Grain Size, in Units of Microns, of Samples in the Hafnia System as a Function of Annealing History Measured on Both the As-Fired Surface and in the Sample Interior

Sample Composition	1600°C 24 h	1800°C 24 h	1800°C 72 h	1800°C 216 h
HfO_2-8.3% Y_2O_3				
Interior	3.99 (1.82)*	12.64 (5.39)	13.56 (6.18)	-
As-Fired Surface	- (3.00)	7.14 (5.78	14.18 (9.94)	26.15
HfO_2-18.3% Y_2O_3				
As-Fired Surface	- (3.13)	6.98 (3.32)	8.29	-
$CaHfO_3$				
Interior	12.41 (7.53)	22.66 (9.94)	32.87 (17.75)	-
As-Fired	-	21.11 (6.42)	22.20	- (13.56)

* Numbers in parentheses represent the standard deviation associated with a best fit of a normal distribution to the data.

CHEMICAL COMPATIBILITY AND MICROSTRUCTURAL STABILITY OF SELECTED MATERIALS

General Electric R&D
Schennectady, New York
Principal Investigator: K. L. Luthra
Report: AFWAL-TR-89-4009

Several key issues associated with interface reactions in potential carbon fiber/oxide matrix and oxide fiber/oxide matrix systems were identified by thermochemical calculations. The program also experimentally evaluated interface reactions with possible coating candidates in these systems.

Thermodynamic analysis was performed to establish the chemical reactions that could be expected between carbon and several oxides, and with many nitrides, borides, intermetallics, and sulfides. The results of chemical reactions with potential oxide matrices are shown in Figure A.2. The criterion used for chemical compatibility was that the equilibrium partial pressure of carbon monoxide (CO) must be less than one bar. Using this criterion, oxides of BeO, Y_2O_3, Al_2O_3, and Ce_2O_3 are least reactive.

Chemical compatibility experiments were performed with two diffusion couples: C/Al_2O_3 and C/Y_2O_3. The diffusion couples were made by imbedding a pyrolytic carbon disk in a hot-pressed oxide powder matrix. They were heated to between 1650°C and 1800°C in argon gas to study chemical compatibility, and in oxygen, to determine the effects of oxygen permeation. Both Al_2O_3 and Y_2O_3 were chemically compatible with carbon after 120 hours at 1650°C when the specimens were heated in an inert (argon) atmosphere; however, when the same samples were exposed to an oxygen environment, severe gas evolution was observed at the carbon/oxide interface and this caused considerable deformation and even fracture in the case of the $C\text{-}Y_2O_3$ buttons. The results illustrate problems associated with oxygen permeability through an oxide matrix that can cause structurally destructive reactions to occur at the fiber interface.

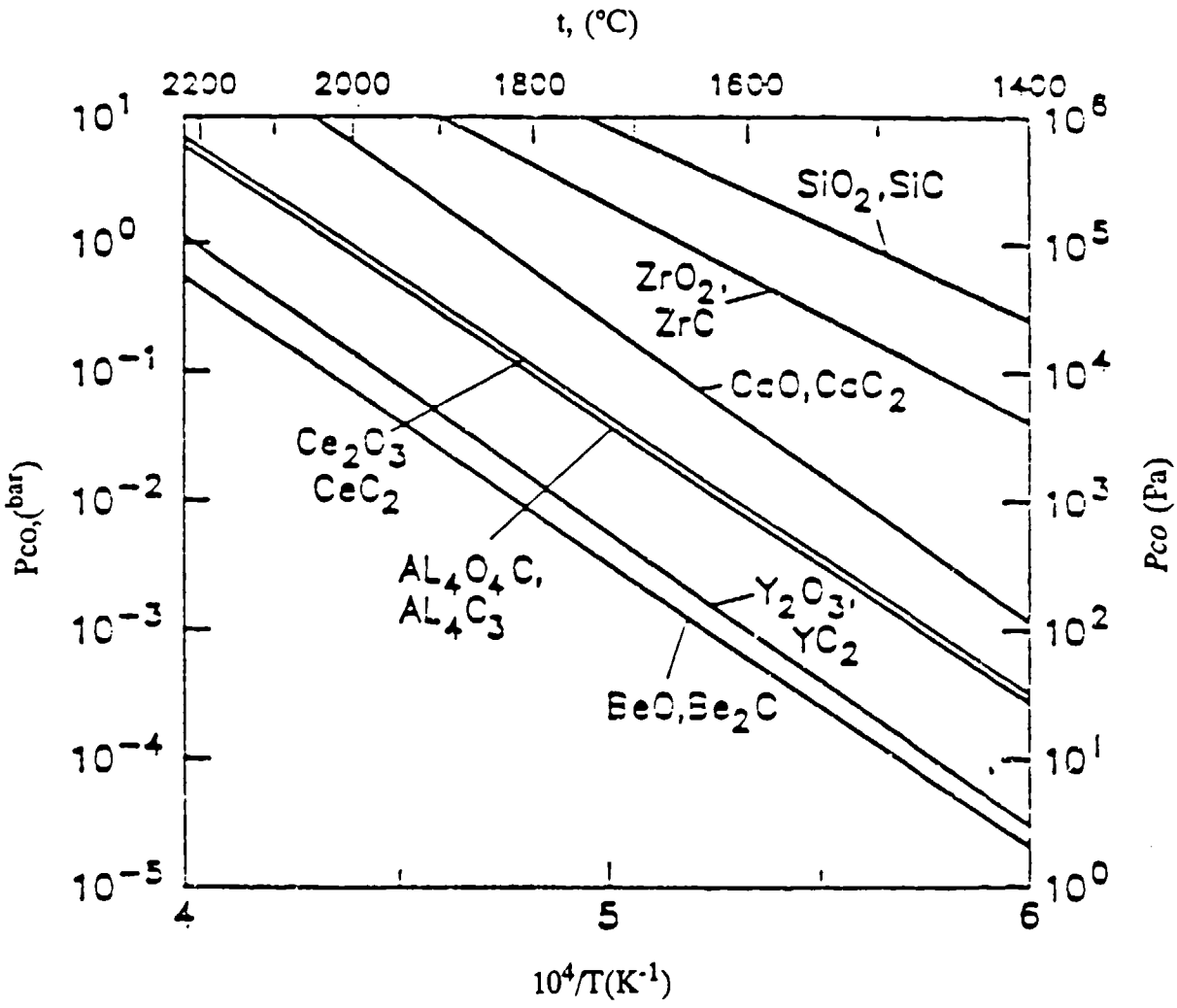

FIGURE A.2. The Equilibrium Partial Pressure of CO for Oxides in Contact with Carbon

Thermodynamic analysis was initially performed to evaluate chemical reactions of oxides with possible fiber coatings. Many metals, intermetallics, borides, and nitrides were considered as candidate coatings. The calculations revealed that while many of the candidates were chemically compatible with oxides, the most attractive coatings were chromium and iridium.

Sputtered coatings were deposited on oxide substrates to confirm the thermochemical stability of chromium and iridium with Al_2O_3, Y_2O_3, and ZrO_2-9.5% Y_2O_3(YSZ). Samples were heated at temperatures up to 1650°C and for times up to 90 hours in argon. No chemical reaction was observed between the

coatings and the oxide substrates. A few attempts to incorporate chromium-coated sapphire fibers in an Al_2O_3 matrix by HIP were unsuccessful because the coating oxidized during processing. However, iridium coated sapphire fibers were successfully embedded in an Al_2O_3 matrix. The iridium-coating was observed to remain stable when samples were exposed at 1650°C for 90 hours in oxygen-contaminated (concentration unspecified) argon.

DETERMINATION OF FUNDAMENTAL THERMODYNAMIC PROPERTIES OF CONSTITUENT MATERIALS AND PERFORMANCE SCREENING OF CANDIDATE SYSTEMS

MSNW
San Marcos, California
Principal Investigators: G. Reynolds/J. Porter
Report: WRDC-TR-89-4035

MSNW, in collaboration with Rice University and the Houston Area Research Center (HARC), examined the applicability of thermochemical modeling, combined with supplemental experimental techniques, for the screening of candidate materials for ultrahigh-temperature composites and for the identification of potential interaction and reaction limitations. The specific experimental techniques employed included mass spectrometric analysis, supplemented by matrix isolation Fourier transform infrared (FTIR); and laser probe spectroscopy. Results obtained from thermodynamic measurements on selected borides, carbides, oxides, and alloys at high temperatures under varying conditions were as follows:

Borides and Carbides

- Metal borides and carbides vaporize under neutral conditions as the atomic metal, boron, and carbon species.
- TiB_2 and HfC begin to react readily with oxygen at temperatures below 1027°C. B_2O_3 and B_2O_2 are evolved at higher temperatures from the boride and carbon monoxide from the carbide.

Metal Oxides

- Strontium zirconate and hafnate lose strontium and oxygen over the temperature range from 1527°C to 2027°C. Above 2027°C, zirconium oxides and hafnium oxides are evolved. The onset temperatures of strontium evolution was observed to increase with oxygen pressure. Under reducing conditions, the strontium evolves at temperatures as low as 1227°C. The vaporization of strontium as a function of temperature is shown in Figure A.3. The reaction $SrO(v) = Sr + 1/2\ O_2$ was assumed and the equilibrium constant defined as $Kp = [(\text{intensity of Sr})*T]^{3/2}$.

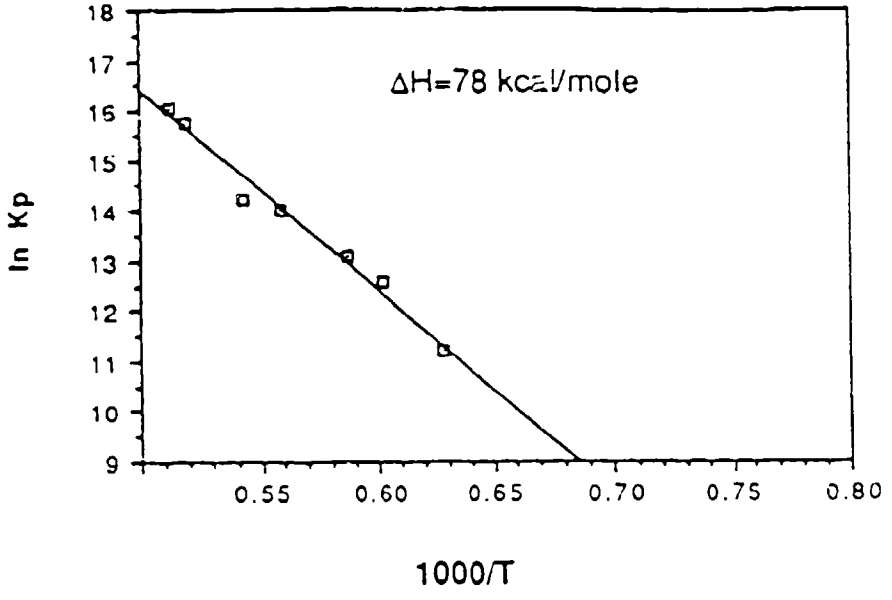

Vaporization of Sr + O_2 from $SrHfO_3$

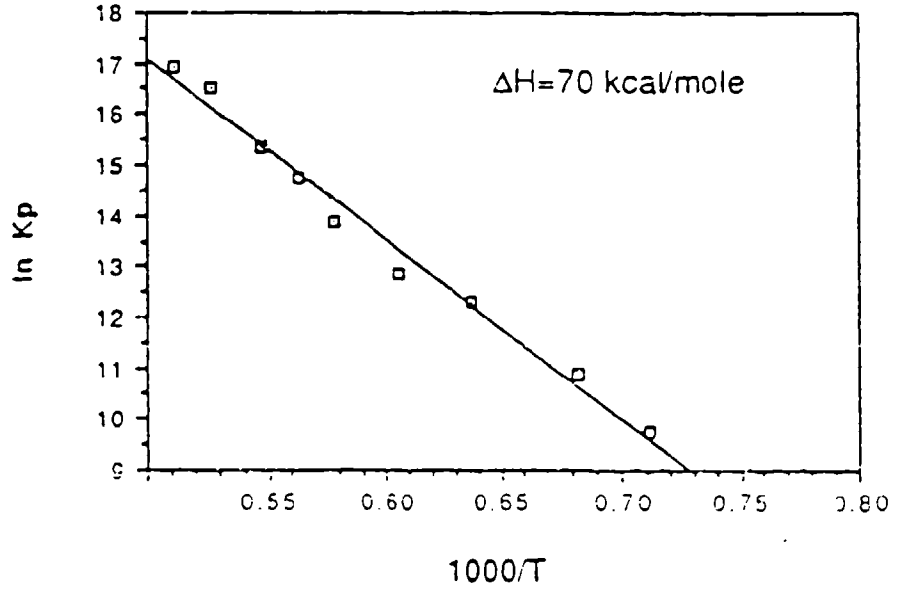

Vaporization of Sr + O_2 from $SrZrO_3$

FIGURE A.3. Vaporization of Sr + O_2 from $SrHfO_3$ and $SrZrO_3$

- Yttria-stabilized zirconia or hafnia vaporize with loss of yttrium, yttrium monoxide, and the respective metals, metal monoxides and metal oxides. Vaporization begins about 2227°C.

Alloys

- Iridium-aluminum alloys ($Ir_{0.4}Al_{0.6}$) preferentially lose atomic aluminum at temperatures below 2027°C. The heat of vaporization of atomic aluminum from the alloy is 2.2 times greater than from elemental aluminum. The presence of oxygen converts atomic aluminum to the Al_2O vapor species.

COMPATIBILITY, STABILITY, AND CREEP OF DIBORIDE/OXIDE SYSTEMS

Case Western Reserve University
Cleveland, Ohio
Principal Investigator: K. Vedula
Report: WRDC-TR-89-4089

This work evaluated potential refractory metal diboride/oxide matrix systems. Particulate composites and diffusion pairs were initially prepared by vacuum hot-pressing. Compatibility studies were then performed in vacuum above 1650°C. Several samples were also induction-heated in air at 1650°C for short periods of time (approximately 15 minutes) to evaluate oxidation resistance.

Neither ZrO_2 nor Y_2O_3 is capable of preventing oxidation of embedded refractory diborides above 1650°C. Oxygen diffused rapidly through the matrix and reacted with the diboride phase to form B_2O_3 vapor, which escaped along the matrix grain boundaries and destroyed the material. See Figure A.4 for schematic of oxidation effects. Aluminum oxide was only slightly better for reducing oxygen ingress. Preliminary tests with $CaZrO_3$ indicated that CaO volatilization was too high to be useful. A $MoSi_2$ + 20% TiB_2 composite formed large amounts of TiO_2 and borosilicate glass when heated in air for 15 minutes at 1600°C.

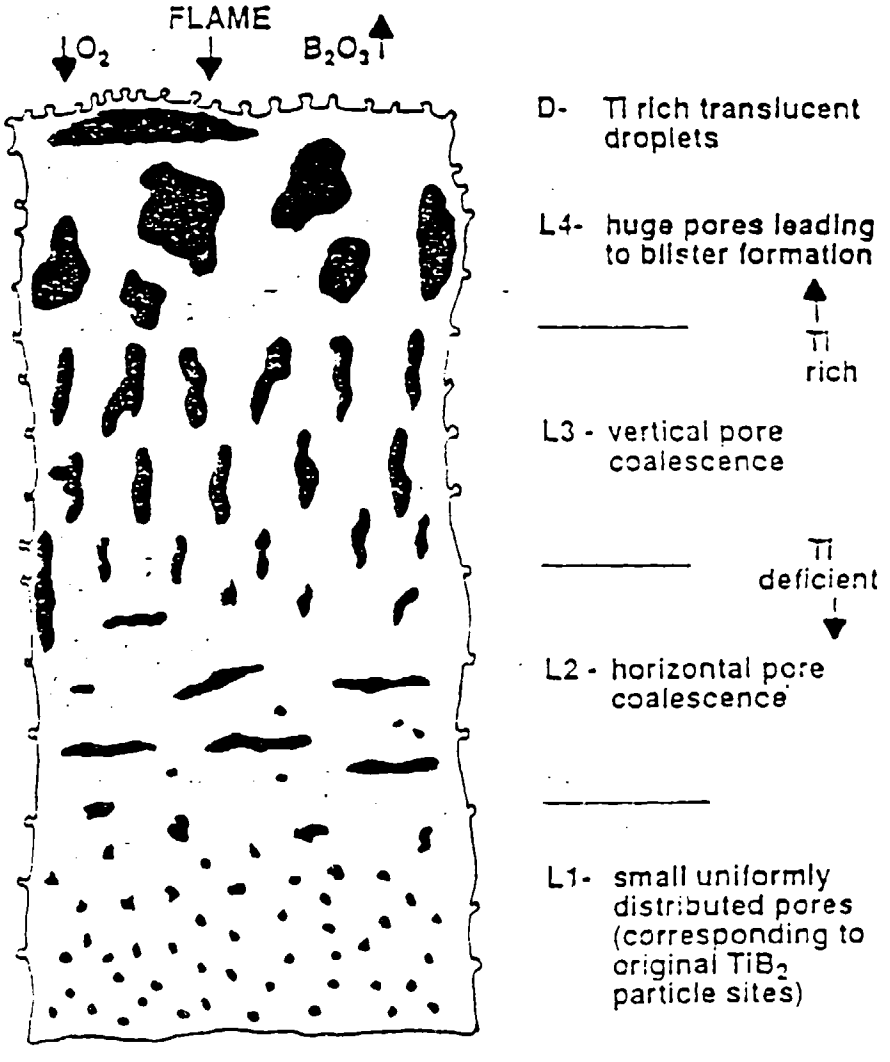

$$TiB_2 + 5/2\ O_2 \rightarrow TiO_2 + B_2O_3$$

FIGURE A.4. Schematic of Oxidation Process Created in Oxyacetylene Flames at 1650°C for Titanium Diboride Particles in a Yttria-Stabilized Zirconia Matrix Composite Specimen

APPENDIX B

PROSPECTIVE COMPOSITE MATERIALS AND SYSTEMS

The four programs summarized in Appendix B studied specific materials that could potentially be developed into composite systems for use in the desired 1650°C to 2200°C service range. Compatibility, strength, and oxidation resistance were evaluated. The initial selections were based on thermodynamic considerations or promising background information. The principal objective of the research was to establish a prior feasibility and to provide supporting data.

PROSPECTIVE COMPOSITES EVALUATED FOR CHEMICAL INTERACTION, OXIDATION, AND CREEP

Babcock and Wilcox
Lynchburg, Virginia
Principal Investigator: J. D. Lee
Report: AFWAL-TR-88-4114

The four composite systems listed in Table B.1 were evaluated for thermal and oxidative stability at 1650°C and 2000°C. Flexural strengths were also measured at 1200°C and 1530°C. The rationale for the selection of the systems investigated was as follows:

Matrix	Reinforcement	Comments
I. AlN-SiC	BN	Reported phase compatibility above 2000°C, low density. Should exhibit oxidation product compatibility with bulk to ~1900°C.
II. ZrB_2-Y_2O_3	ZrC	Representative of M-B-C systems where M = Hf, Zr, Ti. Y_2O_3 included to stabilize cubic phase of ZrO_2.
III. TiB_2	AlN	Phase stability unknown. Ti-Al-B-O oxidation products may provide diffusion barrier to >1800°.
IV. Y_2O_3	TiN	Phase stability unknown. Representative of oxide matrix/nitride reinforcement.

The BN/AlN-SiC system with an AlN-rich composition showed very encouraging results. Boron nitride was added in the form of particulate as opposed to whiskers or fibers, which could increase strength or creep resistance even further. These materials exhibited phase stability to 2000°C and excellent oxidation resistance to 1650°C. The protective scale appears to be Al_2O_3 or perhaps an Al_2O_3-mullite mixture. High-temperature strength retention was quite good and showed little loss between 1200°C (220.7 MPa) and 1525°C (191.7 MPa). Stress-strain curves are presented in Figure B.1. A preliminary

TABLE B.1. B & W Composite Study

Composition Wt. w/o	Hot Press Conditions	Density (g/cc/%TD)	XRD As Fab.	1750°C/5hr Nitrogen	2000°C/5hr Nitrogen	*Oxidation 1200°C/5h 2-3%O_2	(% Wt. Gain) 1650°C/5h 1-2%O_2	Flexural 1200°C MPa	Strength 1530°C MPa
BN_p/AlN-SiC									
I. AlN 67.7 SiC 22.1 BN 10.2	1950°C/ 5 min.	3.09/ 99.4%	AlN,SiC BN	AlN, SiC, BN Amorphous	AlN, SiC, BN	1.5	0.7	32.1	27.8
ZrC_p/Y_2O_3-ZrB_2									
II. ZrB_2 74.6 Y_2O_3 10.9 ZrC 14.5	1850°C 5 min.	6.11/ 100%	ZrB_2.Y_2O_3 ZrC.ZrO_3	ZrO_2.Y_2O_3 ZrC Amorphous	ZrB_2, ZrC Amorphous	4.6	9.6	44.0	15.8
AlN_p/TiB_2									
III. TiB_2 88.7 AlN 11.3	1850°C/ 5 min.	4.23/ 98.1%	TiB_2/AlN TiN	TiB_2, AlN TiN, Amor.	TiB_2 Amorphous	Porous	>50		
TiN_p/Y_2O_3									
IV. Y_2O_3 84.5 TiN 15.5	1520°C/ 5 min.	4.99/ 99.9%	Y_2O_3.TiN	Unstable	Disintigrated				

* Oxidation was performed in a Bickley gas fired furnace with measured oxygen levels as indicated.

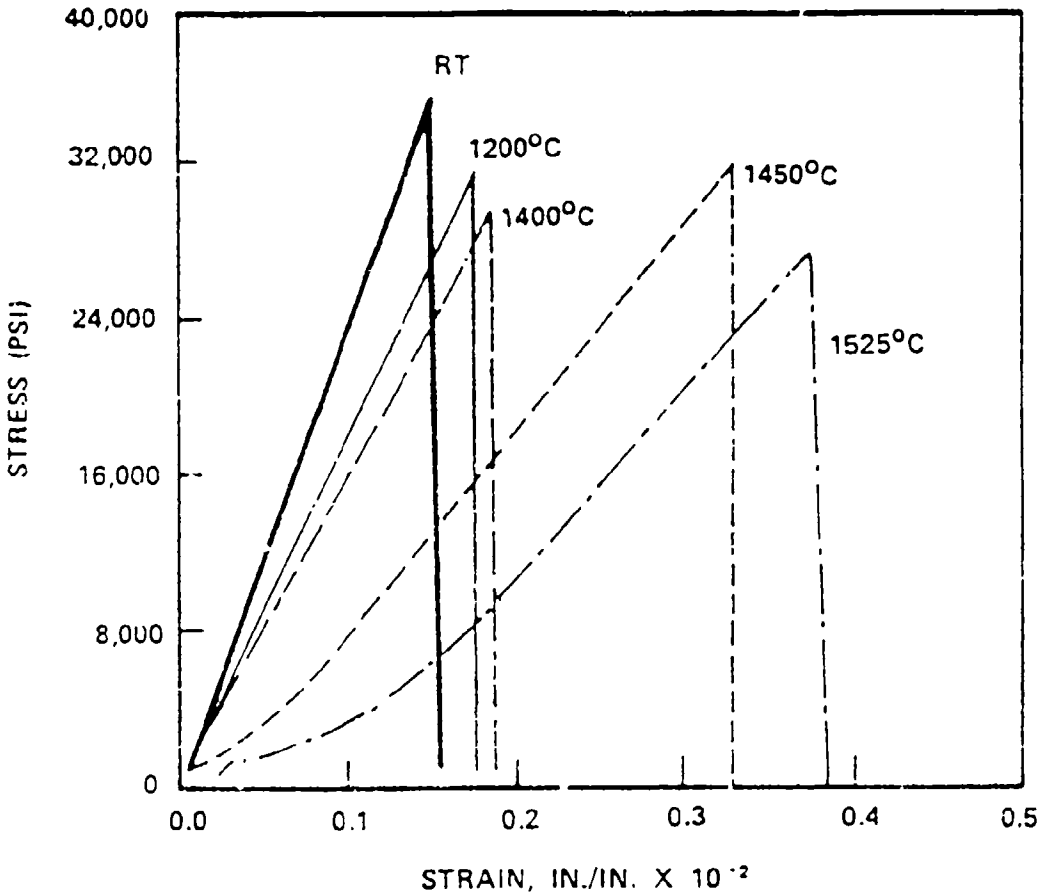

FIGURE B.1. Stress Versus Strain Curves as a Function of Temperature in Air for BN/AlN-SiC Composite

evaluation of creep was made by subjecting samples to compressive loading. Very little deformation occurred up to 1800°C under an applied stress of 186.2 MPa.

The second best composite system consisted of ZrB_2-Y_2O_3/reinforced with ZrC particulate. This composite does not have such good resistance to oxidation, but thermal stability appeared to be adequate.

CHEMICAL AND MICROSTRUCTURAL STABILITY OF ALKALINE EARTH ZIRCONATES

3M - Ceramic Technology Center
St. Paul, Minnesota
Principal Investigators: D. M. Wilson/E. D. Morrison
Report: AFWAL-TR-88-4007

In this investigation, alkaline earth zirconates derived from sol gel precursors were made for a range of $MZrO_3$ compounds where M = Mg, Ca, Sr, or Ba. The flakes were fired to temperatures as high as 1600°C and the resulting microstructures evaluated by optical microscopy, SEM, and XRD.

Alkaline earth carboxylate - colloidal ZrO_2 sol gel mixtures gave ultrafine zirconate microstructures at 800°C; however, grain growth during subsequent densification at 1400°C was quite rapid. A curve of zirconate grain growth is presented in Figure B.2. Trivalent doping with Y^{+3} and Sc^{+3} reduced the sintering rate and hence the grain growth by slowing cation diffusion, but grain enlargement was still significant at high temperatures. On the other hand, this composite appeared to act by reducing cation mobility in the grain boundary region through the formation of oxygen vacancies, thereby lowering boundary mobility. Fe_2O_3 was found to strongly accelerate sintering by a liquid phase mechanism and grain growth was also reduced.

Continuous green fibers were prepared from strontium zirconate with diameters of about 20 μm. Attempts to sinter these into good fibers were not successful due to microstructural instabilities associated with the aforementioned rapid grain growth.

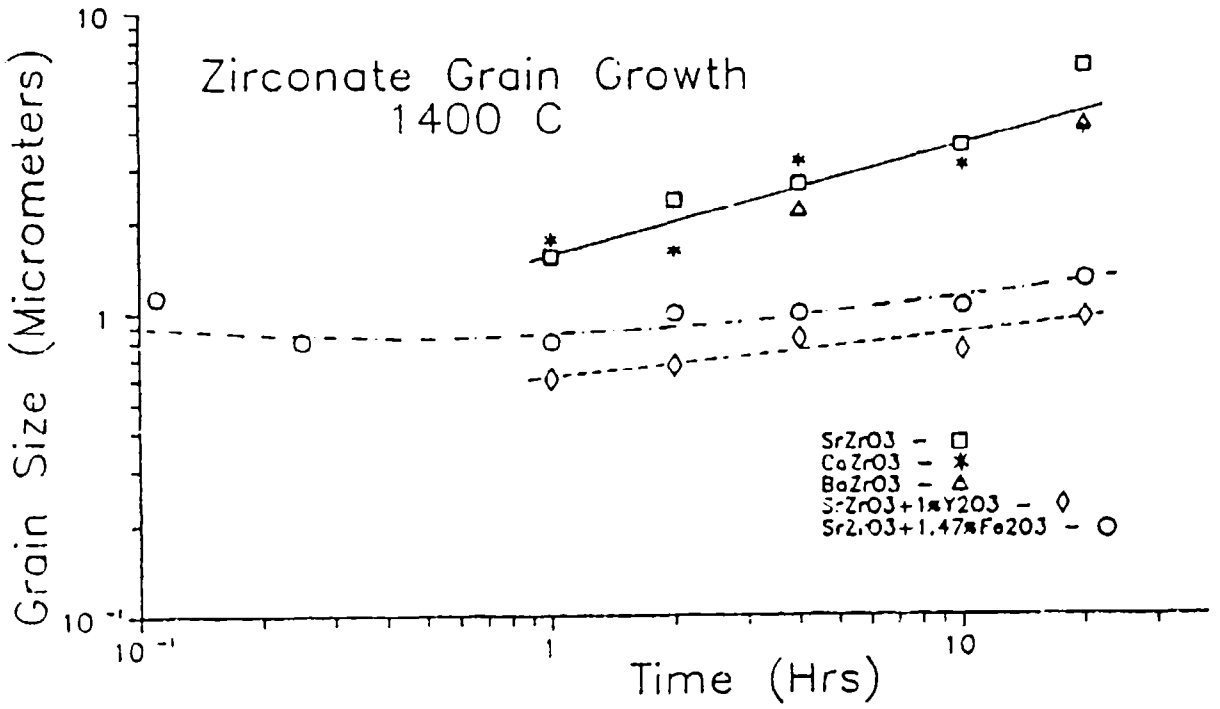

FIGURE B.2. Grain Growth at 1400°C for $CaZrO_3$, $BaZrO_3$, $SrZrO_3$, $SrZrO_3$ + 1% Y_2O_3, and $SrZrO_3$ + 1.47% Fe_2O_3

EVALUATION OF $LaCrO_3$

UCLA
Los Angeles, California
Principal Investigator: J. D. MacKenzie
Report: AFWAL-TR-88-4199

Determining the feasibility of using sol gel methods for the preparation of ceramic oxide fibers with good chemical and mechanical stability above 1650°C in oxidizing atmospheres was a principal goal of this work. After considering several potentially stable high-temperature oxides, efforts were focused towards producing lanthanum chromite ($LaCrO_3$) fibers. Lanthanum chromite was successfully prepared by new solution-based methods, and pre-ceramic precursor fibers were drawn. Discontinuous green fibers or rods could be produced, but small cracks developed during subsequent sintering even though very slow heating and cooling rates were employed. Attempts to draw continuous filaments were not successful.

The stability of $LaCrO_3$ was evaluated by analyzing and characterizing heating elements produced by FUJI SHO for their KERAMAX line of electric furnaces. Analysis showed that the composition, although somewhat variable, could be described by $La_{1-x}Ca_xCrO_3$ where x varied from 0.0038 to 0.0853.

Young's modulus was reported to be 14.2×10^6 psi (97.9 GPa). Oxidative stability was determined, and after 49 hours at 1600°C in air, the weight loss was approximately 0.4 %. Weight losses were improved by a factor of six when the $LaCrO_3$ was coated with aluminum oxide by dipping in an aluminum di (sec butoxide) acetoacetic ester chelate followed by heat treating to 1100°C prior to oxidation exposure. The coating successfully suppressed vaporization of chromia, which can cause loss of structural integrity for this and other chromia containing compounds. A comparison of weight loss for a coated and uncoated $LaCrO_3$ heating element at 1600°C is shown in Figure B.3.

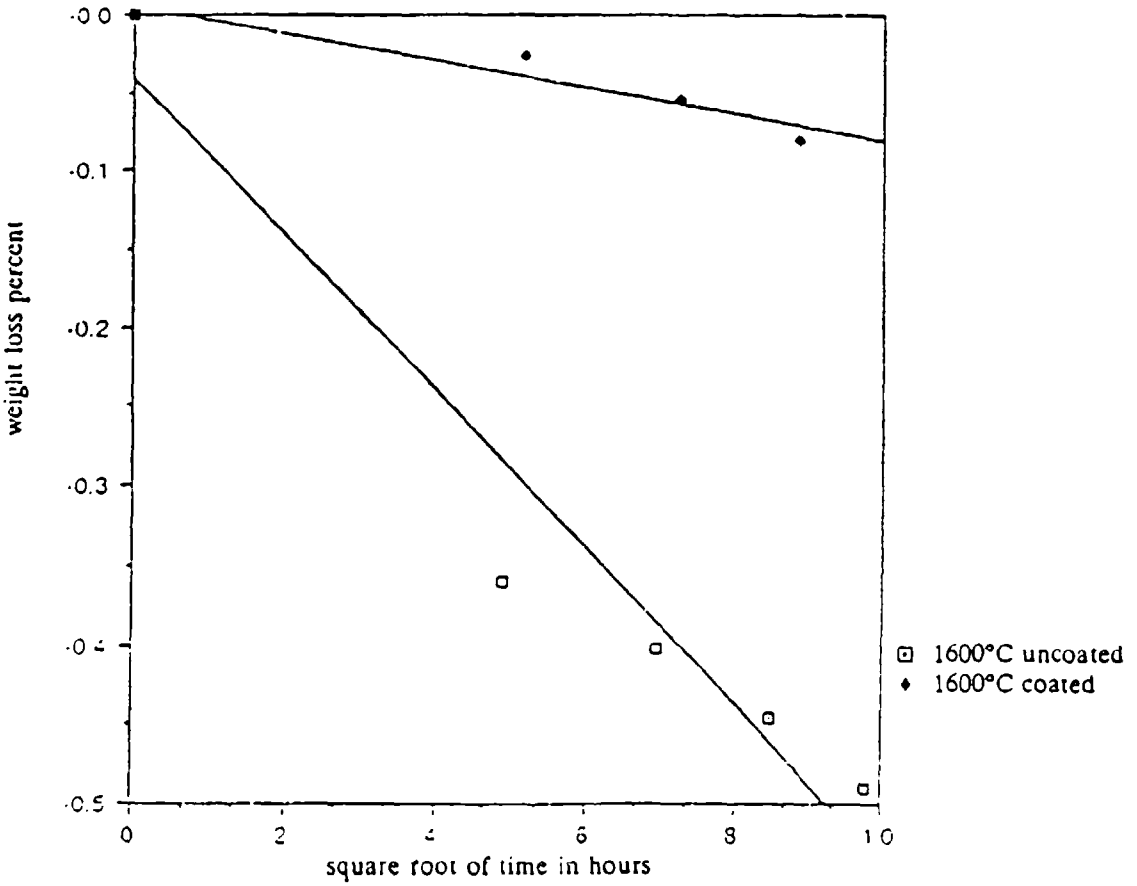

FIGURE B.3. Weight Loss of Al_2O_3 Coated and Uncoated Lanthanum Chromite Heating Element at 1600°C Versus Square Root of Time

MORPHOLOGICAL AND CHEMICAL STABILITY OF Al_2O_3/MULLITE AND DIRECTIONAL SOLIDIFICATION OF OXIDE EUTECTICS

Universal Energy Systems
Dayton, Ohio
Principal Investigator: Tai-Il Mah
Report: AFWAL-TR-88-4015 (Al_2O_3/Mullite)
WRDC-TR-90-4081 (Eutectics)

The first of two programs evaluated the prospects of a single-crystal alumina fiber-reinforced mullite system. Thermochemical stability evaluations showed that while Al_2O_3 dissolves in mullite, the degree of dissolution is quite slow below 1650°C. The sapphire whiskers did not appear to be stable above 1700°C and the whisker reinforced composites degraded after 20 hours at 1650°C in air. Alumina fiber/mullite matrix composites will not likely be suitable for structural applications due to the large difference in thermal expansion (8.8 for Al_2O_3 versus 5.3 x 10^{-6}/°C for mullite) which generates residual stresses sufficient to induce multiple cracking in the fibers.

The second program involved phase studies determining the morphological and chemical stabilities of directionally solidified eutectics. The binary systems consisting of SrO-ZrO_2, CaO-ZrO_2, La_2O_3-Al_2O_3, Y_2O_3-Cr_2O_3, Y_2O_3-ZrO_2 and Al_2O_3/YAG (yttrium aluminum garnet) were selected for evaluation. Initial melting experiments revealed an uncertainty in the eutectic composition of the SrO-ZrO_2 system due to the hydration of $SrZrO_3$. Hydration of calcium oxide also caused low-temperature decomposition in the CaO-ZrO_2 system. This binary oxide system is complicated by the varying solubility of CaO in cubic zirconia with temperature. Lanthana-alumina (La_2O_3-Al_2O_3) proved to be extremely hygroscopic and decomposed after one week of exposure to room temperature and ambient humidity. High vapor pressures of CrO_3 discouraged attempts to melt Y_2O_3-Cr_2O_3.

Good arc melted specimens were made from the Y_2O_3-ZrO_2 system at a composition of 83 m/o Y_2O_3 - 17 m/o ZrO_2. However, subsequent heat treatment at 1625°C and 1750°C in air caused significant degradation and spheroidization of

the eutectic microstructure. The samples had been melted in a Mo-Ta tube at 2400°C in argon and solidified at approximately 40 cm/h.

Eutectic material was made from Al_2O_3-YAG ($Y_3Al_5O_{12}$) at a composition of 81.7 m/o Al_2O_3 - 18.3 m/o Y_2O_3 by melting in molybdenum tubes at 2050°C. The resulting microstructure showed the presence of large Al_2O_3 veins and regions of lamellar eutectic structures that were analyzed by XRD and found to be a metastable eutectic of alumina-$YAlO_3$ (see Figure B.4). When the temperature was lowered to 1950°C, the equilibrium eutectic for alumina-(YAG) was obtained. The composition and microstructure of the Al_2O_3-YAG eutectic remained stable after exposure for 5 hours in air at 1700°C (see Figure B.5).

Flexural strength and the fracture toughness of the Al_2O_3-YAG eutectic were measured in air using four-point-bending and single-edge-notched-beam techniques. The average flexural strengths decreased from 373 MPa at R.T. to 272 MPa at 1375°C and to 265 MPa at 1585°C. Fracture toughness showed little temperature dependence and was reported to be in the range of 4 MPa $\sqrt{m}$.

Constant strain rate compression tests were done on the Al_2O_3-YAG eutectic specimens at 1410°C and 1530°C, and at strain rates ranging from 10^{-5}/s to 10^{-6}/s. The tests were stopped after reaching peak stress and approximately 0.5 to 1% plastic deformation. At 1530°C, the peak stress decreased from 344 MPa at 10^{-5}/s to 139 MPa at 10^{-6}/s.

FIGURE B.4. SEM Photomicrographs of Al_2O_3-$YAlO_3$ Metastable Eutectic Showing Lamellar/Rod Morphology of $YAlO_3$ (Light Phase) and Continuous Alumina (Dark Phase)

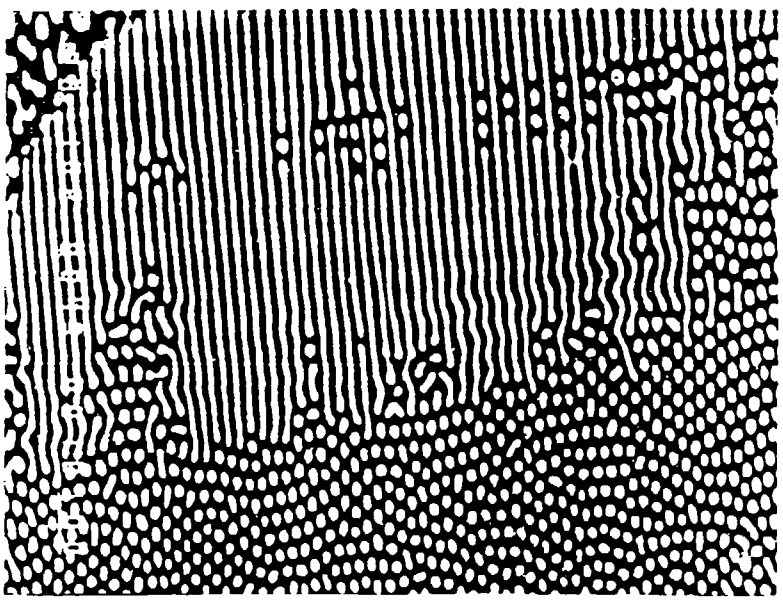

FIGURE B.5. SEM Photomicrographs of Alumina-YAG DS Eutectic After Heat Treatment at 1700°C, 5 hours in Air (Longitudinal Section)

APPENDIX C

HIGH-TEMPERATURE CREEP

Ceramics tend to be weak in tension and extremely strong in compression; thus, many applications are designed accordingly. Creep resistance is perhaps a more important property because creep cannot be easily accommodated in the design and may be a limiting criterion. The rate-controlling mechanisms that dominate creep in ceramics include grain boundary sliding, nucleation of microcracks, porosity in grain boundaries, dislocations, diffusion within grains, and diffusion along grain boundaries.

For composite applications, many of the commercially available fibers are either amorphous or polycrystalline. At very high temperatures, amorphous fibers can degrade by crystallization or creep may be enhanced by viscous flow. Polycrystalline fibers, especially if the grain size is small, often do not exhibit good creep behavior due to grain boundary effects. Single-crystal fibers are, therefore, attractive since grain boundaries can be eliminated and a preferred orientation maximized.

Appendix C summarizes the results of one UHT program that has yielded compressive creep data on several single-crystal oxides. The principal objective of this effort was to identify potential oxide reinforcement candidates for use in composite systems.

CREEP MEASUREMENTS OF SINGLE CRYSTAL OXIDES

General Electric R&D
Schennectady, New York
Principal Investigator: G. S. Corman
Report: WRDC-TR-90-4059

Several refractory oxides were selected for evaluation based on thermal and oxidative stability, high specific modulus, and process-related factors. The experimental approach was to obtain high-purity single-crystals and test them in uniaxial compression using a constant load system. To date, creep data have been obtained for [100], [110], and [111] yttria-stabilized zirconia and for [100], [110] thoria. Creep dependency of yttria-stabilized zirconia single crystals followed the relationship:

$$\epsilon = \frac{A \cdot G}{T} \left[\frac{\sigma a}{G} \right]^n e^{-(Q/RT)}$$

where A is a constant, G is the shear modulus, S is the Schmid factor, σa the applied stress, and Q is the activation energy for diffusion. G can be approximated at high temperatures using the relationship:

$$G = G_0 - \Delta G T$$

where $G_0 \simeq 64.5$ GPa and $\Delta G \simeq 18.6$ MPa/K. A fit to the general creep equation gives n as approximately 4.07 and Q = 436 kJ/mol for [111] and [110] yttria-stabilized zirconia. This activation energy is very close to that for the diffusion of zirconium and suggests a creep mechanism limited by cation diffusion controlled climb. In the case of [100] yttria-stabilized zirconia, the estimated activation energy was found to be slightly higher (497 kJ/mol), and the exponent n changed with increasing stress, indicating a change in mechanism. While the data for thoria also fit the same generalized creep equation, the rate-controlling mechanism does not seem to be as clearly associated

with cation diffusion. The stress limits associated with 1%/1000 h (~2.8 x 10^{-9}/s) creep rates at 1650°C were 14 MPa for [100] yttria-stabilized zirconia and 46 MPa for [100] thoria.

The creep behavior of yttrium aluminum garnet (YAG) for three single-crystal orientations is shown in Figure C.1. These creep rates are significantly (almost three orders of magnitude) lower than those reported for thoria and zirconia for comparable temperatures and stresses. Unusual creep behavior was observed for the [100] and [110] YAG orientation in that there appears to be two regimes and the transition between the regions is dependent on temperature and stress. The stress dependence of the creep rate for the [100] orientation is much lower than for the [110] or [111] direction. The reason for this peculiar behavior is not clear at this point. However, creep in single-crystal YAG appears to be comparable to, or slightly less than, c-axis sapphire, which is very encouraging. Further, the creep rates are significantly less orientation dependent than for sapphire.

Preliminary testing of beryllium oxide produced mixed results. Specimens tested along a [1011] axis (~46° from the c-axis) crept severely at relatively low temperatures. (This behavior is similar to sapphire where orientations that activate basal slip are found to creep easily.) On the other hand, c-axis specimens are so creep-resistant that measurable data have been difficult to obtain.

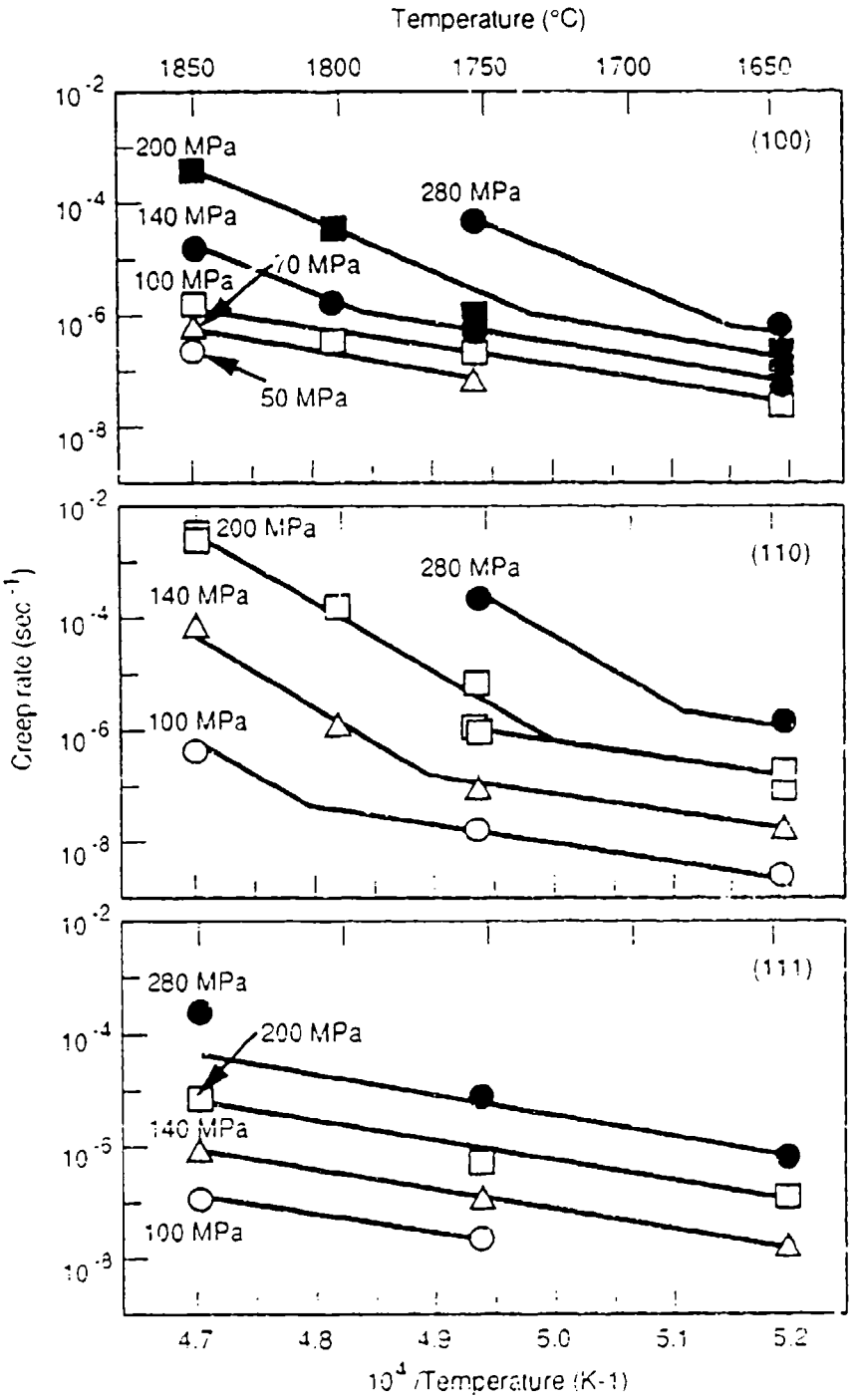

FIGURE C.1. Temperature-Dependent Creep of $Y_3Al_5O_{10}$

APPENDIX D

OXIDATION OF NONOXIDE CERAMICS

Three UHT programs studied the oxidation behavior of borides and carbides to help establish a better understanding of how these, and perhaps other, nonoxide ceramics will perform in oxidizing environments. One study is complementary to the information presented in Appendix F, which is a review of prior Air Force work on diboride/silicon carbide materials.

COMPATIBILITY AND OXIDATION OF REFRACTORY METAL BORIDE/OXIDE COMPOSITES AT ULTRAHIGH TEMPERATURES

University of Texas-El Paso
El Paso, Texas
Principal Investigators: A. Bronson, Yu-Tao Ma, and R. Mutso
Report: WL-TR-91-4060

The objectives of this research were to investigate the effect of silicides on a boride/oxide interface and to determine the oxidation behavior of boride/oxide composites at ultrahigh temperatures.

A reaction couple of $HfO_2/HfSi_2/HfB_2/HfO_2$ was hot-pressed at 2000°C under 4000 psi for 1 hour. The foregoing process created a block of HfO_2-4 wt% Y_2O_3 with an internal core consisting of a boride/silicide couple. The reaction couple was then annealed under high-purity argon at 1800°C (2073K) for 4, 8, 16, and 50 hours to investigate compatibility between phases.

Examination of the boride/silicide and boride/oxide interfaces with optical and scanning electron microscopes revealed distinct interfaces, suggesting no boride reaction with either the oxide or silicide. The reaction couple was analyzed with an electron microprobe for boron. At the boride/silicide and boride/oxide interfaces, a sharp decrease in boron content occurred. At the silicide/oxide interface, a product layer formed and grew with annealing time. The thickness of the product layer was measured along the interface at each annealing time, and followed a parabolic growth pattern, as shown in Figure D.1. The formation of the Hf_2Si in the $HfO_2/HfSi_2/HfB_2$ mixture, as indicated by X-ray diffraction, suggests a reaction between the oxide and silicide.

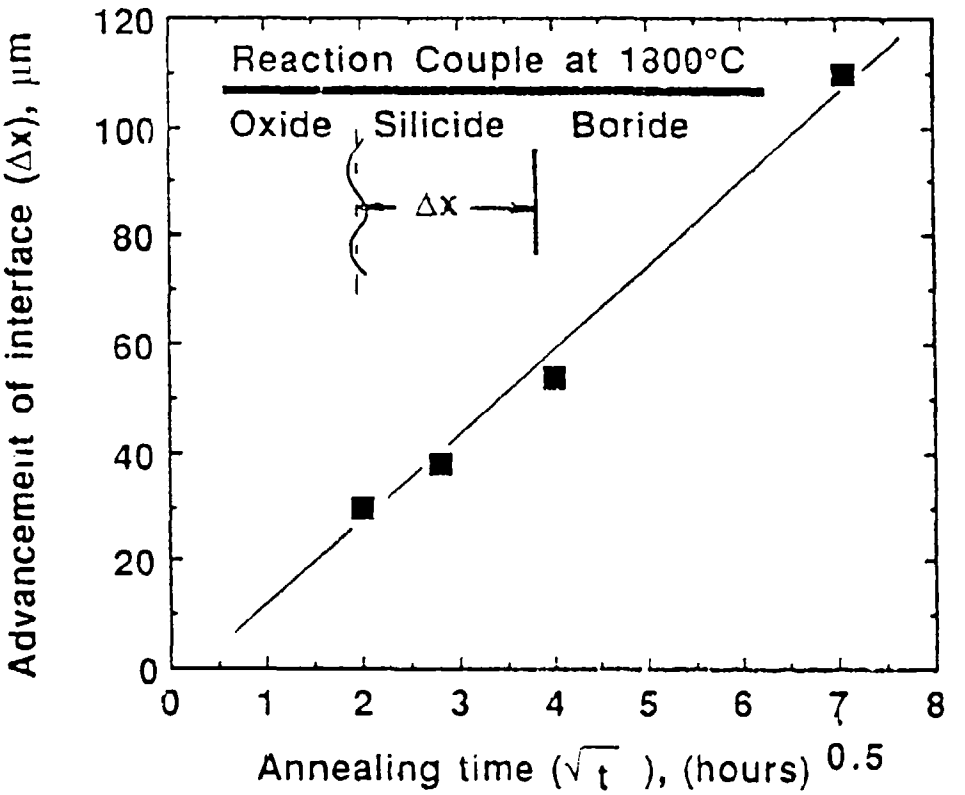

FIGURE D.1. Advancement of the Silicide Interface on a $HfO_2/HfSi_2/HfB_2/HfO_2$ Reaction Couple at 1800°C

DIBORIDE/CARBIDE CERAMICS FOR ELEVATED TEMPERATURE OXIDATION RESISTANCE

Refractory Composites, Inc.
Whittier, California
Principal Investigators: M. Simpson and E. Paquette
Report: WRDC-TR-90-4077

Mixed diboride-silicon carbide composites were oxidation tested in flowing air at temperatures near 2000°C. A 80% hafnium diboride (HfB_2) - 20% silicon carbide (SiC) mixture exhibited the most resistance to oxidation. In general, the mixed $H_f(Zr)B_2$/SiC ceramics lack long-term oxidation stability at these elevated temperatures.

The samples were heated under an argon atmosphere and then subjected to flowing air. As the air reacted with the sample, the surface temperature increased to ~2100°C. An oxide film rapidly formed on the surface and considerable bubbling was observed with the zirconium diborides, and to a lesser extent, on the hafnium systems. A silica-rich surface layer was found over a SiC depletion zone as depicted in Figure D.2, where compositional plots of different species are identified across the oxide layer and conversion zone of a fractured HfB_2 + 20% SiC test coupon. The oxidation rates of both oxide film and depletion zones were measured up to 90 minutes for the hafnium systems.

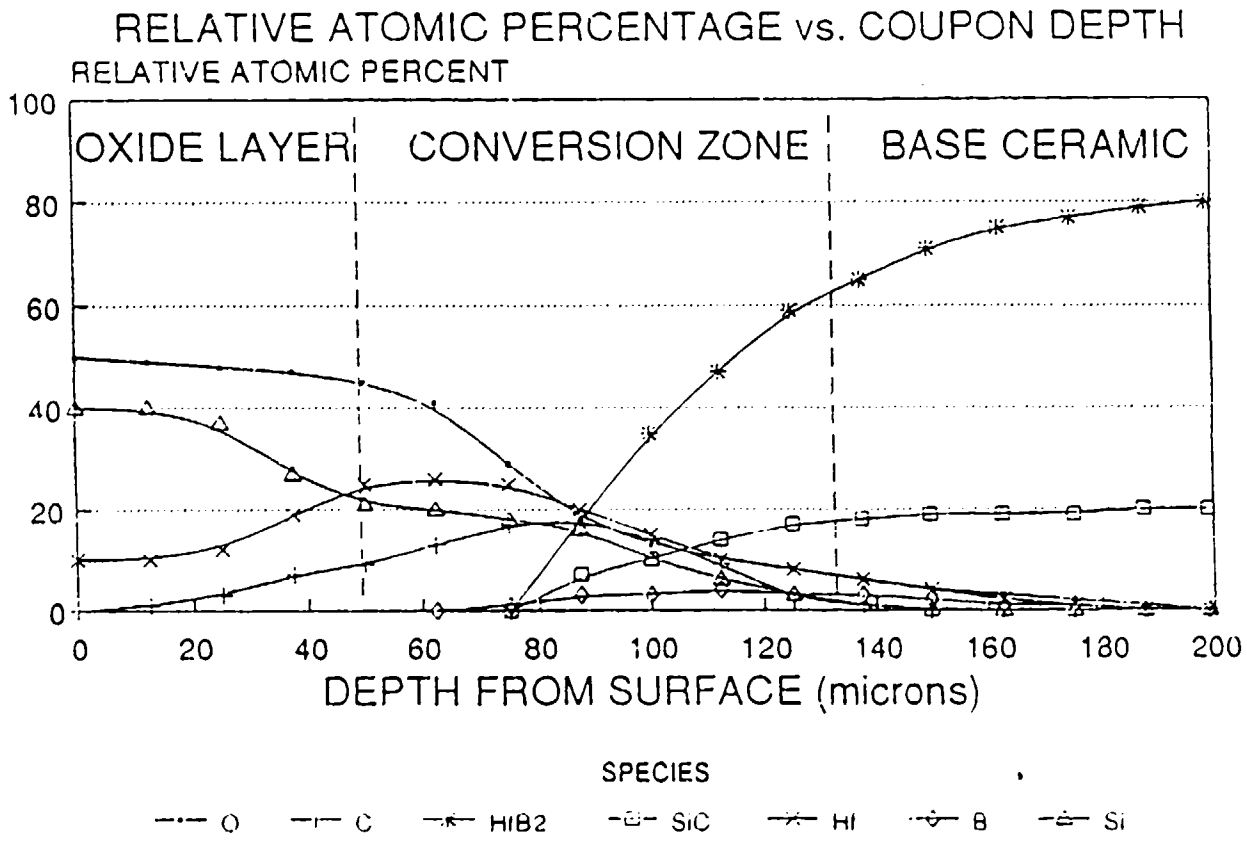

Diboride/Carbide Ceramic Oxidation Test

(1960 C) HfB2 + 20% SiC COUPON (15 min)

FIGURE D.2. Relative Atomic Percentage of Species Across the Oxide Layer and Conversion Zone of HfB_2 + 20% SiC Sample. The coupon had been oxidized at 1960°C for 15 minutes. Data obtained by scanning auger electron spectroscopy.

MODIFICATION OF HAFNIUM CARBIDE FOR ENHANCED OXIDATION RESISTANCE THROUGH ADDITIONS OF TANTALUM AND PRASEODYMIUM

Pacific Northwest Laboratory
Richland, Washington
Principal Investigator: J. T. Prater
and
Ohio State University
Columbus, Ohio
Principal Investigator: G. R. St. Pierre
Report: AFWAL-TR-88-4141

A joint study performed by Pacific Northwest Laboratory and Ohio State University was directed at understanding the oxidation kinetics of HfC. It was postulated that oxidation resistance might be improved by additions of tantalum or praseodymium. Prior work performed on Hf-Ta metallic alloys had indicated that the addition of 20 to 30 wt% tantalum improved the oxidation resistance of pure hafnium. In a tantalum alloy, Hf is internally oxidized to form tetragonal HfO_2, thereby preventing a damaging phase change while promoting the growth of a dense tenacious oxide layer that contains a small amount of glassy phase to aid in sealing cracks and defects. Praseodymium was added to promote the formation of a pyrochlore ($Hf_2Pr_2O_7$) compound with a lower permeability to oxygen. The results, however, indicated that neither tantalum nor praseodymium additions improved the oxidation resistance of pure hafnium carbide.

A protective HfO_2 scale does form on pure HfC upon exposure to oxygen at high temperatures, and the growth kinetics are parabolic above 1800°C (see Figure D.3). Below 1600°C, oxidation was controlled by the coupled diffusion of reactive and product gas species through a porous scale; the oxidation kinetics actually decreased as the scale sintered and became more dense. A gaseous diffusion model was developed to account for the $CO/CO_2/O_2$ reactions occurring within the scale. This model calculates the net counterflow of oxygen and carbon across the oxide layer by accounting for (a) diffusion of

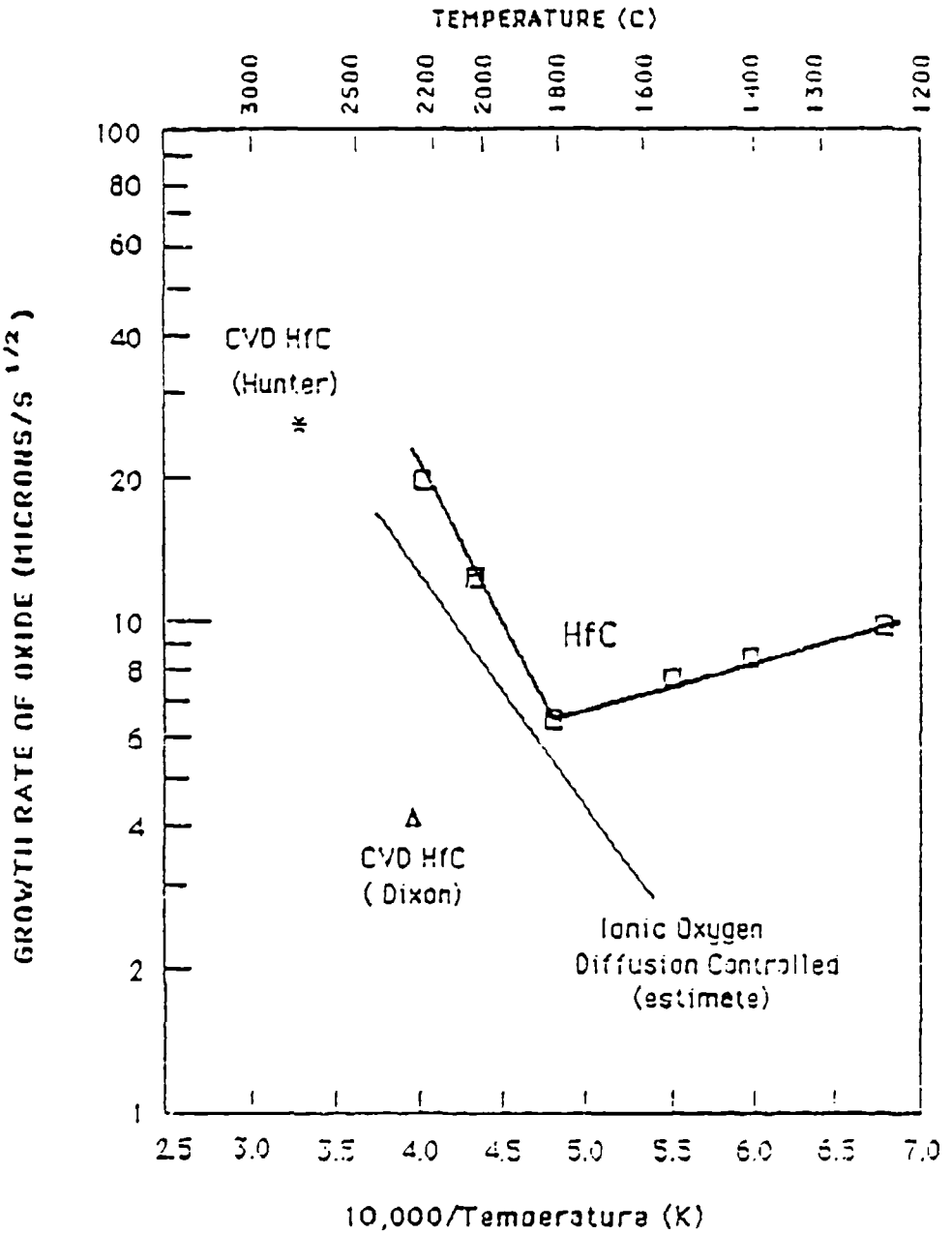

FIGURE D.3. Parabolic Rate Constant for Oxide Growth on HfC

molecular oxygen through the porous oxide where it eventually reacts with CO to form CO_2, (b) the migration of CO_2 to the carbide interface where it reacts with HfC to form CO, (c) the outward diffusion CO to combine with inward diffusing molecular oxygen to form CO_2, and (d) the eventual exhausting of CO_2 to the atmosphere. These mechanisms can occur in a porous scale on any carbide, and are an important part of understanding oxidation protection of porous scales. At higher temperatures, the oxide scale that forms on HfC is more dense and the kinetics become parabolic, controlled by a combination of diffusion in the oxide lattice and augmented by gas diffusion in the sintered pore network.

APPENDIX E

DIFFUSION OF OXYGEN IN OXIDE CERAMICS

In view of the importance of oxygen diffusion in ceramic composites, several UHT programs studied the oxygen diffusivity and permeability in selected oxides with emphasis on ternary compounds where very little data currently exist.

Diffusion coefficients were typically obtained using isotopic tracers. Under these conditions, there is virtually no chemical concentration gradient of oxygen, but there is an isotopic concentration gradient. The relationship between chemical diffusion coefficient D_i and the tracer diffusion coefficient D* can be written as follows:

$$D_1 = D^*\left(1 + \frac{d\ln\gamma}{d\ln N_1}\right) \qquad (C.1)$$

where γ_1 is the activity coefficient and N_1 is the mole fraction of the component. In concentrated nonideal solutions, the chemical diffusion coefficient could be significantly different from the tracer diffusion coefficient.

Another measure of diffusion is the permeability, which is defined as the steady-state flux across a membrane of known thickness (x) for a given pressure drop. Permeability is often expressed in terms of a permeability constant ($P \cdot X$). To obtain the diffusion coefficient from a permeability measurement, the value of dc/dx in the membrane must be known.

THERMODYNAMIC AND DIFFUSIVITY MEASUREMENTS IN POTENTIAL ULTRAHIGH-TEMPERATURE COMPOSITE MATERIALS

Ohio State University
Columbus, Ohio
Principal Investigator: J. D. Cawley
Report: WRDC-TR-90-4058

The purpose of this research was to provide fundamental thermodynamic and kinetic data in the temperature range 1650°C to 2200°C for calcium, barium, and strontium zirconates. The evaluation of the kinetics of vaporization of these materials addresses such issues as the weight-loss per unit area per hour ($mg/cm^2/h$) anticipated for zirconates if they are used as the wall of the combustion compartment of jet engines operating at about 2000°C. In this manner, the potential of the material to serve as a matrix or coating for high-temperature composites can be evaluated.

Dry-pressed $CaZrO_3$ and hot-pressed $BaZrO_3$ were tested at three different temperatures each to study vaporization characteristics with results shown in Figure E.1. The materials were characterized using the SEM, EDS, and X-ray diffraction techniques.

Both $CaZrO_3$ and $BaZrO_3$ appear to have a fairly high rate of evaporation at high temperatures. However, dry-pressed $CaZrO_3$ shows a smaller rate of evaporation than hot-pressed $BaZrO_3$. In both the materials, solid-state diffusion appears to play a key role in the kinetics of vaporization.

Results of the diffusion experiments indicate that $CaZrO_3$ exhibits the largest penetration and $BaZrO_3$ the smallest. Apparent oxygen tracer diffusion coefficients were measured for $CaZrO_3$ and $SrZrO_3$ at 1000°C and for $BaZrO_3$ between 900°C and 1100°C. The apparent tracer diffusion coefficients are compared with literature values for oxygen diffusivities in other oxides in Figure E.2. The curve for $BaZrO_3$ extrapolates to about $10^{-9} cm^2/s$ at 1650°C.

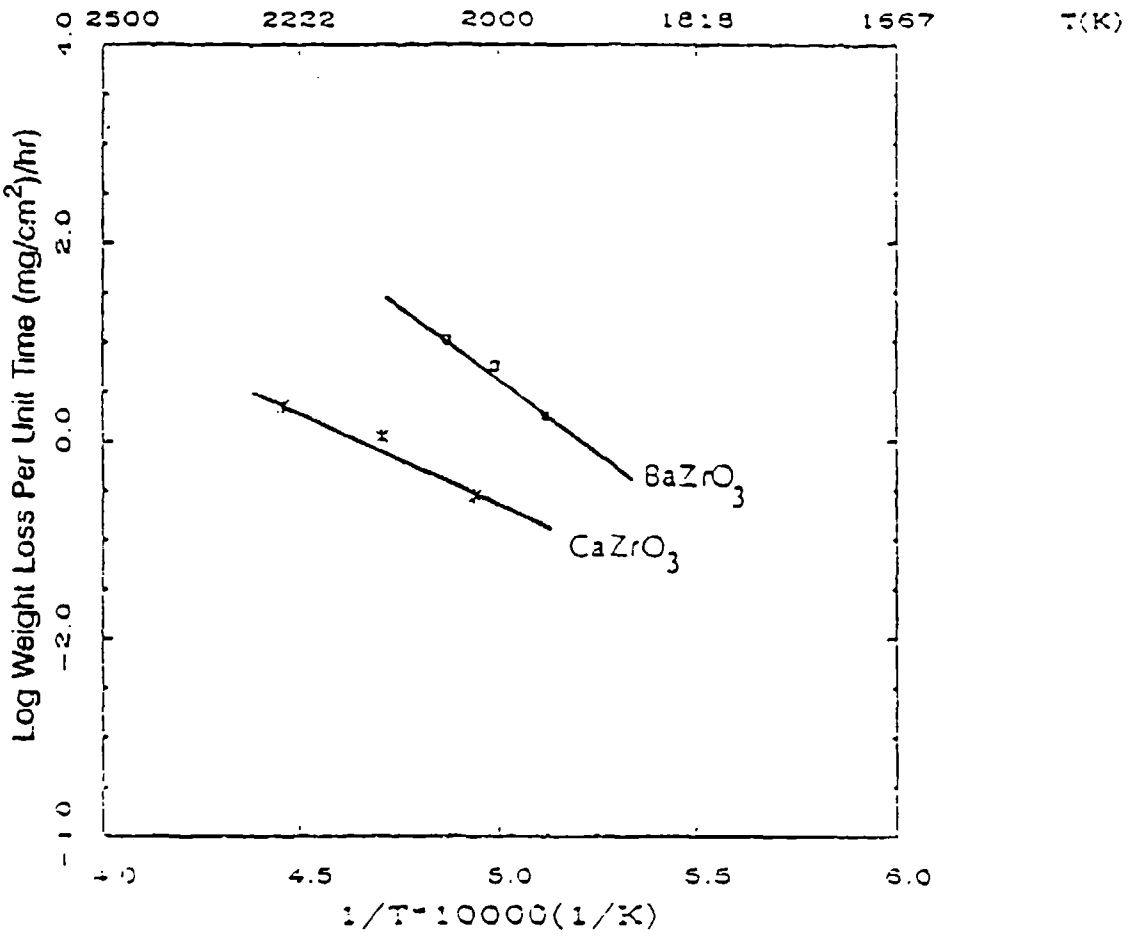

FIGURE E.1. A Plot of the Logarithm of the Weight-Loss per Unit Time for Dry-Pressed $CaZrO_3$ and Hot-Pressed $BaZrO_3$ as a Function of Temperature

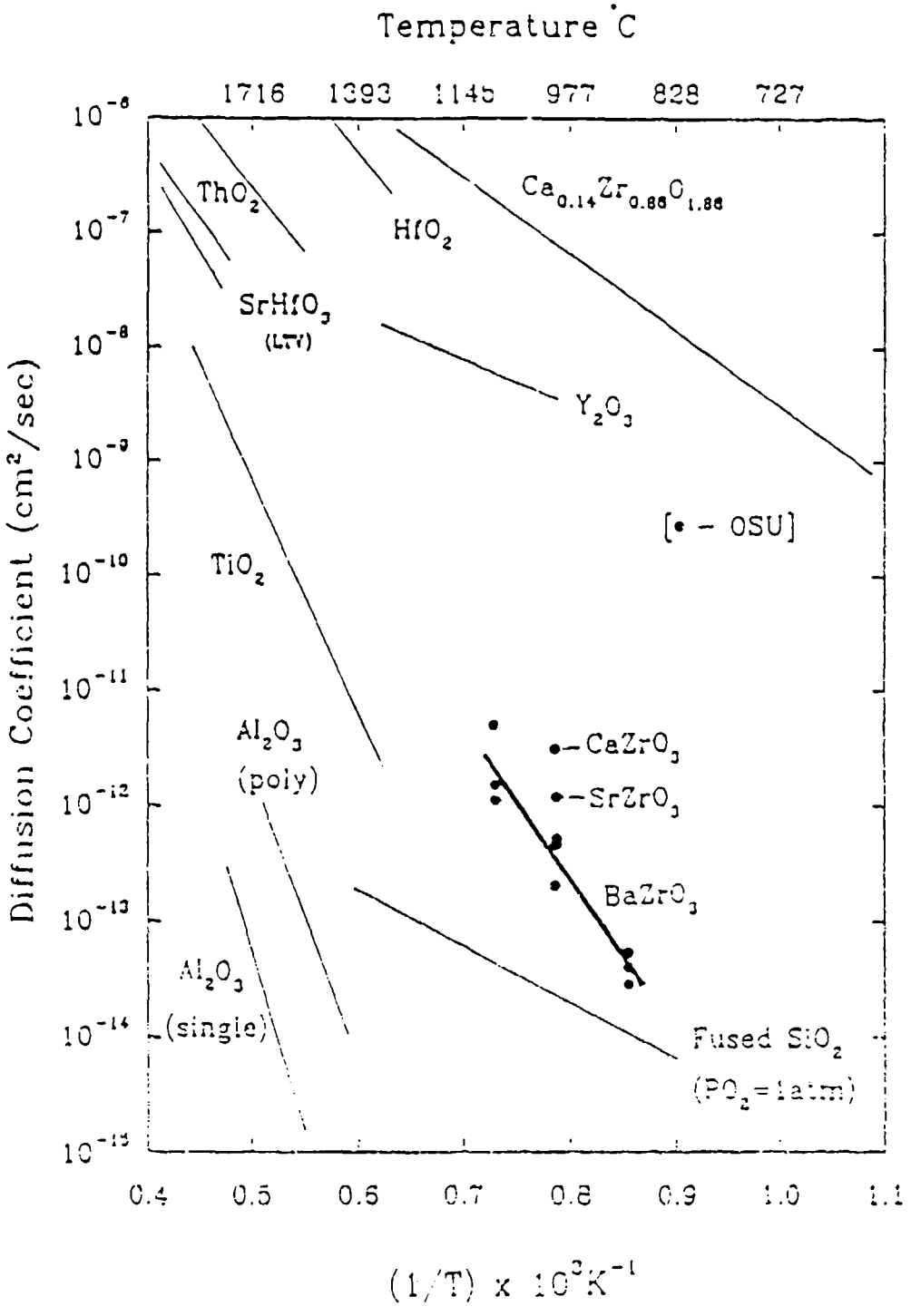

FIGURE E.2. Arrhenius Plot of the Apparent Tracer Diffusion Coefficients for the Alkaline-Earth Zirconates Together with Literature Values of Oxygen Diffusivities in Other Oxides

OXYGEN DIFFUSION IN $SrHfO_3$ FOR USE IN CERAMIC MATRIX COMPOSITES AT ULTRAHIGH TEMPERATURES

LTV Aerospace
Grand Prairie, Texas
Principal Investigator: D. W. Freitag
Report: WRDC-TR-89-4029

Specimens of strontium hafnate ($SrHfO_3$) and hafnia + 8 m/o yttria were prepared by the densification of alkoxide-derived ceramic powders. Pressureless sintered material was found to be compositionally, crystallographically, and physically stable when heat-treated to 2000°C in air for up to 340 hours; however, excessive grain growth was observed in both materials. The $SrHfO_3$ grain size increased from 20 μm to approximately 50 μm after 100 hours at 2000°C and then to over 120 μm after 340 hours. Strontium hafnate samples also showed signs of intergranular degradation that apparently resulted from strontium evaporation.

A novel technique was employed to prepare diffusion couples and to measure diffusion concentration gradients. A thin layer of $SrHf^{18}O_3$ was sandwiched between isotope-free yttria-stabilized hafnia and $SrHfO_3$ wafers. Diffusion profiles for very high temperatures up to 2200°C were established by the measurement of $^{18}O/^{16}O$ ratios with SIMS analysis. The results shown in Figure E.3 are compared to reported values for other high-temperature oxides. The tracer oxygen diffusivity, D_O^*, for strontium hafnate is about three orders of magnitude below that for hafnia.

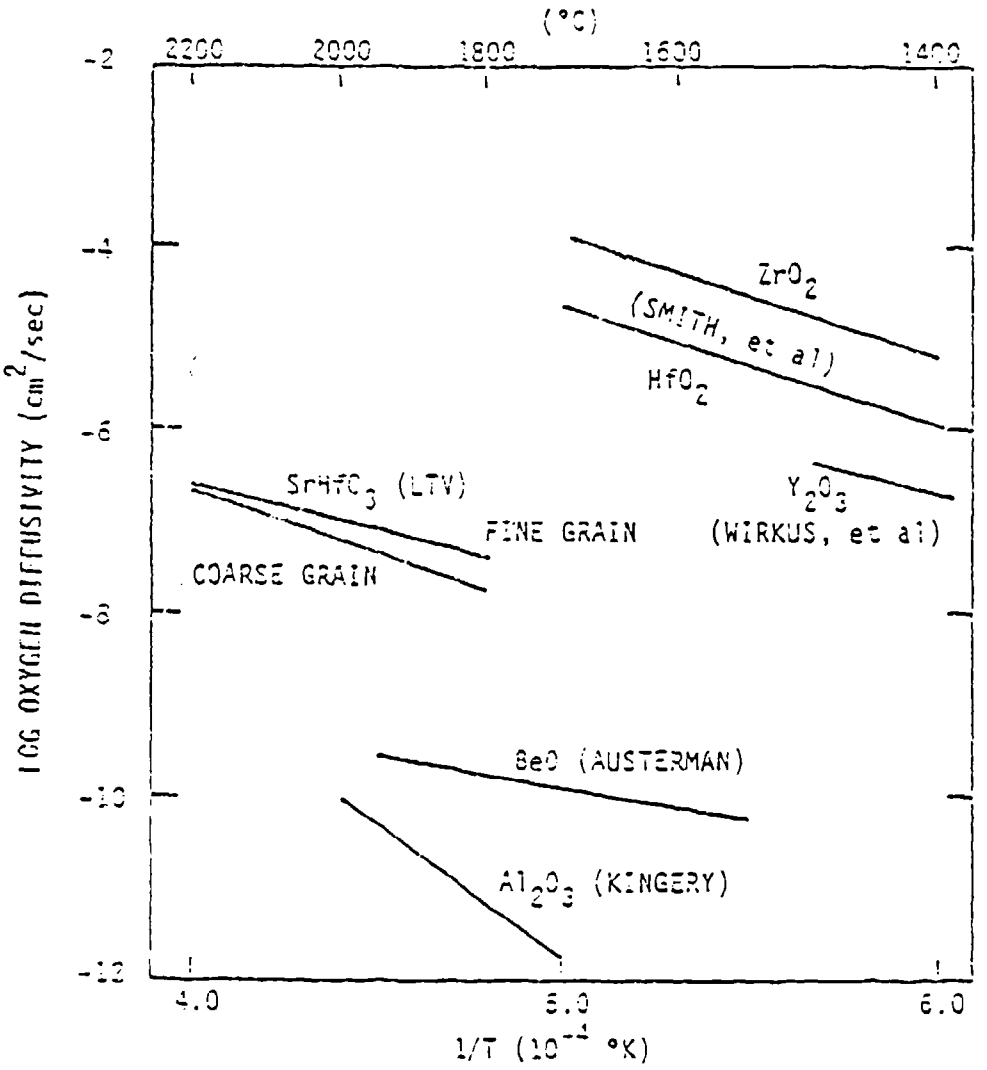

FIGURE E.3. Oxygen Diffusivity for $SrHfO_3$ as Compared to Other High-Temperature Oxides

OXYGEN DIFFUSIVITY MEASUREMENTS IN PYROCHLORE COMPOUNDS

Basic Industry Research Laboratory
Northwestern University
Evanston, Illinois
Principal Investigator: R. P. Turcotte
Report: WL-TR-91-4059

Based on thermodynamic stability and crystal structure considerations, several mixed oxides with composition $Zr_3M_4O_{12}$ were prepared as candidate ceramics having significantly reduced oxygen diffusion coefficients compared with cubic-stabilized zirconia. Colloidal processing and conventional sintering produced samples with density near 98% of theoretical. $Zr_3M_4O_{12}$ compositions with M = Sc, Y, La and Gd, as well as Y_2O_3 and cubic-stabilized zirconia were studied using the ^{18}O-exchange method to measure diffusivity in the range 800°C-1200°C.

Figure E.4 summarizes the results of the study in the form of an Ahrennius plot showing the temperature dependence of the diffusivities. The materials span about three orders of magnitude in diffusivity, with D ranging from 10^{-7} to 10^{-10} cm^2/s at 1135°C. $Zr_3Sc_4O_{12}$ and Y_2O_3 were found to have the lowest diffusivity. The temperature dependence for all of the rare earth-containing ceramics was similar. Although scandium has the smallest trivalent cation radius and lowest D values, there was no regular trend correlating diffusivity and the crystal lattice dimensions. Porous microstructures in some of the materials, especially cubic-ZrO_2 and $Zr_3Gd_4O_{12}$, led to experimental ^{18}O-exchange versus time curves which could not be easily fit to theoretical curves. Doping studies of Sc^{3+} and Ta^{5+} in $Zr_3La_4O_{12}$ showed no significant effect on diffusivity at 1135°C.

Based on this study, pure Y_2O_3 is considered the most attractive material evaluated.

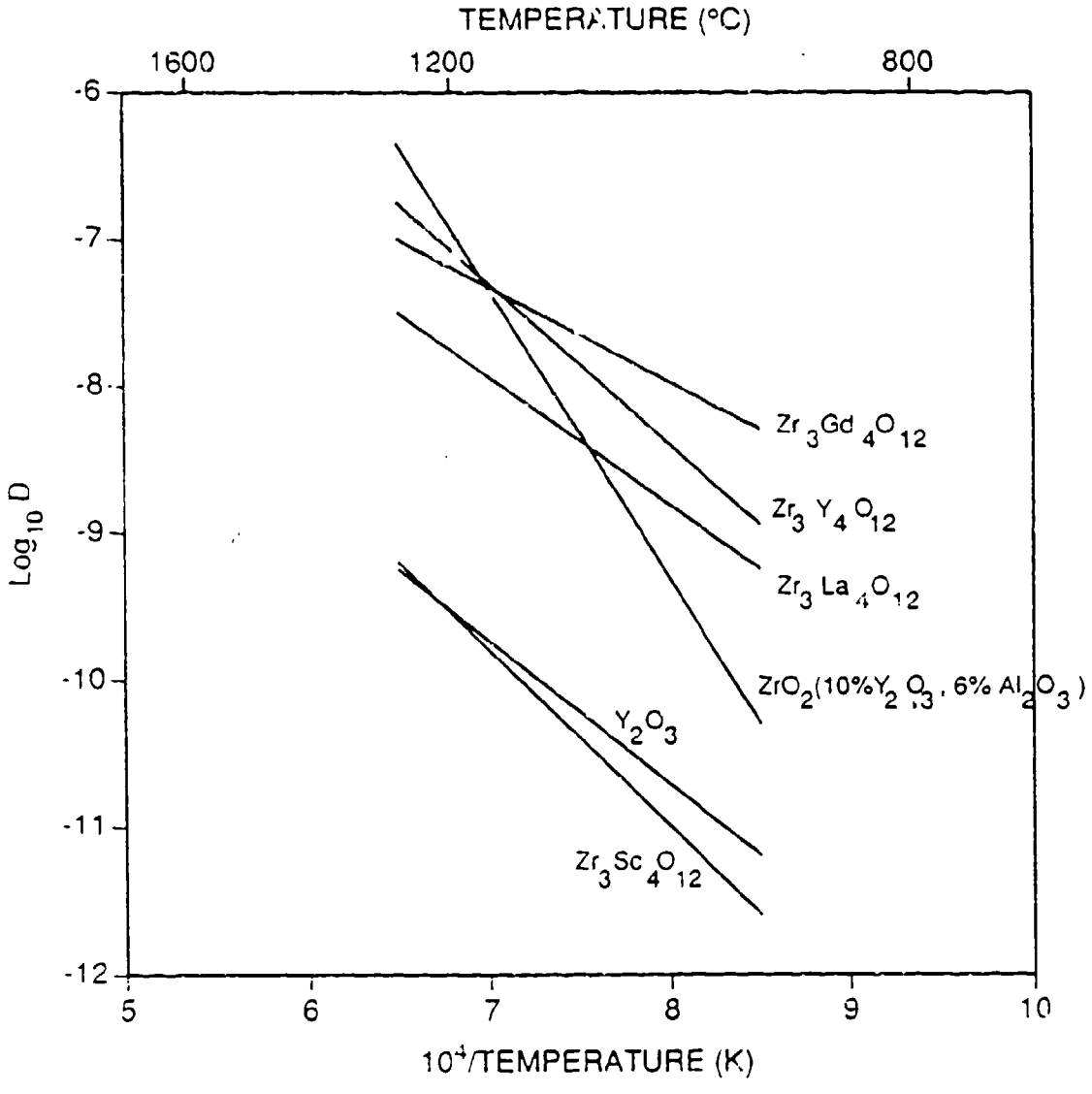

FIGURE F.4. Log of Diffusion Coefficient Versus Temperature for Complex Pyrochlore Type Oxides

OXYGEN PERMEABILITY IN SELECTED REFRACTORY OXIDES IN THE RANGE 1200-1700°C

Pacific Northwest Laboratory
Richland, Washington
Principal Investigators: J. T. Prater and E. L. Courtright
Report: WL-TR-91-4006

Oxygen permeability in several single and ternary oxides was measured at Pacific Northwest Laboratory. High-density thin wafers (≈1 mm in thickness) were prepared by hot-pressing and by sintering. These wafers were heated to various temperatures and subjected to an oxygen pressure of 0.21 atm (air) on one side and high-purity argon on the other. An electrochemical gas sensor was used to measure the flux of oxygen diffusing through the membrane.

The temperature dependence of the oxygen permeability for a range of crystallographically different oxides is shown in Figure E.5. Lanthanum hafnate ($La_2Hf_2O_7$) and calcium zirconate ($CaZrO_3$) appear to have the lowest permeabilities of the ternary oxides. The single oxides with the lowest measured permeabilities were aluminum oxide (Al_2O_3), beryllium oxide (BeO), and yttria (Y_2O_3), respectively. The permeability of oxygen through strontium zirconate is nearly the same as that for yttria-stabilized zirconia.

Cation segregation occurred for several of the mixed oxides as shown in Figure E.6. In the case of the strontium zirconate ($SrZrO_3$) sample, there was almost complete segregation, as measured by EDX analysis, with the strontium migrating to the high pressure oxygen (air) side of the sample. While a small amount of demixing, about 10%, was reported for yttria-stabilized hafnia, this is probably within experimental error. The most stable material was $La_2Hf_2O_7$. Steady-state demixing of homogeneous oxides in an oxygen potential gradient has been discussed by Schmalzried and Laqua.[117] If a stable ternary oxide ABO_x is subjected to an oxygen potential gradient, with the diffusion coefficient $D_A > D_B >> D_O$, the crystal enriches in AO at the side of the

higher oxygen potential. This demixing phenomenon can occur in practical situations and is important to the application of multicomponent ceramics at high temperatures.

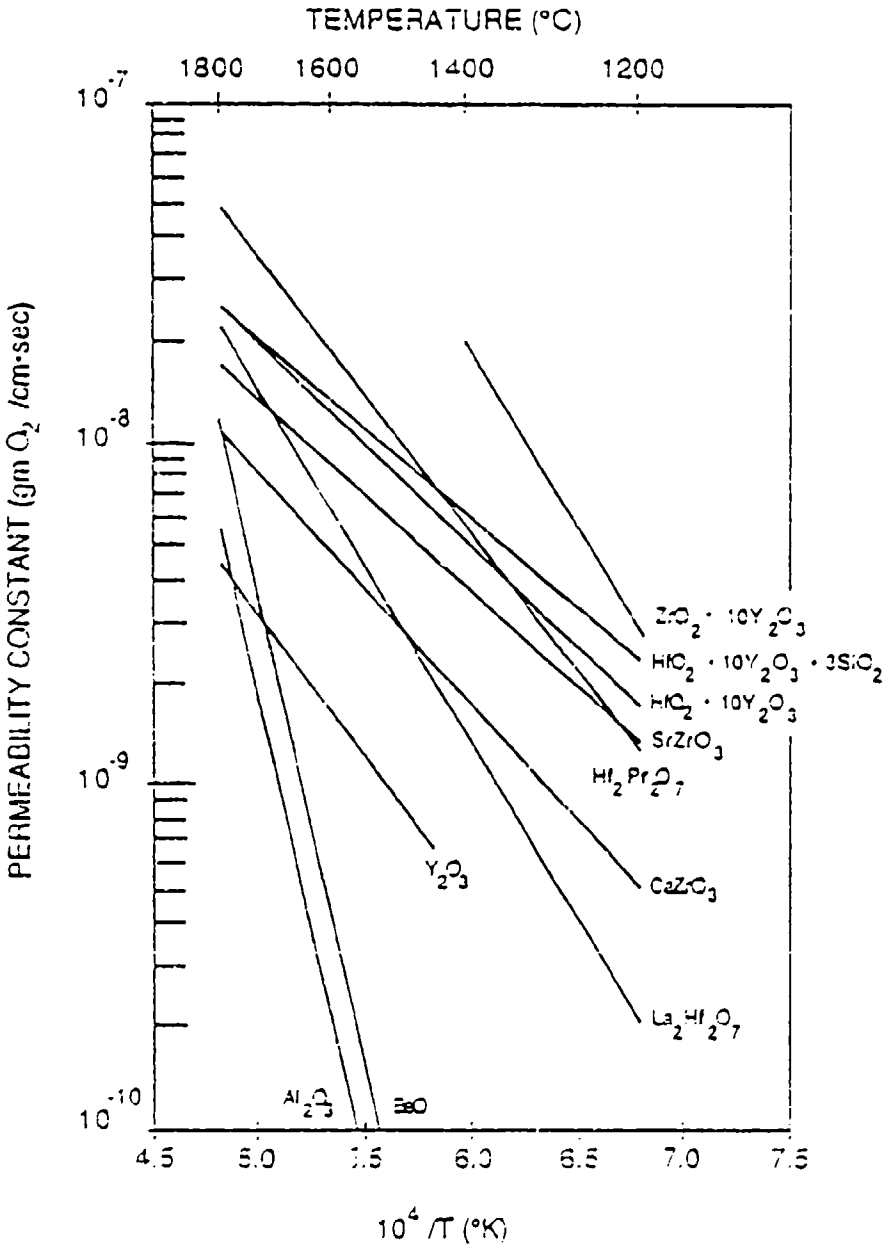

FIGURE E.5. Temperature Dependence of Permeability Constants for Several Oxide Ceramics

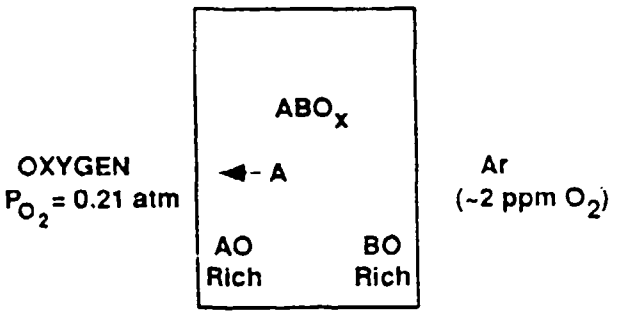

	COMPOSITION		
OXIDE	INITIAL	FINAL (AIR SIDE)	FINAL (Ar SIDE)
$SrZrO_3$	A Sr: 50 B Zr: 50	Sr: 100 Zr: 0	Sr: 0 Zr: 100
$Pr_2Hf_2O_7$	A Pr: 50 B Hf: 50	Pr: 60 Hf: 40	Pr: 40 Hf: 60
HfO_2-Y_2O_3	A Y: 10 B Hf: 90	Y: 11 Hf: 89	Y: 9 Hf: 91
$La_2Hf_2O_7$	A La: 50 B Hf: 50	La: 50.5 Hf: 49.5	La: 49.5 Hf: 50.5

FIGURE E.6. Segregation in Oxygen Gradient After Exposure to 1700°C

APPENDIX F

PRIOR AIR FORCE STUDIES

In the mid to late 1960s, the Air Force Materials Lab sponsored a program performed by Man Labs to identify the most promising material(s) for advanced aerospace applications. The first major effort was carried out under Contract No. AF33(657)-8635 entitled, "Investigation of Boride Compounds for Very High-Temperature Applications." The objectives of this work were aimed at acquiring a knowledge of the properties of refractory transition metal diborides pertinent to application under high-temperature, high-velocity oxidizing conditions.[141-143]

This initial effort was followed by an interdisciplinary program that coupled materials studies with representative environmental testing. In the materials centered framework, Contract AF33(615)-3671 (Research and Development of Refractory Oxidation-Resistant Diborides), efforts were directed towards establishing the physical, thermal, thermodynamic, and oxidation characteristics of refractory diborides in terms of temperature, composition, phase constitution, and oxidation response.[144-151] The companion study was performed under Contract AF33(615)-3859 (Stability Characterization of Refractory Materials Under High Velocity Atmospheric Flight Conditions).[152-160] Several classes and types of materials were selected for evaluation: refractory diborides, graphites and JT graphite composites, hypereutectic carbide-graphite composites, refractory metals, coated refractory metals, metal/oxide composites, and iridium-coated graphites. The testing methodology encompassed representative heat flux and boundary layer shear conditions expected during re-entry or high velocity atmospheric flight as well as those conditions found in conventional furnace tests. Particular focus was directed towards establishing the relationships between hot wall/cold gas and cold wall/hot gas surface effects in terms of mass transfer rates at high temperatures.

DEVELOPMENT OF REFRACTORY OXIDATION RESISTANT DIBORIDES

Man Labs, Inc.
Boston, Massachusetts
Principal Investigator: L. Kaufman
Report: (Ref. 141-160)

A comprehensive review of the refractory diboride studies performed by Man Labs, in addition to other related Air Force sponsored efforts, was provided by Fenter.[57] A compilation of the original reports is given by references (141-160). Processing conditions, materials characterization, mechanical and physical properties, and thermochemical stability were summarized. Significant improvements in oxidation resistance and mechanical strength were obtained by adding 20 to 30 v/o SiC to a refractory diboride matrix. Both HfB_2-20SiC and ZrB_2-20SiC were found to have good short-term oxidation resistance in hot flowing gas environments. Bend strengths were on the order of 276 MPa (40,000 psi) at 1800°C, see Figure F.1, which is about 70% retention of the room temperature values. Stress rupture life at 100 MPa (14,500 psi) was approximately 100 hours at 1040°C. Creep rates were on the order of 1 x 10^{-5}/s at 1600°C under compressive loads of 172 MPa (25,000 psi).

Carbon was added to the SiC/Hf(Zr)B_2 material in concentrations up to 30 to 50 v/o without significant losses in oxidation resistance and/or reduction in high-temperature creep. This addition had the beneficial effect of improving fracture toughness, thermal shock resistance, and machinability. The oxidation rates of specimens exposed to furnace air for ZrB_2, 20SiC/ZrB_2, and 20SiC/ZrB_2-(C) were 10, <.5, 2.5 mil/h at 1650°C, and 100, 10, and 40 mil/h at 1927°C, respectively.

The recession rates for the refractory diborides (e.g., HfB_2 and ZrB_2) were a factor of ten lower in arc plasma exposures compared to furnace testing due to the effects of reaction-limited conditions and temperature gradients. A comparison of high- and low-velocity oxidation for zirconium diboride is shown in Figure F.2. In general, materials that form solid oxide protective

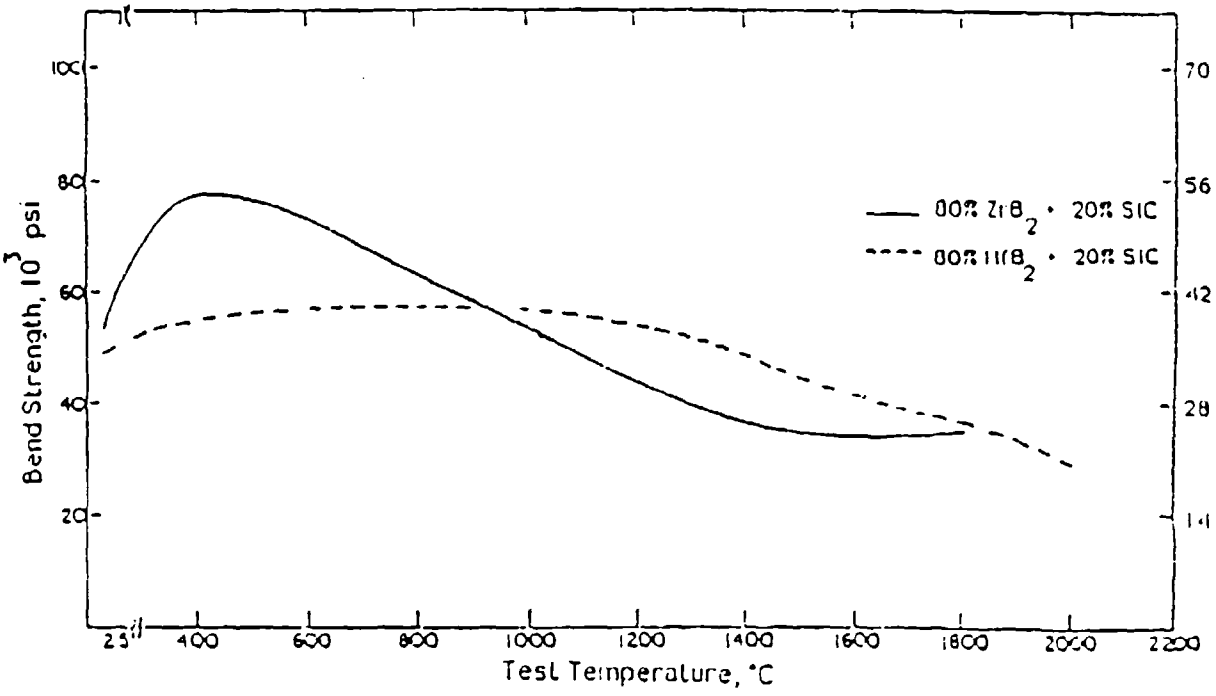

FIGURE F.1. Bend Strength-Temperature Relationship for Two Diboride Compositions

scales showed lower recession rates in the hot-gas/cold-wall test for a given surface temperature than in the cold-gas/hot-wall situation, but the reverse was true for ablating materials. The difference between arc plasma and furnace oxidation was not as great for the diborides when SiC was added.

A significant effort was also made to translate the flux/enthalpy profiles into equivalent altitude-velocity characteristics to permit comparison of stagnation point performance with relative trajectories. Materials were ranked at a stagnation point pressure of 1 atm and the superiority of SiC and composites containing SiC was evident. The widest range of applicability was afforded by the SiC/HfB_2 composite.

Two of the composite systems, 20SiC/ZrB_2 and 14SiC/ZrB_2-3C, were tested as segments of a full-scale engine intake leading edge. The diboride elements appeared to withstand all loads imposed in the test, which simulated velocities approaching Mach 5.9 condition at 89,000 feet altitude, 2400°F

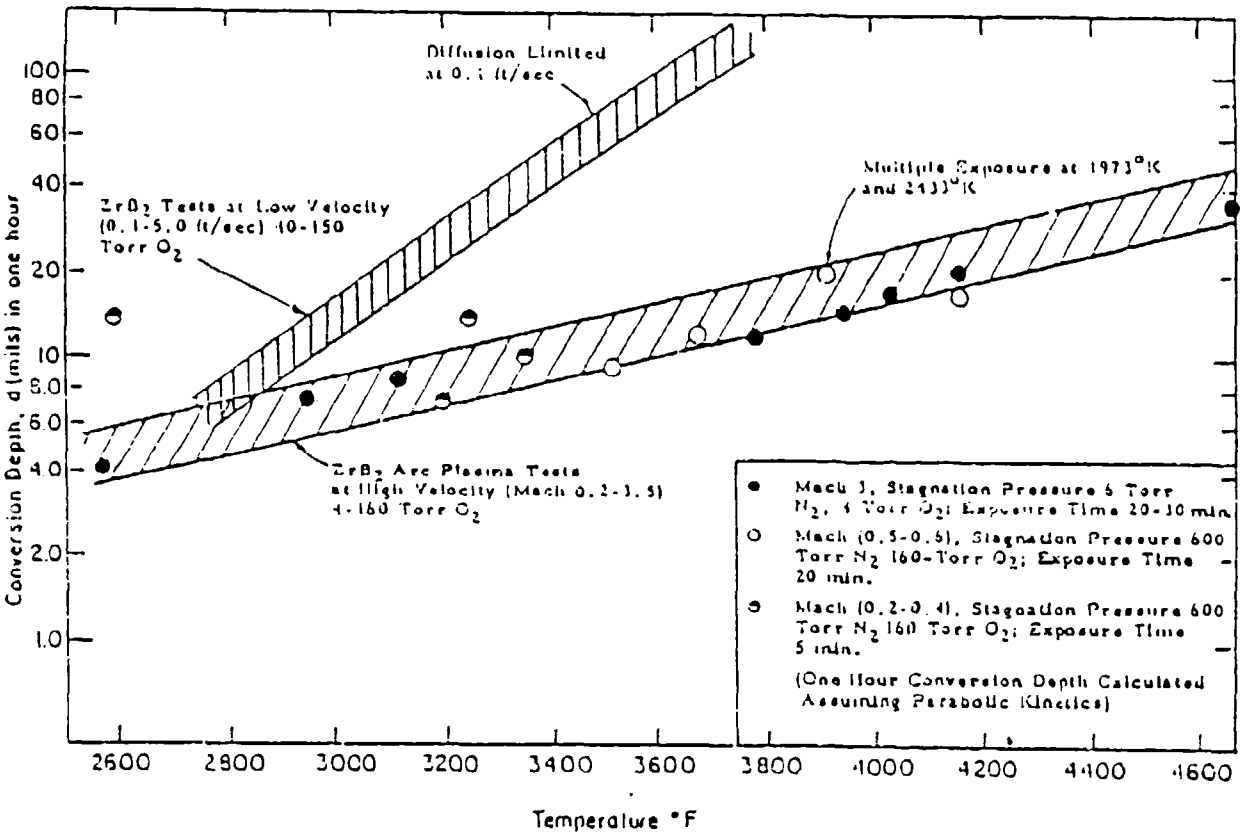

FIGURE F.2. Comparison of High- and Low-Velocity Oxidation of ZrB_2

temperature, a 50 psi (0.34 MPa) steady-state pressure differential, and a starting-shutdown transient pressure differential up to 150 psi (1.03 MPa).[57]

☆U.S. GOVERNMENT PRINTING OFFICE : 1991 - 750-111/80096